Department of Precision and Microsystems Engineering

Design of a fluorescent measurement method for compliant hydrostatic bearings

S.J. Siers

Report no : 2020.036
Coach : ir. J. P. A. Nijssen
Professor : dr. ir. R. A. J. van Ostayen
Specialisation : Mechatronic System Design
Type of report : Master of Science Thesis
Date : 3 September 2020

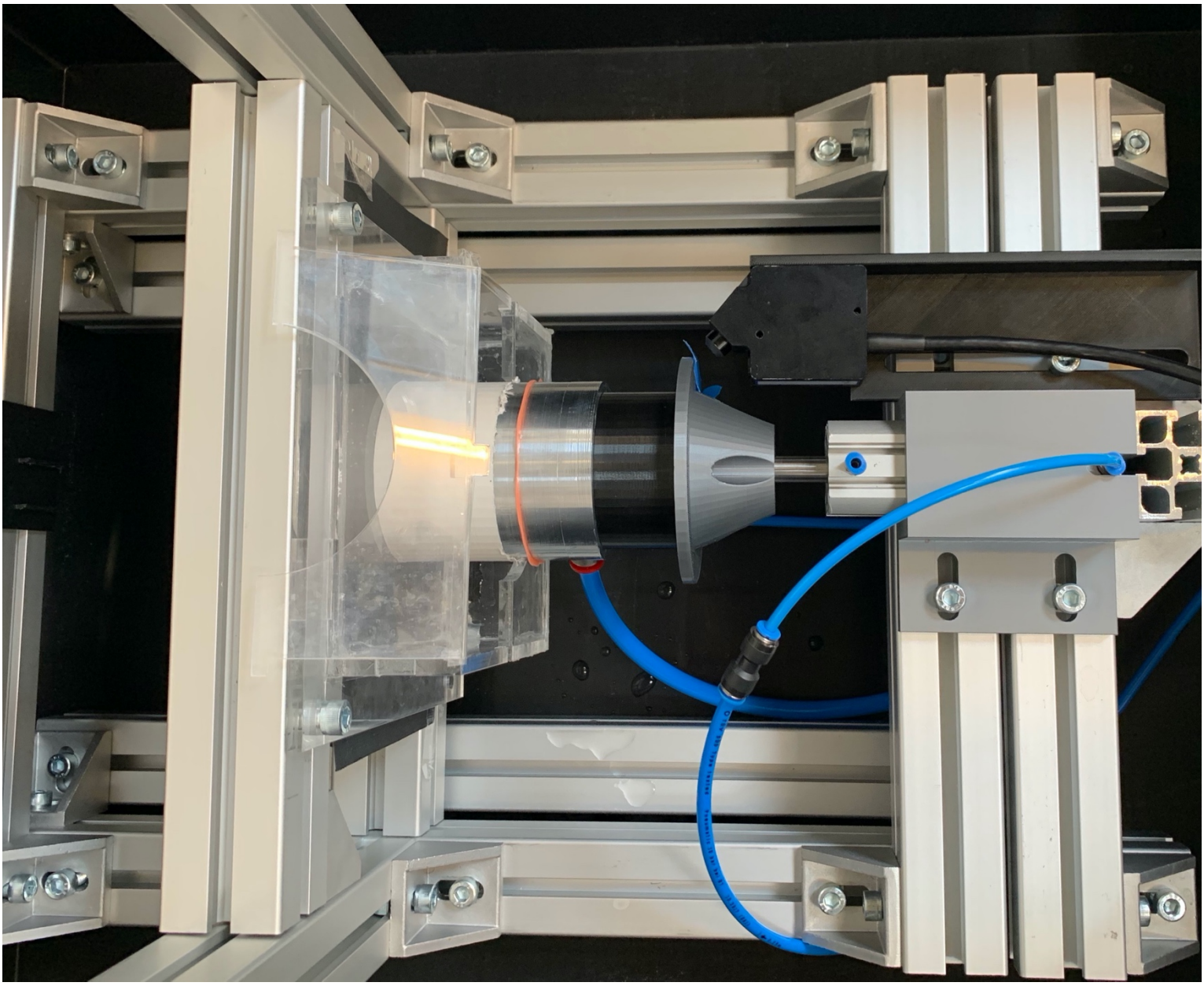

Design of a fluorescent measurement setup for compliant hydrostatic bearings

by

S.J. Siers

to obtain the degree of Master of Science
at the Delft University of Technology,
to be defended publicly on Tuesday September 29, 2020 at 13:15 AM.

Student number:	4219910	
Project duration:	September 20, 2019 – September 29, 2020	
Thesis committee:	Dr. ir. R. A. J. van Ostayen,	TU Delft, supervisor
	Ir. J. P. Nijssen,	TU Delft, supervisor
	Dr. Ir. J. F. L. Goosen,	TU Delft

This thesis is confidential and cannot be made public until May 20, 2021.

TU Delft

Preface

From a young age, I was always interested in mechanics and everything that comes with it. This inspired me to start my study mechanical engineering at the TU Delft. From the first moment, I was encouraged to extend my mechanical engineering skills. There was not a moment were I regret my choice for this study. Now an end has come to my time as a student in Delft and it is time to start my career. The fundation has been laid to have enough analytical skills as well as soft skills. I am very grateful for this time in Delft for forming me as a person. This was not possible without the peeplo surrounding me and I would like to thank them.

First of all, I would like to thank my parents, Paul Siers and Corien Sluijter, for always supporting me in ups and in downs. Furthermore, by giving me the freedom to find things out by myself, I grew as a person. Due to their thrust, I had the strength to push on and able to finish my study. Many, many thanks!

Secondly, I would like to thank my girlfriend Aliex. We have met during our time in Delft and grew closer to each other. She always stood by my side and supported me wherever it was needed. Therefore, I would like to thank you with all my heart.

Furthermore, I would like to thank Joep Nijssen and Ron van Ostayen for their time and support, giving me greater insights and helping me to finish my research project. Without their help this was not possible.

Finally, I would like to thank everybody else who contributed to my thesis and to my time as a student in Delft. There are too many to name them all. But know that I am very grateful for your support and help.

S.J. Siers
Amsterdam, September 2020

Abstract

A hydrostatic bearing is a bearing type where the friction is reduced by creating a thin film of liquid between a bearing and its counter surface. These types of bearings are typically highly reliable and have very high performance capabilities.
The main limitation of this type of bearing is that they are highly dependent on the shape and smoothness of the running track surface. This means they only work properly when the running track is flat or has a constant curvature. Improvements to these bearing systems can therefore be made by reducing the dependency to the geometry and smoothness of the running track. A method of achieving this is through the use of a compliant hydrostatic bearings [27]. An embodiment of such a bearing is by using elastic materials for the bearing support. Such bearings will be able to follow the imperfections of the running track, whilst maintaining a sufficient film of liquid between the surfaces.

To determine the performance of these compliant hydrostatic bearings a method has to be implemented that is able to map the film height. In the case of rigid bearing, the film height and tilt can be determined using three laser sensors. For the compliant bearing this is not suitable due to the elastic behavior, therefore a fluorescence based measurement technique will be implemented in a setup for determining the film height. This can be achieved because the fluorescent intensity is proportional to the thickness of the solution.

A LED, with a dominant wavelength of 540 nm, will be used to excite a solution containing water and Rhodamine B as fluorescent dye. This dye has an excitation wavelength of 540 nm and an emission wavelength of 570 nm. The shift in colour due to this fluorescent effect is captured by a RGB camera were the different channels can be used as a digital filter. Using a ratioed technique the increase in intensity is determined and by using a calibration method coupled to a film height.

To obtain the performance of the measurement method, a setup has been design using a rigid hydrostatic bearing with multiple features. The method is then validated by the use of a laser sensor which determines the actual film height and tilt. It is found that this method can obtain an average accuracy of 6.4 % with an average confidence interval of 95 % of 15.4 μm.

A second setup has been designed which is able to test a compliant hydrostatic bearing. The goal of this setup is to show the potential of the measurement by introducing a deformable bearing made of silicon rubber. Using COMSOL, the measured results are compared to the FEM results. A noticeable difference in result can be explained due to the fact the bearing contains air bubbles in the silicon. This silicon has therefore not a uniform stiffness and thus behaves different than the model.

Concluding, this work shows a fluorescent based measurement method that has an operating range of 15-1400 μm. By further reducing the leakage and the noise this range can be extended and the method becomes valuable for even more applications.

Contents

1 Introduction

1.1. Background

Almost all mechanical systems contain some sort of relative motion of solid components. Where two systems are sliding or rolling over each other, friction and wear will occur. The performance of a mechanical system is majorly influenced by friction, lubrication and wear. If a passenger car is taken as an example, almost 1/3 of the energy consumption goes to overcome friction [14].Furthermore, wear and friction also determines the precision, accuracy and lifetime of mechanical systems. The continuous pursuit of higher-performing systems requires higher design demands in the industry. One method to improve the efficiency and reduce friction between the moving parts, is the use of bearings. Over the years bearings have been designed to minimize friction and to meet the requirement set by the industry. But a rising demand for better performing bearing keeps existing.

Bearings can be divided into two types. The contact bearing, such as ball-bearings or slider bearings, are widely known for their versatility and used in almost all mechanical systems. The big disadvantage of these bearing is that they still have contact between the surfaces which means friction occurs. Due to the friction, the system wears down and consequently, these components need to be replaced. A replacement of components means that the system needs to be shut down which results in extra costs costs for a company.

The other type of bearings are contactless bearings, such as hydrostatic bearings or magnetic bearings. These bearing systems do not have contact between the two surfaces. This means no friction will occur and therefore there is no wear and the lifetime improves drastically. These systems are mostly used in high tech systems were precision and accuracy needs to be as high as possible. Therefore more research is being carried out into contactless bearings.

In this report, I will focus on hydrostatic bearings and in particular compliant hydrostatic bearings, see figure 1.1.A. A compliant hydrostatic bearing has an elastic layer within the bearing so that it can deform. Although compliant hydrostatic bearings are very suitable for non-constant tracks, the design aspect is a more complicated and there sits the problem. Most hydrostatic bearings are designed for a certain load capacity. This load capacity depends on the distributed pressure between the bearing and the running track. Because this pressure profile is depending on the film height it is crucial to know the film height between the bearing and the running track. Due to compliance and elasto-hydrostatic effects, the film height is not easily predicted. That is the reason why verifying the fly height by doing experiments becomes valuable.

1.2. Research approach

In this thesis the goal is to find and implement a measurement method that is able to measure the film thickness of a compliant hydrostatic bearing. Multiple methods are found in literature that are able to measure a film thickness. In order to compare these multiple methods, I have defined some criteria of which these methods should comply with.

Using the requirements as a guideline, methods found in relevant literature can be divided into three categories: Optical, Acoustic and Electromagnetism. Methods like magnetic reluctance [5], capacitance [6] [9], ultrasound [23] [8] or light of internal reflection [17] are limited by their resolution or have the disadvantage to only measure discrete points. Another method such as optical interferometry [18] [11] has the proper

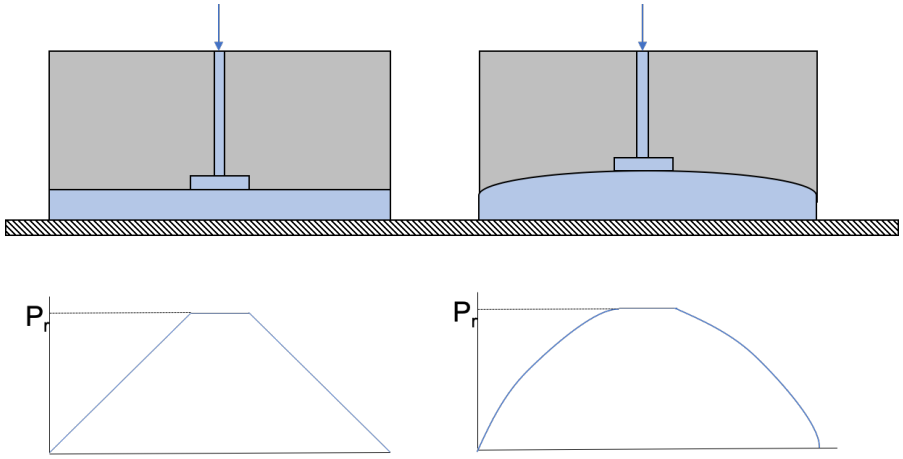

Figure 1.1: (A.Left) Classic hydrostatic bearing with corresponding pressure profile(B.right) Compliant hydrostatic bearing and its corresponding pressure profile

Design requirement	Quantification	Definition
Film height range	1-1000 μm	Defined as $10 \cdot h_0$ with h_0 being the film height
Resolution of method	1-5 μm,	Because small changes in the fly height have great influence on the load capacity and these need to be captured
Large measurement area	$\geq 80x80\text{mm}^2$	Self defined
Applicable on elasto surface	-	Because an elasto-hydrostatic bearing will probably be of some sort elastic material and the method should work with that.
Non intrusive method	-	Be able to test different bearing, so the bearing should not have to be altered to be tested.
Fast measurement	-	An instantaneous film thickness map is required.

Table 1.1: Design requirements

resolution but has the disadvantage of being limited by its area of measurement. This method is expensive, hard to implement and requires a scanning motion. Therefore it is not suitable for compliant bearing measurements. Other methods such as dye attenuation [20] [25] and fluorescence [13] have the ability to make a 2D map of the film height with a sufficient resolution to obtain the deformation of a compliant hydrostatic bearing. Both methods use a colour shift to obtain the film height, but dye attenuation, in contrast with fluorescence, needs some adaptations to measure the colour shift. Because the desired method is non intrusive and does not need adaptations to the bearing itself, it has becomes useful to use fluorescence as the method to implement. Besides the ability to measure the film height, fluorescence can also give information about the lubricant behaviour [22]. Husen (2018) has succesfully used fluorescence to obtain the thickness of a thin oil film. This experiment has been used in air-oil-wall configuration. However, hydrostatic bearings need a counter surface, this method will be used to measure the thickness between a transparent wall-lubricant-bearing wall configuration. In this thesis I will make use of fluorescent behaviour to obtain film height maps.

1.3. Thesis Layout

Chapter 2 will give some background theory about hydrostatic bearing and fluorescence. This theory is used in the design of two measurement setups. Chapter 3 will explain all the design steps made in the construction of the measurement setups. Chapter 4 is a paper containing the results of this thesis. Chapter 5 will elaborate on the measurement itself. Multiple settings have been tested to obtain the best result. Chapter 6 will consider the FEM model used. Results concerning the FEM model will be discussed as well. Chapter 7,8 and 9 will contain the discussion, conclusion and recommendations respectively. A critical look will be taken on all the considerations and this will be used in the conclusion. Recommendations for further research will finalize this thesis.

2

Theory

2.1. Hydrostatic bearings

2.1.1. Classic hydrostatic thrust bearing

A hydrostatic bearing is a contactless bearing. It creates a layer of liquid or gas between two surfaces, such that the two moving parts are not in contact with each other. This is also called full film lubrication. Due to the layer of liquid or air, a system is created which has almost no mechanical friction and therefore almost no wear. A cross-section of a schematic classic hydrostatic bearing with pressure distribution is shown in figure 2.1. In this example, a cylindrical hydrostatic trust bearing is used. The system works as follows:
The bearing is being fed through an external pump with a certain supply pressure(**1**). In order to reduce the supply pressure to the rescess pressure, the liquid is fed through a restrictor(**2**). The restrictor has as purpose to create a variable recess pressure which results in giving the bearing its stiffness. Restrictors come in two different types. 1. There are linear restrictors that have a linear relation between the pressure drop and flow rate through the restrictor. Such a restrictor is called a capillary tube. 2. there are non-linear restrictors. Here the relation of the pressure drop is non-linear with the flowrate. These types of restrictors are called orifice restrictors. What type of restrictor is chosen for a system does not matter for the function it delivers, but the orifice restricotr does make calculations more complex.
So the restrictor lowers the supply pressure to the recess pressure. Via the recess the liquid is pushed outside the bearing through the gap between the surface and the bearing (**3**). This gap is in order of 100 micrometers [26]. This can be considered as a thin film and such a thin film has the property of having a laminar flow. This thin film is important because it determines the pressure profile between the bearing and the surface. This pressure profile determines the load capacity of the bearing and the load capacity is one of the most important characteristic of the bearing[21].
Classic hydrostatic bearings are considered rigid, which means that deformations of the bearing compared to the height of the film is negligible. This also means that when the bearing is being pressurized the film thickness is equal throughout the whole film. In order to measure the film height of the bearing, A measurement of one discreet point can be done. Forces that are not normal to the bearing can make the bearing tilt. Therefore, three discrete measurement points are desired, because the bottom side of the bearing does not deform. Although having great performance characteristics such as high load capacities and low friction, still some disadvantages arise. A limitations is that a perfectly straight running track is desired which is hard to obtain.

2.1.2. Reynolds equations

A hydrostatic bearing is noting more than two static parallel plates separated by a thin film of liquid. This thin film of liquid creates a pressure distribution in y direction when the liquid is flowing. This flow is caused by a pressure difference between the entry and the exit of the path. Because the film is considered a thin film, laminar flow is assumed between two stationary parallel plates. The flow is resisted by shear stresses in the liquid. Figure 2.2 gives an example. At the boundary of these plates the flow velocity is zero and in the middle a maximum is reached. Pressure across the flow is assumed to be constant which results in $\delta p/\delta y = 0$. The equilibrium of the force of an element with a width z [4] is

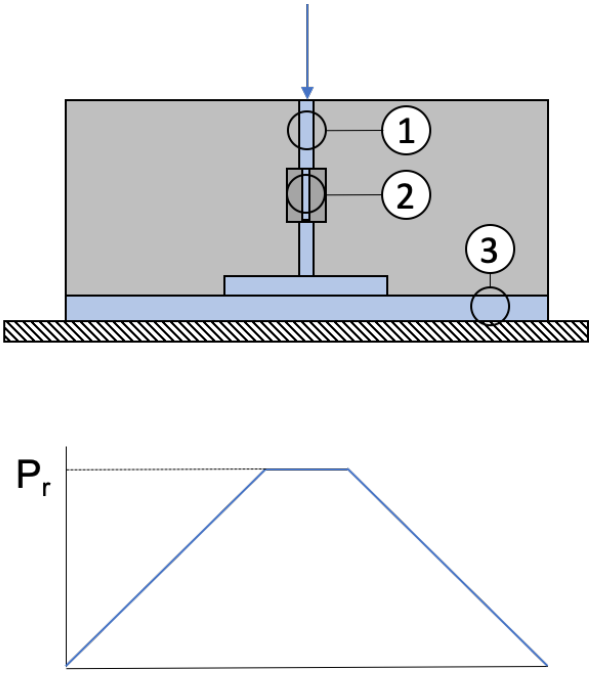

Figure 2.1: Classic hydrostatic bearing with highest recess pressure and its distribution for an infinitely long bearing.

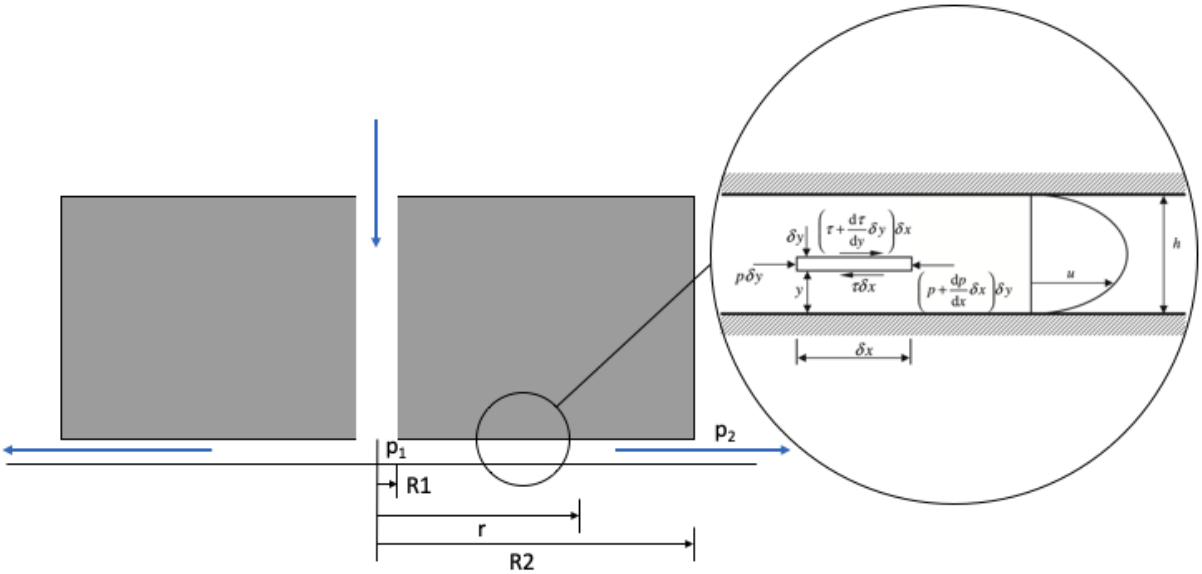

Figure 2.2: Pressure induced poiseuille flow, (Rowe 2013)

$$pz\delta y - (p + \frac{dp}{dx}\delta x)z\delta y - \tau z\delta x + (\tau + \frac{d\tau}{dy}\delta y)z\delta x = 0 \tag{2.1}$$

which leads to:

$$\frac{d\tau}{dy} = \frac{dp}{dx} \tag{2.2}$$

If we substitute $\tau = \eta\frac{du}{dy}$ in equation 2.2, it leads to:

$$\eta\frac{d^2u}{dy^2} = \frac{dp}{dx} \tag{2.3}$$

Integrating equation 2.3 twice and applying its boundary conditions $u = 0$ at $y = 0$ and $y = h$, and $\frac{du}{dy} = 0$ at $y = \frac{h}{2}$ results in:

$$u = \frac{1}{2\eta}\frac{dp}{dx}(y^2 - yh) \tag{2.4}$$

Integrating this to find the volumetric flow:

$$q = \frac{zh^3}{12\eta}\frac{dp}{dx} \tag{2.5}$$

If we look at two parallel circular plates this equation becomes:

$$q = \frac{-\pi r h^3}{6\eta}\frac{dp}{dr} \tag{2.6}$$

If we now integrate this flow rate for $p_2 = 0$ and $r = R_1$ the flow rate of the bearing becomes:

$$q_{\text{bearing}} = \frac{-\pi p_1 h^3}{6\eta \ln(R_2/r_1)} \tag{2.7}$$

2.1.3. Compliant hydrostatic thrust bearing

To make a system that does not have the limitation of only performing on a straight running track, compliant hydrostatic bearings are being developed. Such a compliant hydrostatic bearing will consist of an elastic material that is in contact with the fluid film. Figure 2.3 shows a schematic example of such a bearing with its deformations. This means that the bearing itself will deform due to the pressure profile(**4**). So when a higher load is applied to the bearing, the bearing will fly lower and therefore the pressure underneath the bearing surface gets higher. This results in a deformation of the elastic material and consequently leads to a higher load capacity. This higher load capacity will make the bearing fly higher and thus resulting in a lower pressure. This is a iterative process which will lead to a equilibrium. Compared to a classic hydrostatic bearing the compliant one will have better performance characteristics. But to determine these performance characteristic such as load capacity, hard complex calculations are needed. Therefore it becomes valuable to do fast measurements instead.
In the past research has been done into these compliant hydrostatic bearings[27] [26]. But that research was only conducted for small deformation. For instance, the Prins Willem Alexander lock, which has a waviness of 0.5 mm/m with corresponding nominal film height of 0.1 mm and width of the bearing of 0.75 m [27]. Current research is being done in large deformation compliant hydrostatic bearings with a waviness of 100 mm/m. For these large deformable surfaces film height profiles are desired.

2.1.4. Restrictors

To maintain a stable bearing it is required to have some form of a flow control device. A restrictor will be able to control the flow resulting in a stable bearing that has a stiffness as well. In the situation where there is no restrictor the recess pressure would be equal to the supply pressure. If the bearing has a certain film height and you would increase the load, the film height becomes smaller and the recess pressure has to become higher to carry the extra load, but the supply pressure can not increase and therefore the film height becomes zero. If we add a restrictor, which determines the flow and the pressure drop, the supply pressure is not equal to the recess pressure. This means that if the load is increased, the film height will decrease and therefore the outflow of the bearing decreases. Due to continuity the flow from the restrictor also decreases and therefore the pressure drop becomes smaller. This means that recess pressure becomes higher and the bearing will be able to carry the extra load. The flow continuity is as follows:

$$q_{\text{restrictor}} = q_{\text{bearing}} \tag{2.8}$$

The two kind of restrictors are explained as follows:

1. Capillary restrictor

A capillary restrictor is a tube with length l_c and a diameter of d_c. To ensure the resistance of the restricor work properly (Re > 5000) a ratio of 20 should be achieved [26]. This is to obtain the effect of restricting the flow for low Reynolds numbers and negligible losses at the entrance and exit. The flow over such a restrictor is give by:

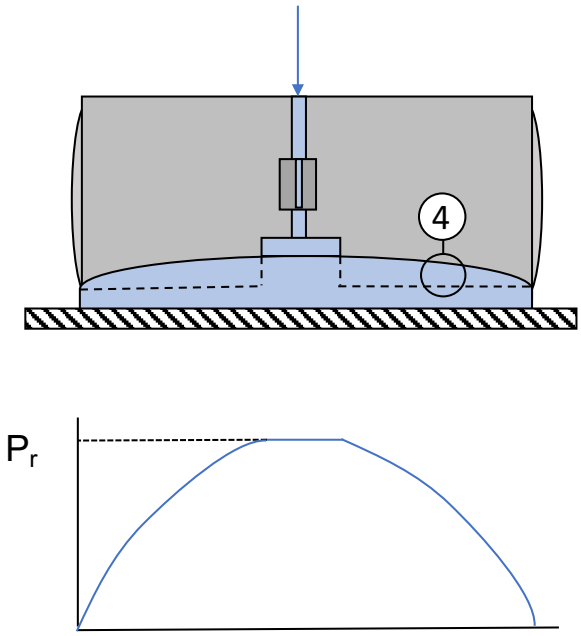

Figure 2.3: Schematic compliant hydrostatic bearing with corresponding pressure distribution.

$$q = \frac{(p_s - p_r)\pi d_c^4}{128\eta l_c} \tag{2.9}$$

Where p_s is the supply pressure, p_r is the recess pressure and η is the viscosity of the liquid.

2. Orifice restrictor

An orifice is a hole with a very small length to diameter ratio. The flow rate for an orifice restrictor is as follows

$$q = C_f A_o \sqrt{\frac{2(p_s - p_r)}{\rho}} \tag{2.10}$$

where C_f is the discharge coefficient of the orifice. This is typically equal to 0.55 for a Reynolds number of $Re = 10^6$. The A_o is the area of the orifice. This restrictor is also dependent on the density of the liquid. Therefore it is also dependent on the temperature of the liquid.

2.1.5. Load

The load of the bearing is dependent on the pressure distribution under the bearing surface. For a circular bearing pad this can be found by rewriting equation 2.6 and integrating this across the bearing lands gives

$$p_1 - p = \frac{6\eta q}{\pi h^3} \ln(\frac{r}{R_1}) \tag{2.11}$$

If we know that $p_1 = p_r$ this equation becomes

$$p = p_r - \frac{6\eta q}{\pi h^3} \ln(\frac{r}{R_1}) \tag{2.12}$$

The bearing load can then be calculated using

$$W = \int_{R_1}^{R_2} p(2\pi r) \mathrm{d}r \tag{2.13}$$

The load of a bearing can be increased using a pocket in the bearing. Figure 2.4 gives schematically the load distribution of a bearing with and without a pocket. This pocket will have a greater area of where the recess pressure is present. The equation to calculate the load becomes

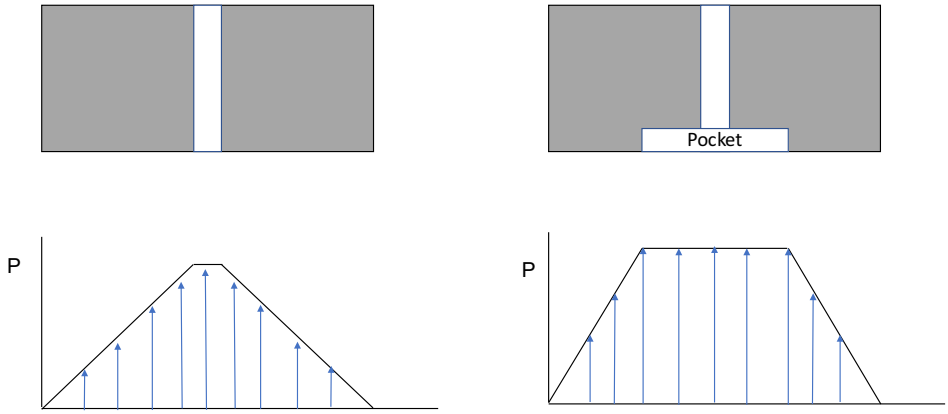

Figure 2.4: Pressure distribution over the bearing surface with and without pocket.

$$W = p_r \pi R_1^2 \int_{R_1}^{R_2} p(2\pi r) \mathrm{d}r \tag{2.14}$$

if we now implement equation 2.12 and integrate by part the load will become:

$$W = \frac{\pi p_r (R_2^2 - R_1^2)}{2\ln(\frac{R_2}{R_1})} \tag{2.15}$$

2.2. Fluorescence

In this section, fluorescence will be explained. Furthermore, derivation of the fluorescence principle will be used to obtain valid equations which will give the relation between film thickness and fluorescence.

2.2.1. How does fluorescence work

Fluorescence dye which can be dissolved in liquids can absorb light of one wavelength and re-emit light of a higher wavelength. This fluorescence process has three stages [12]. These three stages are schematically shown in figure 2.5

- *Excitation*: An external energy source supplies a photon that is absorbed by the fluorescent dye. The fluorescent dye, which initially is in ground state (S_0), then is excited by this photon to an electronic singlet state (S_1).
- *Excited-state lifetime*: The time of which the molecule normally exists in such a state is between 1 and 10 ns. In this time the molecule undergoes a change due to its environment. By dissipation of energy, the molecule goes into a relaxed electronic singlet state (S_2). This new state is from a lower energy level than its first excited state. from this new state it will start emitting. There are also other means by which the molecule returns to its ground state, such as coalitional quenching, fluorescence energy transfer and intersystem crossing. The quantum yielding is a property of the fluorescent dye, which is the ratio of photons absorbed and photons emitted, which give a relative level of these processes.
- *Fluorescence emission*: In this stage the molecule emits a photon of its energy level. This energy level is lower due to the dissipation of energy in the previous state. Therefore the photon has a higher wavelength. This difference in wavelength is called a stoke shift and is the main property of the fluorescent dye.

The excitation and emission wavelengths of these fluorescent dyes, as well as the intensities, are determined by their chemical structures. These emission absorption spectra, as what they are called, define the properties of the fluorescent dye. Such dyes can be dissolved in liquids and the fluorescence can be measured at low concentrations [22]. An example of such an emission absorption spectrum is given in figure 2.6. You can clearly see the stoke shift of this dye. The fluorescent dye in this example is Rhodamine B and has a shift from 545 nm to 575 nm.

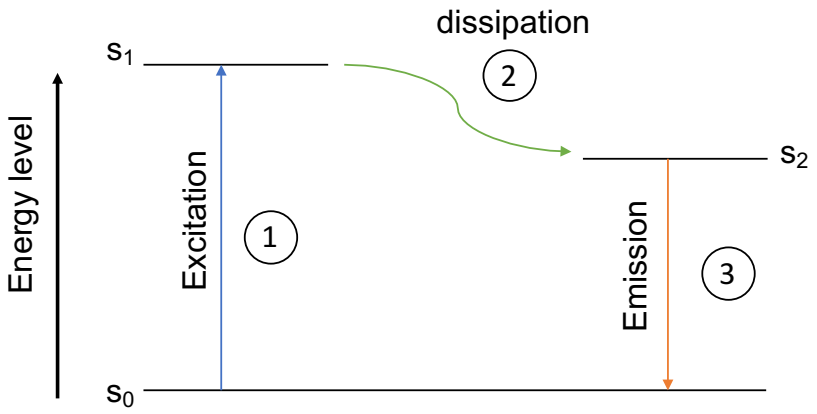

Figure 2.5: schematic overview of the three stages of fluorescence.

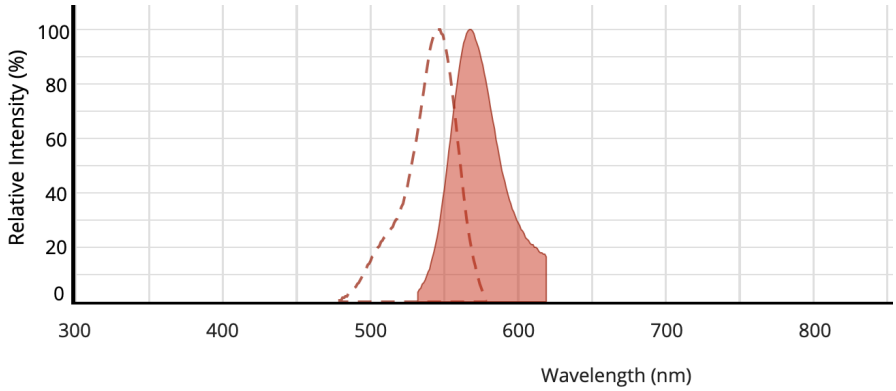

Figure 2.6: An emission absorption spectrum of Rhodamine B, where the dashed line is the absorption wavelength (545 nm) and the coloured line the emission wavelength (575 nm)

[1]

2.2.2. Fluorescence theory

The basic fundamentals of fluorescence are described in the previous section. These fundamental can be put into equations and are described in this section. With these equation measurement can be performed resulting in film heights [7].

We consider a rectangular differential volume of fluid properly mixed with a fluorescent dye and cross-section A, schematically shown in figure 2.7. The fluorescence, F, emitted by this differential volume when excited by a uniform intensity I_{inc} is given by

$$F = I_{\text{inc}} \epsilon_{\lambda_{\text{inc}}} C \phi \mathrm{d}V \tag{2.16}$$

where:

- I_{inc} is the incident light cast upon the differential element with intensity I.
- $\epsilon_{\lambda_{\text{inc}}}$ is the molar absorption (extinction coefficient) at the incident light wavelength, that determines the amount of incident light intensity is being absorbed.
- C is the concentration of the fluorescent dye in to the fluid.
- ϕ is the quantum efficiency. This determines how much of the absorbed energy is being converted to fluorescent energy.
- dV is the differential volume element, this is the control volume over which fluorescence takes place.

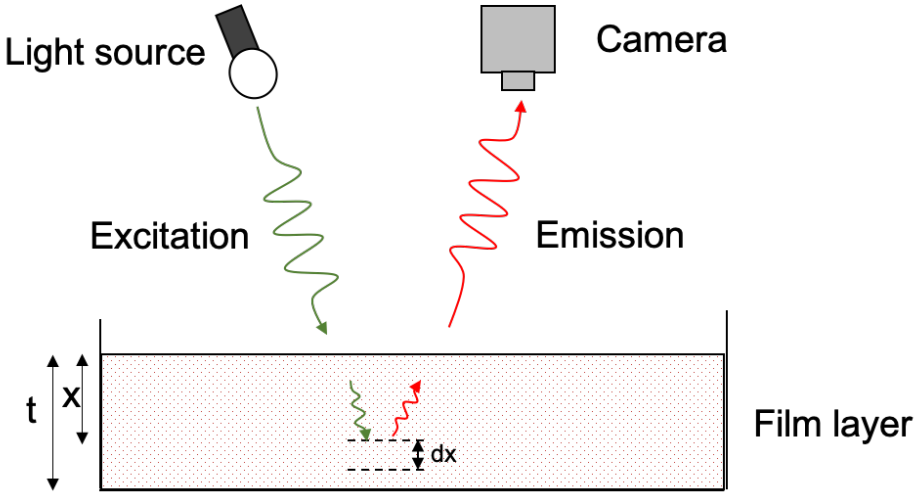

Figure 2.7: Schematically shown how fluorescence works on a differential element dx.

Because the length of the volume element is infinitely small we can divide equation 2.16 by area A, that results in

$$I_{\mathrm{f}} = I_{\mathrm{inc}} \epsilon_{\lambda_{\mathrm{inc}}} C \phi \mathrm{d}x \tag{2.17}$$

Where I_f is the intensity of the fluorescence normal to area A. In this equation it is assumed that the incident light intensity is constant through the fluid, this is valid for thin films. A more accurate representation of the fluorescence equation can be obtained if the Lambert-Beer law [24] is implemented for the excitation intensity. The Lambert-Beer Law takes into account the absorption of light intensity when going through a finite fluid.

$$I_{\mathrm{e}}(x) = I_{\mathrm{inc}} e^{-\epsilon(\lambda) C x} \tag{2.18}$$

If we consider the differential element shown in figure 2.7. The fluorescent intensity becomes:

$$\mathrm{d}I_{\mathrm{f}} = I_{\mathrm{e}}(x) \epsilon_{\lambda} C \phi \mathrm{d}x \tag{2.19}$$

This means for a given fluid thickness t, the total intensity emitted by the fluorescent fluid is:

$$\begin{aligned} I_{\mathrm{f}} = \int_0^t \mathrm{d}I_f = \int_0^t I_{\mathrm{e}}(x) \epsilon_{\lambda} C \phi \mathrm{d}x = \\ \int_0^t I_{\mathrm{inc}} e^{-\epsilon_{\lambda} C x} \epsilon(\lambda) C \phi \mathrm{d}x \end{aligned} \tag{2.20}$$

Which results in:

$$I_{\mathrm{f}}(t) = I_{\mathrm{inc}} \phi [1 - e^{-\epsilon_{\lambda} C t}] \tag{2.21}$$

For small values of t a Taylor expansion can be used resulting in

$$I_{\mathrm{f}}(t) = I_{\mathrm{inc}} \phi \epsilon_{\lambda} C t \tag{2.22}$$

This means the relation between the fluorescence intensity and the incident light intensity becomes linear. This relation is also called optically thin. The relation is called optically thick when the relation between I_{f} and I_{inc} is exponential. What is thick or thin depends on the product of $\epsilon_{\lambda} C$.

3

Design of an experimental setup

In order to validate the model and compare it to measured results a design of an experimental setup is needed. This is done in two different setups. The first setup has been made to validate the fluorescent measurement method, where the bearing itself is a non deforming bearing and the recess height is known. This first setup has the advantage that it is easy to handle and to implement the proper settings. Furthermore, it only uses gravity to give a load to the bearing. This load depends on the weight of the bearing and the manifold. The second experimental setup will be larger and force regulated. Then, after the validation of the fluorescent measurement technique, the setup will be used to test a deformable hydrostatic bearing which is used to test two load cases.

3.1. Setup A

3.1.1. Analytical design

For this setup a hydrostatic bearing is designed which has a diameter of 60 mm and a recess diameter of 20 mm. From these dimensions and the load that is going to be applied, the recess pressure can be determined. In setup A no external force is applied, so the load comes from the weight of the bearing and the manifold. Both have been weighted and found was that they deliver a force of 12 N. A force derived from the pressure can be determined as follows:

$$F = \int_A p_\mathrm{r} \mathrm{d}A \tag{3.1}$$

This equation, as derived in the previous section, can be described as follows:

$$F = \frac{\pi p_\mathrm{r}(R_2^2 - R_1^2)}{2\ln(\frac{R_2}{R_1})} \tag{3.2}$$

By rewriting this equation the recess pressure becomes the unknown and can be solved from this equation. This means that for a load (F) of 12 N, the supply pressure is $p_\mathrm{r} = 10491$ Pa. Now that we have the recess pressure required to carry the load, we can calculate the flow rate of the bearing. This flow rate as explained in the previous chapter, equation 2.6 depends on the film height and on the recess pressure. A film height (h) commonly used in literature is 100 micrometer [26]. This results in a flow rate of $Q = 5.62 \cdot 10^{-6} \frac{\mathrm{m}^3}{\mathrm{s}} = 0.34 \frac{\mathrm{L}}{\mathrm{min}}$. This flow rate can be used to determine a restrictor. As explained in the previous section, due to continuity, the flow must be equal through the restrictor and through the thin film. To determine a restrictor also a waterpump must be used. A membrame pump has been used which can deliver a flow rate of 4.3 L/m and can apply a pressure of 2.4 bar. This amount of pressure is too high for this setup, so a pressure reducing valve is used to bring the pressure back from 2.4 bar to 0.5 bar. With 0.5 bar of supply pressure the restrictor can be determined. For the restrictor an orifice restrictor is used. This orifice restrictor is chosen because it is very easy to implement in the design, but the disadvantage is that the discharge coefficient is not easily predicted. Therefore an additional measurement needs to be carried out. To determine the actual discharge coefficient, a laser sensor measurement has been performed determining the film height by different supply pressures. The analytical film height and supply pressure can be fitted to the measured one by varying the discharge

coefficient. Using equation 2.10 a figure can be plotted with a variable discharge coefficient. Before this can be done, an initial value for the discharge coefficient needs to be determined as well as a orifice diameter. A common discharge value is found to be 0.6 [28]. With this initial discharge coefficient a diameter(d_o) for the orifice can be determined, this was found to be 1.2 mm. Figure 3.1 gives the measured results plotted with the analytical film height with a discharge coefficient of 0.65. Using a coefficient of 0.65 could fit the measured film height and pressure figure sufficient.

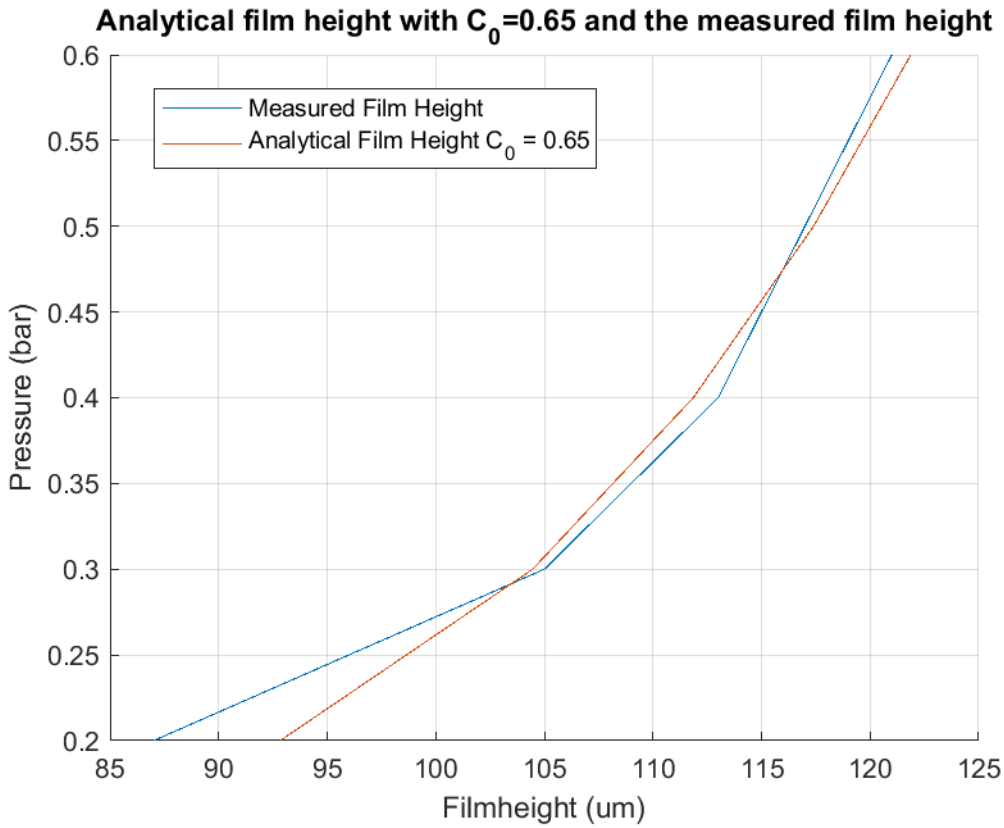

Figure 3.1: Determining the discharge coefficient by comparing measured results with a analytical approximation

In table 3.1 a summary of all the used variables is given:

Variable	Value
h	100μm
W	12 N
p_r	10491 Pa
p_s	50000 Pa
Q	$5.62 \cdot 10^{-6} \frac{m^3}{s}$
d_o	1.2 mm

Table 3.1: Design variables

3.1.2. Hydraulic scheme

To further design the experimental setup a hydraulic scheme was made. This hydraulic scheme gives a clear overview of what is going on, shown in figure 3.2. In this scheme an overflow valve is implemented to regulate the the pressure difference and to maintain a constant pressure. Furthermore, a pressure reducing valve is installed to regulate the supply pressure going into the restrictor and the bearing.

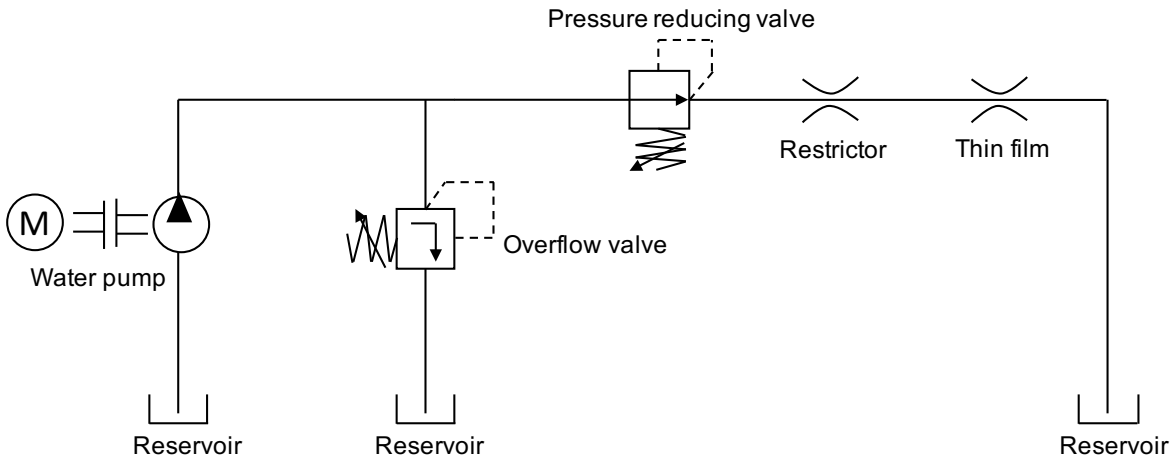

Figure 3.2: Hydraulic scheme of the experimental setup

3.1.3. Bearing and Frame Design

In figure 3.3 a cross-section is given of the hydrostatic bearing used in setup A. In this design both the manifold and the bearing are made from aluminum. To first validate the measuring method a stiff material such has aluminum is used because we would like a non-deformable surface. This non-deformable surface accomodates the use of a laser sensor in order to determine the film height. Thereafter a comparison with the fluorescent measuring method is made. The gasket is made from rubber, in order to make the bearing watertight. The orifice restrictor has been made of PMMA, by using a laser-cutting machine the exact dimensions could be applied. The frame of the setup has been made by using Thorlabs newton profiles. The sensing equipment and the bearing itself could easily be attached to this frame. The tray was made from PMMA, resulting in a transparent plate. To suspend the bearing but also guarantees it stays in the same position, a flexure has been used. This flexure is nothing more than a polycarbonate plate which is connected to the bearing. This plate is very flexible and therefore has a very low stiffness in the z-direction and rotationally, but has a very high stiffness in the xy-plane. This means it can freely move up, down and rotate but keeps its position in its plane. Figure 3.4 give an overview of the setup used (left) and a schematically drawn setup (right). The camera was placed 210 mm beneath the bearing surface and the LED was placed on the same height as the camera but with a distance of 120 mm. During a measurement the setup will be cover with a black cloth in order to minimize the influence of external light.

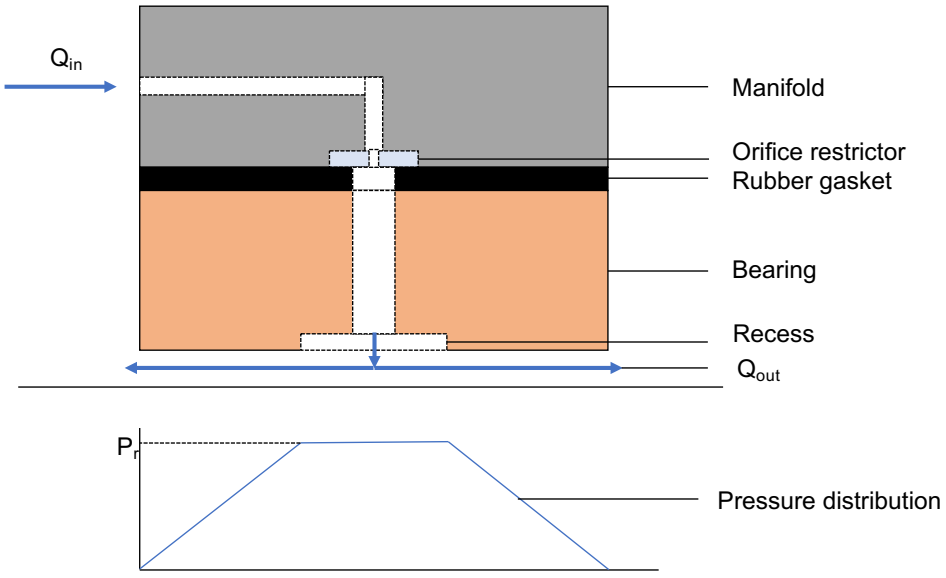

Figure 3.3: Schematic overview cross-section of a hydrostatic bearing design

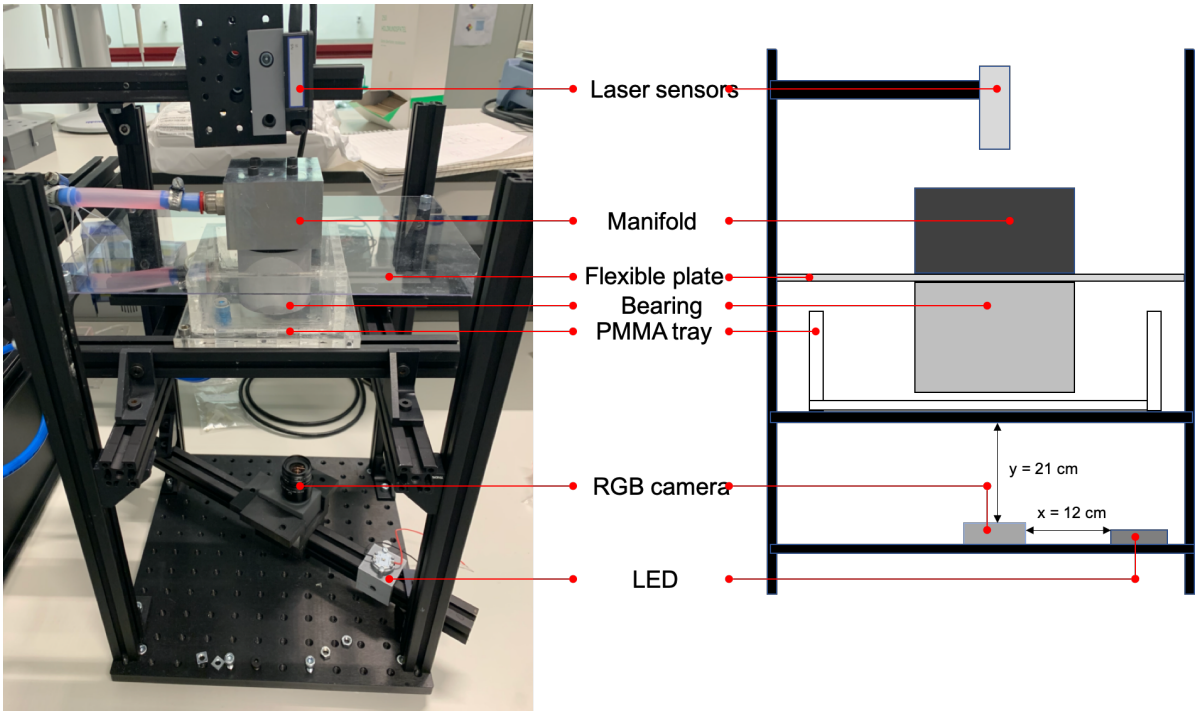

Figure 3.4: (Right)Schematic overview of setup A and (Left) the actual setup

3.2. Setup B

To implement the measurement method using a compliant hydrostatic bearing, some adaptation needed to be done. Multiple load cases will be used and therefore it becomes useful to add a force actuator. A pneumatic cylinder has been chosen as force actuator. The pneumatic cylinder has been connected to the frame by a 3D printed holder piece. This force actuator needs to be connected to the manifold and bearing, therefore a coupling has been designed in a way that it facilitates the force to the bearing. Furthermore, a new manifold is designed such that it is able to connect the bearing to it as well as the coupling piece. Moreover, the setup has been rotated 90 degrees such that the alignment is horizontal. This still guarantees a full film and therefore should not affect the measurement. Figure 3.5 shows the schematically setup and Figure 3.6 shows the actual setup. The camera is placed at the side of the setup, with a connector piece for the LED in order to guarantee the distance between the camera and the LED is the same. In Setup A the alignment of the bearing was accomplished by self-alignment due to the nature of the flexure. Because the bearing is now being actuated by the pneumatic cylinder, some sort of alignment needs to be done. The frame to which the tray is connected to is able to be adjusted such that the bearing and the tray will be aligned. This method would not have been precise enough if a rigid bearing was used, but due to the compliance of this flexible bearing it will self-align, creating an even distributed film height. During a measurement the setup will be placed in a large black box. This light proof box will exclude all external light guaranteeing a proper measurement. Figure 3.7 shows the setup with the LED turned on and placed in the box.

3.2.1. Bearing design

The design of a compliant hydrostatic bearing is done with silicon rubber and a mold. The silicon has a white color such that it reflects the incident light. To make sure the light is reflected diffusely the mold counter surface has been finely sanded such that it creates a fine roughness on the surface bearing. To connect the bearing to the setup, an aluminum piece is placed on top of the mold when the silicon is still liquid resulting in when it is hardened the aluminum piece is form enclosed to the silicon rubber. Figure 3.9b shows a cross section of the bearing. The Young's modulus is required to obtain the analytical deformation of the compliant bearing. Because greater forces will be applied than with setup A, a larger diameter of the bearing is chosen. This diameter will be 80 mm. The undeformed compliant bearing does not contain a pocket, this is because the effect of pocket forming will occur when applying higher loads.
To obtain the Young's modulus of the silicon rubber a tensile test has been performed. Three test pieces

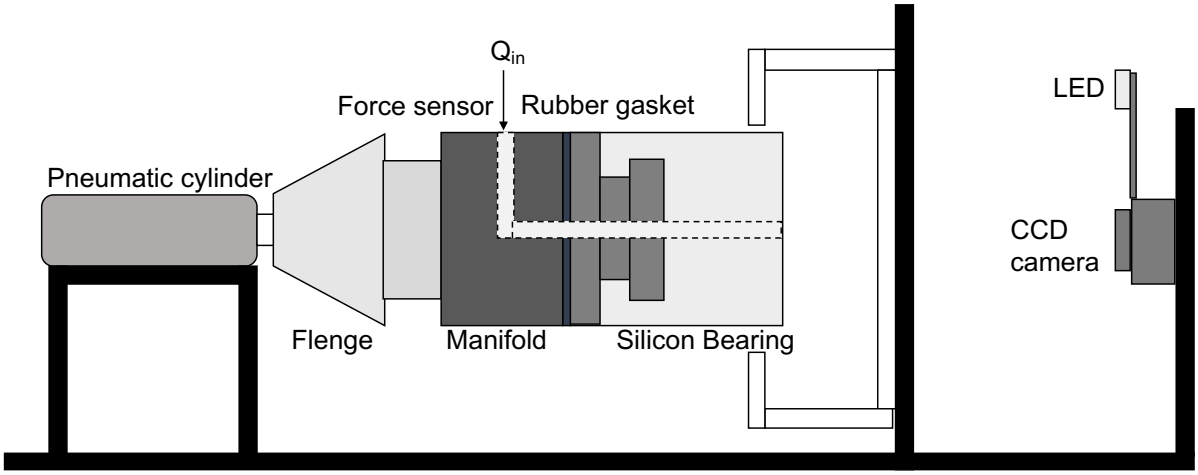

Figure 3.5: schematically overview of measurement setup B

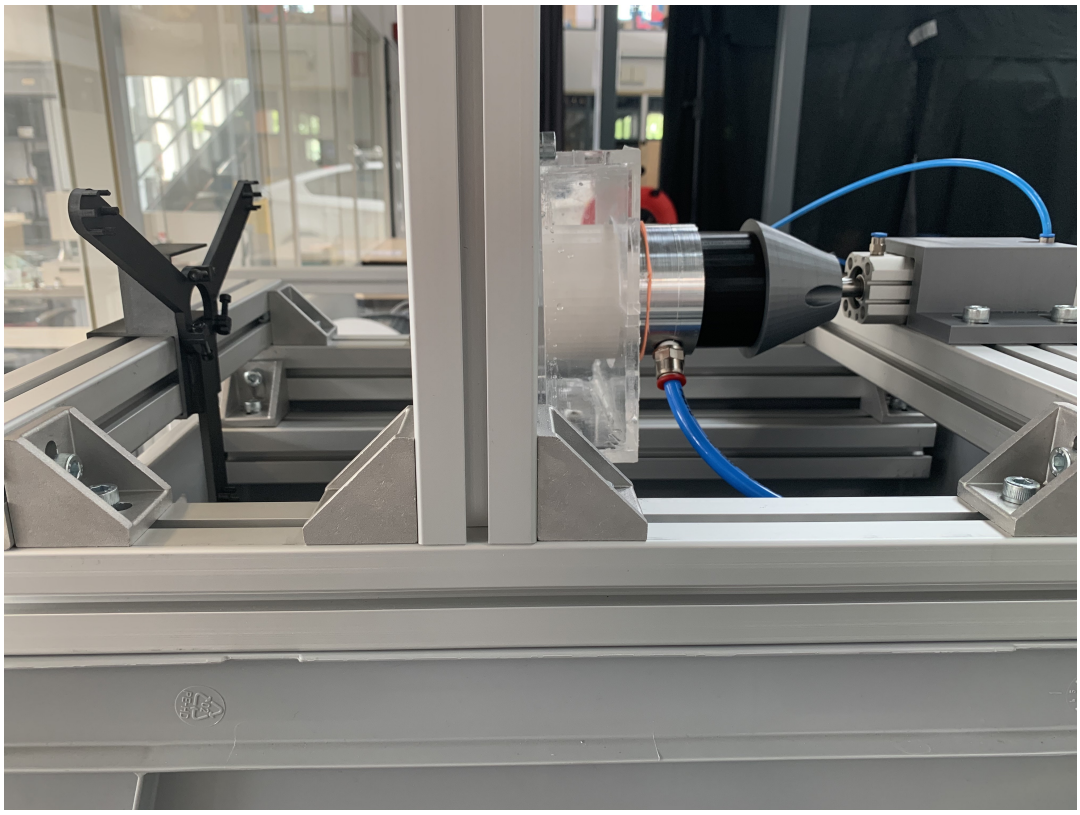

Figure 3.6: Side view of setup B

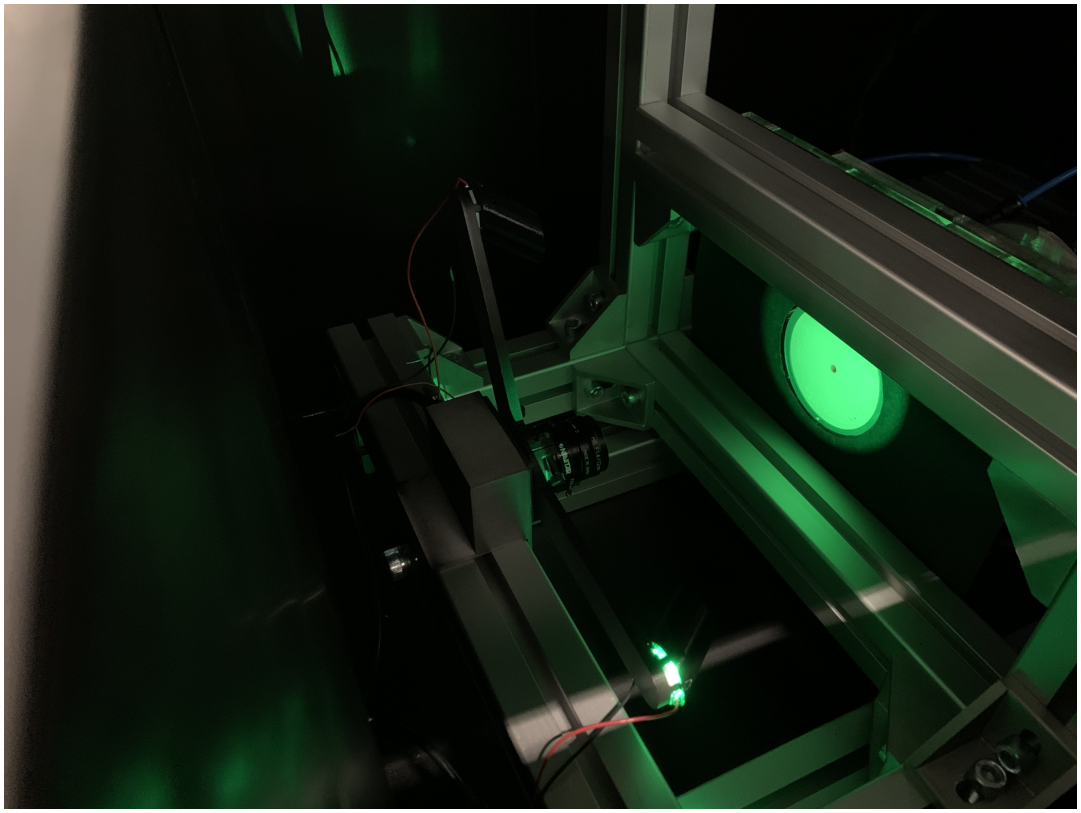

Figure 3.7: Measurement with LED shined upon the compliant hydrostatic bearing

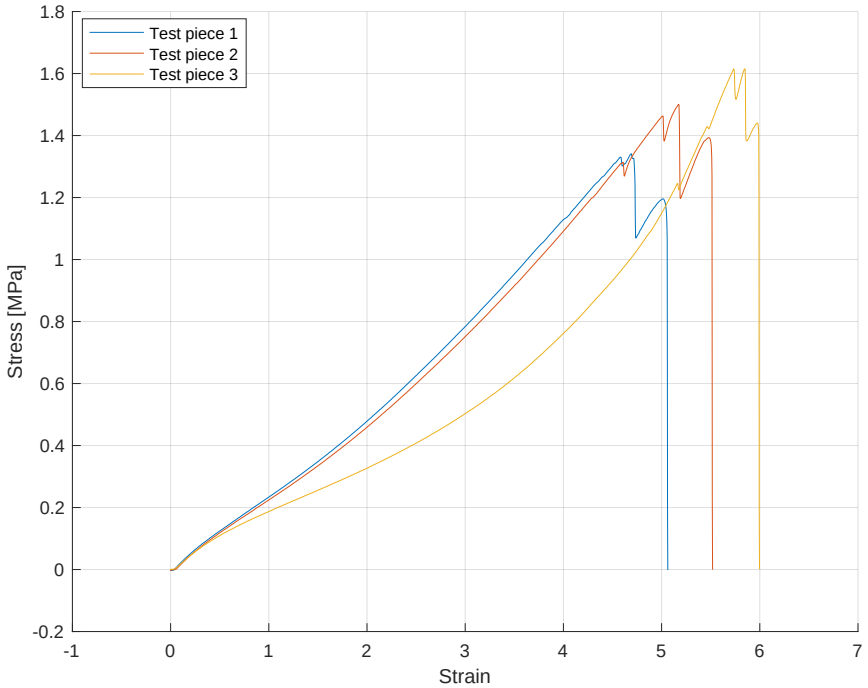

Figure 3.8: Stress/strain curve for three test dogbones of silicon rubber.

were obtained by casting the silicon into a dogbone mold, see Figure 3.9a. These pieces were tested and a force/displacement diagram was obtained. This force/displacement was, by using the dimensions of the

dogbone, redefined to a stress/strain curve. Figure 3.8 shows the stress/strain curve obtained. The Young's modulus can be determined as follows:

$$E = \frac{\Delta\sigma}{\Delta\epsilon} \tag{3.3}$$

This resulted in a Young's modulus of 0.3 MPa and this value is used in the deformations analyses in a later chapter.

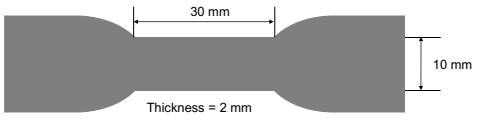

(a) Dogbone and its dimension used in the tensile test

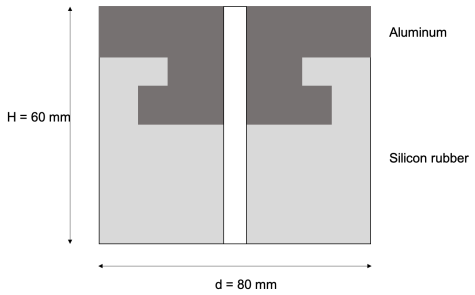

(b) Cross section of the compliant hydrostatic bearing

Figure 3.9: Dogbone dimensions the bearing mold design

3.2.2. Restrictor

With this setup, multiple and higher loads are applied. Therefore a higher supply pressure needs to be used to maintain a measurable film height. The supply pressure used for this setup will be 0.8 bar. Besides increasing the supply pressure, the restrictor has been altered as well. For this setup it is chosen to take a capillary restrictor instead of a orifice restrictor. The reason this is chosen is because the orifice restrictor needs a discharge coefficient determination. A capillary restrictor is easier to determine by applying different pressures and measuring the flow. In figure 3.10b is the measured flow plotted against the pressure difference. For the restrictor dimension, there has been chosen for a diameter of 1.3 mm and a length of 25 mm, shown in figure 3.10a. If the restrictor equations are being used a resistance of this bearing is: $R_{\text{restrictor}} = \frac{\pi d^4}{128\mu l_c} = 3.1 \cdot 10^{-9}$. However, when determining the resistance value by measuring the flow rate and the pressure a different outcome is the result. This results in $R_{\text{measured}} = \frac{\Delta Q}{\Delta P} = 9.3 \cdot 10^{-11}$. This differs a lot and a possible reason for this difference can be the due to the capillary length. This length is perhaps to small and therefore turbulent flow arises resulting in a lower resistance value. The resistance value determined by the measurement will be used in chapter 6 in the finite element analysis of the bearing deformation.

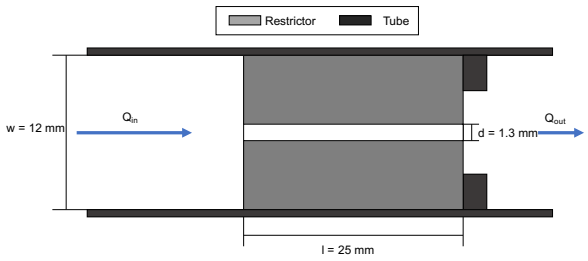

(a) Capillary restrictor inside a tube with its dimensions

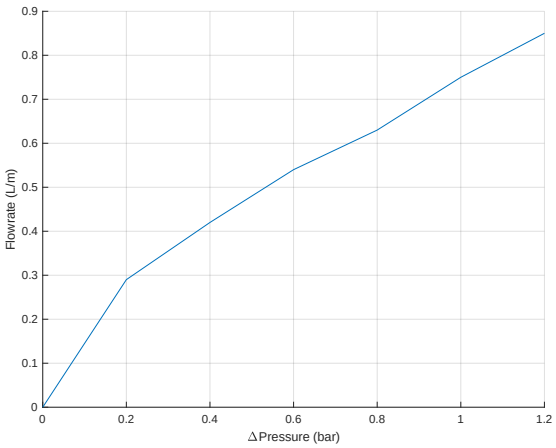

(b) Measured flow plotted against the pressure difference

Figure 3.10: Design of the capillary restrictor and the measured flow

3.2.3. Analytical Deformations FEM

To compare the analytical FEM model of a compliant hydrostatic bearing COMSOL Multiphysics is used. Within COMSOL the flow equations are implemented and thus the pressure profiles and film heights are calculated. The pressure profile is then applied to the surface of the bearing and with solid mechanics the deformations are determined. Then, after the deformations a new pressure profile is determined. This iterates to a film height profile. These deformations and film heights can be determined for multiple external loads. In this thesis there has been looked at 4 load cases: 50 N,75 N,100 N,150 N. Chapter 6 will further elaborate on this.

4

Paper: Design of a fluorescent measurement system for compliant hydrostatic bearings

Design of a fluorescent measurement system for compliant hydrostatic bearings

Sebas Siers, Joep Nijssen, Ron van Ostayen
Departement of Precision and Microsystems Engineering
Delft University of Technology
Mekelweg 2, 2628CD, Delft, the Netherlands

September 15, 2020

Abstract

A LED induced fluorescent technique based test setup is introduced , which is used to measure the water film thickness of compliant hydrostatic bearings. Fluorescent particles have the characteristic of absorbing light of a certain wavelength and emitting light of a higher wavelength. A LED with a wavelength of 540 nm (green light) is used to excite the Rhodamine B fluorescent particles, which have a excitation wavelength of 545 nm. The emission wavelength of the particles is 570 nm (red light) and this colour shift is captured by a RGB colour camera where the red and green channels have been used as an optical filter. The increase of intensity due to the excitation of the thin film can be coupled to the thickness of the film. The performance of the technique is validated by comparing the film height to a laser sensor measured film height for a rigid bearing containing features with known dimensions. A film thickness measurement technique is presented that is able to measure 15-1400 μm and an average accuracy of 6.4% is achieved.

Index Terms **– Deformable hydrostatic bearings, Fluorescence technique, Film thickness measurement**

1 Introduction

A hydrostatic bearing is a bearing type where the friction is reduced by creating a thin film of liquid between a bearing and its counter surface. These types of bearings are typically highly reliable and have very high performance capabilities. An example of such a bearing is shown in figure 1.A
The main limitation of this type of bearing is that they are highly dependent on the shape and smoothness of the running track surface. This means they only work properly when the running track is flat or has a constant curvature. Improvements to these bearing systems can therefore be made by reducing the dependency to the geometry and smoothness of the running track. A method of achieving this is through the use of a compliant hydrostatic bearings [1]. An embodiment of such a bearing is by using elastic materials for the bearing support as seen in figure 1.B. Such bearings will be able to follow the imperfections of the running track, whilst maintaining a sufficient film of liquid between the surfaces. These type of bearings could be implemented in a wide variety of applications, such as axial and radial water pumps [2] [3], cutting and milling tools or stadion rooftops.

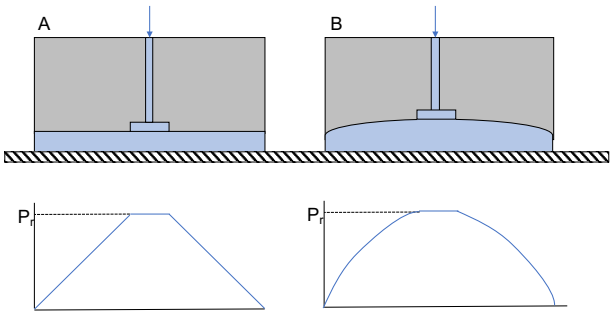

Fig. 1: (A.Left) A classic hydrostatic bearing (B.right) A compliant hydrostatic bearing, both with corresponding pressure profile over the bearing surface

A common performance parameter for hydrostatic bearings is their load capacity and the resulting film height [4]. Therefore it is useful to map these parameters and use them to compare different bearings. Inherently, load can be measured with relative ease through the use of force sensors. However, determining the film height for compliant hydrostatic bearings is a more complex issue. Classic hydrostatic bearings are considered rigid and

the film height considered constant over the surface. This means the film height can be determined by defining a set of points, while taking tilt of the bearing in consideration. For the compliant embodiment this obviously does not apply, since the film height will not be constant due to elastic deformation. Because film height and its corresponding pressure profile are not easily predicted, it is desired to obtain the film height by measurement. The whole bearing surface is desired to be known and therefore this is a key criterium for a measurement method.
In literature various methods can be found that measure thin films. Methods like magnetic reluctance [5], capacitance [6] [7], ultrasound [8] [9] or light of internal reflection [10]. However, these methods are either limited by their resolution or having the disadvantage to only measure discrete points. A different method such as optical interferometry [11] [12] has the proper resolution but is limited by its area of measurement. This method is expensive, hard to implement and requires a scanning motion. Therefore it is not suitable for compliant bearing measurements. Other methods such as dye attenuation [13] [14] and fluorescence [15] have the ability to make a 2D map of the film height with a sufficient resolution to obtain the deformation of an elasto-hydrostatic bearing. Both these methods use a colour shift to obtain the film height, but the dye attenuation method needs some adaptations to measure the colour shift. In terms of general use, a method is desired that is non intrusive and does not need adaptations to the bearing itself. Fluorescence based methods have seen to show great potential. Beside the ability to measure the film height, fluorescence can also provide information about the lubricant behaviour [16]. A fluorescence method to obtain a the thickness of a thin oil film has been successfully used[17]. However, his research made use of a air-oil-wall configuration. Because the nature of hydrostatic bearings, this configuration needs to be adjusted for feasibility and therefore not directly suitable. Such a measurement system has been implemented for elasto-hydrodynamic-lubricating bearings[18], where a transparent plate-water-wall configuration has been used. In his work, a fluorescence measurement method was researched for small (0-20 μm) film heights and a region of interest of 40x40 mm^2, where only the fluorescent emission wavelength used to determine the film height was investigated. This is in general not sufficient for compliant hydrostatic bearings, where significantly larger deformations are expected in relation to the bearing dimensions [2]. In this work, an adjusted method based on the work presented in [17] is implemented in a setup, which is able to measure significantly larger film heights (50 - 1000 μm) and larger regions of interest (80x80 mm^2).

2 Methods

The basic fundamentals of fluorescence are as follows [19]: When a fluid, containing a fluorescent dye, is excited by an external light source with a certain wavelength λ_1, the excitation energy of this external light source will bring the fluorescent molecules into an excited state. The molecules will be in this state for a certain amount of time (ns) in which they will dissipate some of its energy. When returning to the ground state, the energy level has been reduced and therefore will emit light of a higher wavelength λ_2. This change in absorption and emission wavelength is called a stoke shift.

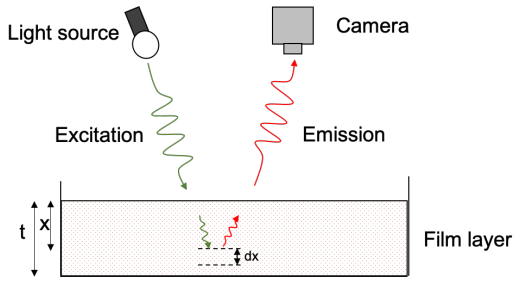

Fig. 2: Schematically shown how fluorescence works on a differential element dx.

We consider a rectangular differential volume of fluid properly mixed with a fluorescent dye and cross-section A, schematically shown in figure 2. The fluorescence, F, emitted by this differential volume when excited by a uniform intensity I_{inc} is given by:

$$F = I_{\text{inc}} \epsilon_{\lambda_{\text{inc}}} C \phi \mathrm{d}V \tag{1}$$

where:

- I_{inc} is the incident light cast upon the differential element with intensity I.
- $\epsilon_{\lambda_{\text{inc}}}$ is the molar absorption (extinction coefficient) at the incident light wavelength, that determines the amount of incident light intensity is being absorbed.
- C is the concentration of the fluorescent dye in to the fluid.
- ϕ is the quantum efficiency. This determines how much of the absorbed energy is being converted to fluorescent energy.
- $\mathrm{d}V$ is the differential volume element, this is the control volume over which fluorescence takes place.

Because the length of the volume element is infinitely small we can divide equation 1 by area A, resulting in:

$$I_{\mathrm{f}} = I_{\mathrm{inc}} \epsilon_{\lambda_{\mathrm{inc}}} C \phi \mathrm{d}x \tag{2}$$

Where I_{f} is the intensity of the fluorescence normal to area A. In this equation it is assumed that the incident light intensity is constant through the fluid, this is valid for thin films. By integrating this equation this results in:

$$I_f = \int_0^t \mathrm{d}I_f = \int_0^t I_{\mathrm{inc}} \epsilon_\lambda C \phi \mathrm{d}x = I_f(t) = I_{\mathrm{inc}} \phi \epsilon_\lambda C t \tag{3}$$

This means the relation between the fluorescence intensity and the incident light intensity is linear. Therefore, the thickness can be determined by the ratio of I_{inc} and I_{fl}.

2.1 A ratioed image technique

The measurement method in this work is primarily based on the work of Husen (2018)[17]. Husen implemented fluorescence to determine the thickness of a fluid when there is only liquid-wall interaction, see Figure 3. He states that the film thickness is proportional to the ratio of I_{inc} and I_{f}.

$$h \propto \frac{I_{\mathrm{f}}}{I_{\mathrm{inc}}} \tag{4}$$

Where h is the film thickness, I_{f} is the intensity of the emitted fluorescence and I_{inc} is the intensity of the incident light which has another wavelength. For these two different wavelengths it should apply that $\lambda_{\mathrm{inc}} < \lambda_{\mathrm{f}}$. This ratio($R$) is only valid when the liquid can be seen as an optically thin liquid, meaning that R behaves linearly to h. To make use of this ratio, multiple images need to be taken and processed:

$$R = \frac{E_{\lambda_{\mathrm{fl}}} - D}{E_{\lambda_{\mathrm{inc}}} - D} - R_{h=0} \tag{5}$$

Where $E_{\lambda_{\mathrm{f}}}$ and $E_{\lambda_{\mathrm{inc}}}$ are the images containing the fluorescent intensity and the incident light intensity, respectively. These images can be obtained using a RGB camera can be used where the R,G,B-channels can be used as a filter. The advantage of a RGB camera is that the E_{λ_f} and $E_{\lambda_{inc}}$ can be obtained simultaneously. D is the baseline image where a lenscap is placed on the lens to make sure the background noise of the camera sensor will not affect the measurement. Finally, $R_{h=0}$ is the ratio of the two images when there is no liquid present. To address the leakage of the incident light through the λ_{fl}-filter, the $R_{h=0}$ will have to be subtracted. Only the increase of fluorescent intensity relative to the incident light is measured. From this ratio the film thickness can be achieved.

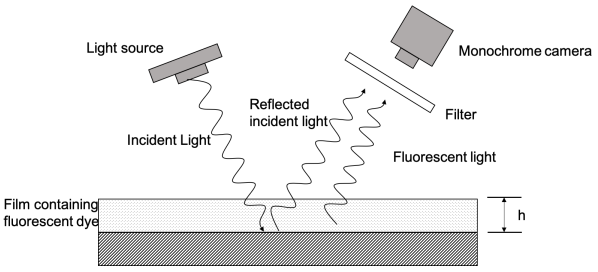

Fig. 3: Approach of a fluorescent measurement method used by [17].

$$h = aR \tag{6}$$

Here a is a scaling constant to determine the actual film height. This constant is dependent on the concentration of the fluorescent dye, the quantum efficiency of the dye, the lambertian surface and the reflectance of the multiple interfaces. Determining a can be difficult because the parameters that make up a are hard to specify, such as the reflectance of the lambertian surface or the exact quantum efficiency. In order to obtain a for the setup this scaling factor will be determined by calibration. This way the actual film height will be measured and R is also known, therefore a can be obtained.

2.2 Setup approach

In order to adjust the principle Husen presented in a way that it can be used to measure hydrostatic bearings a new interface has to be introduced. Changing the bearing to obtain desired optical properties is undesirable from a design standpoint, since the bearing is the designed machine component, the running track is therefore further investigated.

By making the running track transparent, the proposed method remains relevant while the required images can be made. The proposed configuration can be seen in Figure 4a. The introduction of this transparent plate creates and additional interface for the incident light source to be reflected on. In this work this plate is assumed to be smooth and perfectly flat. Furthermore, the effect the plate has on the light properties will be canceled out. The reason for this is because both the incident light and the fluorescent light decrease in intensity due to the partly reflecting of the light. The percentage of the light that is being transmitted is for both the same. In the method for determining the film height a ratio is taken, resulting in a factor that is canceled out. Figure 4a gives a schematic overview of the method proposed in this paper.

To obtain a reliable measurement system that can be used for compliant bearings, the choice was made

to divide the development into two setups. Setup A will have a constant mass and will make use of a rigid bearing with cavities of which the dimensions are known. This setup will be used to do initial experiments to obtain the specifications such as accuracy and resolution of the measurement method, while having minimal additional affects such as deformation that could influence determining the specifications. Also setup A is useful to obtain the best camera settings. Setup B will be used for a compliant hydrostatic bearing where multiple load conditions can be applied through the use of a pneumatic cylinder. Figure 4 will give a schematic overview of the two design approaches. Furthermore, the final adaptions made to [17] is the use of water instead of oil as operating fluid. From the perspective of applications such as gate-locks [1] and water pumps, the use of water becomes necessary. The use of water will have no implications on the method presented by [17]. It does have an effect on the embodiment of the test setup, because a water solvable fluorescent dye needs to be used. This will influence the spectral sensitivity that is needed to be observed.

2.3 Setup A

Figure 5 shows measurement setup A. The bearing is suspended by a flexible plate and also connected to the manifold. The flexible plate has a stiffness in-plane, such that the bearing will stay in the same position, but has low rotational stiffness and low out-of-plane stiffness. The only force applied to the hydrostatic bearing comes from the weight of the manifold and the bearing itself, being equal to F = 12N. Additionally, a laser sensor is added to measure the film height and underneath the transparent plate a LED and a CCD camera are placed. For the measurement only one LED is used, this is placed a 120 mm from the camera. This distance is based on the specular reflection not influencing the measurement. During the measurement the setup will be placed in a completely dark environment, preventing external light from influencing the measurement.

The hydrostatic bearing used in this setup is made of aluminum and has a diameter of 60 mm. The bearing is designed with a recess, with a diameter of 20 mm and a depth of 400 μm. The bearing also contains four features with dimension of 10x10 mm^2, shown in Figure 6. These features have four different depths that are originally designed to be 100 μm, 200 μm, 300 μm and 400 μm in depth respectively. These different features are used to check the range of the measurement method as well as the resolution. Using a Bruker ContourGT-K white light interferometer the actual depth of the feature and the recess is determined after applying a layer of matt white paint so the reflection of the bearing surface is diffuse. This layer of paint is important to get an even distribution of light along the bearing surface and therefore a clear fluorescent signal. The realized depths are 95 μm, 165 μm, 270 μm and 330 μm respectively, and the recess depth is determined to be 355 μm.

For this setup multiple sensing devices are used. A MEL Mikroelectronic M7L/0.5 laser displacement sensor is used to measure the actual film height and the tilt of the bearing. This laser displacement sensor has an operating range of 500 μm and a resolution of 0.2 μm. One laser sensor is placed above the bearing and on three different places a measurement is done so the actual height and tilt can be measured. The camera used is a Pixelink PL-D795. This camera contains a SONY IMX264 camera sensor, with the spectra response for the indiviual RGB-channels shown in Figure 7. Furthermore, The LED used is a LUXEON-C circular LED that has a dominant wavelength of 535 nm.

An important criterium for the measurement is the fluorescent dye and its concentration. In this work Rhodamine B is chosen as dye. This is chosen because it is solvable in water and has a stoke shift that is measurable by the CCD camera, such that the channels red and green can be used as filter, see Figure 7. The properties of Rhodamine B are that it has an excitation wavelength of 540 nm and an emission wavelength of 570 nm. To obtain a useable result, the concentration of the fluorescent dye needs to be chosen properly. In equation 2 the incident light is assumed constant. A more accurate representation of the fluorescence equation can be obtained if the Lambert-Beer law [20] is implemented for the excitation intensity. The Lambert-Beer Law takes into account the absorption of light intensity when going through a finite fluid.

$$I_e(x) = I_{inc} e^{-\epsilon(\lambda) C x} \tag{7}$$

The intensity of the reflected light beam can be approximated by a Taylor expansion resulting in $I_{\text{refl}} = I_{\text{inc}} C \epsilon h + I_{\text{inc}}$. According to Husen(2017) [21] the first term of this linearization can be neglected if it is of an order 10^{-3}, defined by variable A.

$$A = C \epsilon x \tag{8}$$

where A is the absorption, C is the concentration, ϵ is the absorption coefficient of the fluorescent dye and x is the distance the light travels. The absorption coefficient of Rhodamine B at the wavelength of the light source (535 nm) is $1.08 \cdot 10^5$ Lmol^{-1}cm^{-1}. The distance the light will travel is up to 600 μm. The concentration of Rhodamine B

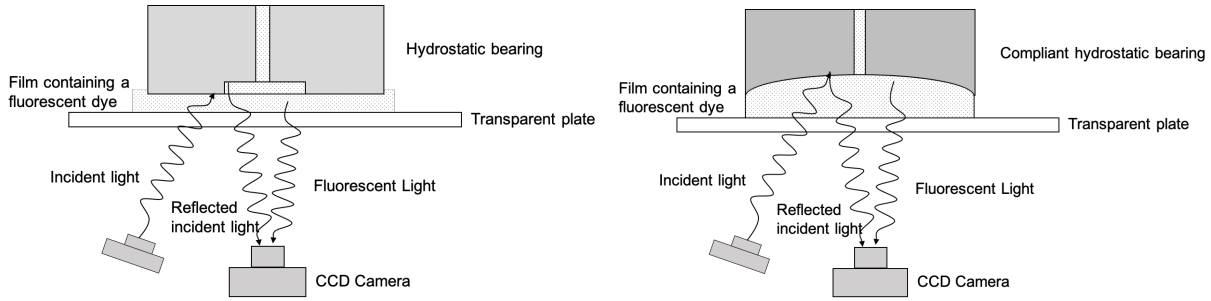

(a) Setup A, where a classic hydrostatic bearing is used under one load condition.

(b) Setup B, where a compliant hydrostatic bearing is used under several load conditions.

Fig. 4: Two measurement design approaches used in this paper.

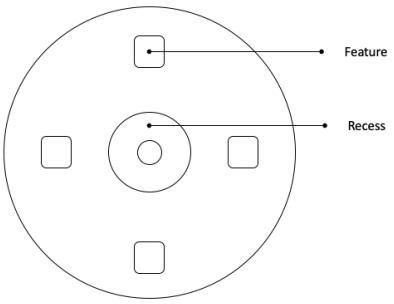

Fig. 6: schematically the bearing surface containing four features and the recess, with a depth of approximately 100, 200, 300 and 400 μm respectively for the features and 400 μm for the recess.

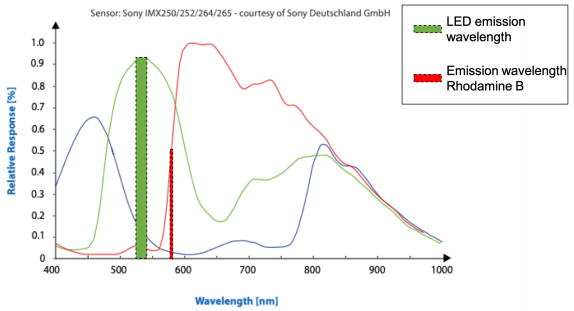

Fig. 7: The spectral respons of a SONY IMX 264 camera sensor with excitation and emission of Rhodamine B.

is chosen to be 4 μM. This results in an absorption A of $2.6 \cdot 10^{-3}$ which is sufficient to be neglected for the reflection of the incident light beam. This also determines whether the solvent is opti-

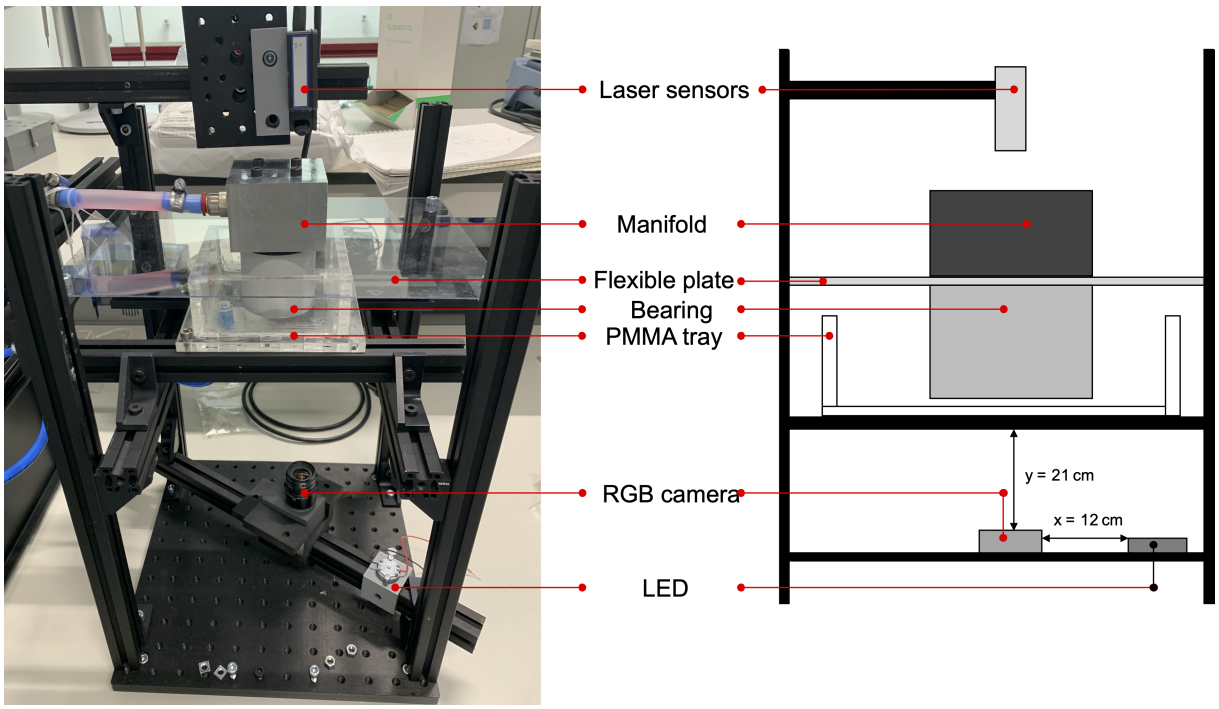

Fig. 5: Side view of test setup A.

cally thick or thin. When the solvent is optically thin the relation between the fluorescent light intensity and film thickness is linear. This optical thickness is determined by the concentration, quantum efficiency, thickness and absorption coefficient. For this measurement method the solvent is supposed to be optically thin, because we can measure the reflected incident light beam and assume that it is the incident light beam. In Figure 8 the fluorescent light intensity is plotted against the film thickness, also, the linearization at h=0 of the fluorescent light intensity is plotted. For this measurement method, the incident light will be assumed linear up to a film thickness of 1 mm, because the absorption becomes in order of 10^{-2}.

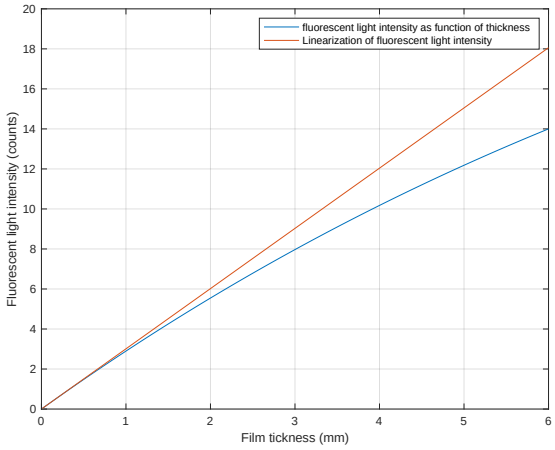

Fig. 8: The fluorescent light intensity as function of the film thickness and the linearization of the fluorescent light intensity at h=0.

To get the information from the RGB camera and convert it to a film height some steps need to be taken. First, the different channels of the camera will be used as a digital filter, described before. If we look at the two different dominant wavelengths of the LED and the fluorescence it can be seen how the red and green channels can be used as a filter (Figure 7. To minimize the effect of leakage, described in section 2.2, we first have to take an image where the film height $h = 0$. Another adjustment that needs to be made is a mask around the region of interest, being the surface of the bearing. Figure 9b shows the result of such a mask. This mask makes sure only the area of the bearing is excited by the light and the background noise of the liquid which is not underneath the Bearing is minimized. Furthermore, in the post-processing a Gaussian filter is used to reduce the independent pixel noise. By using a Gaussian filter a trade-off was made between the spatial resolution and precision.

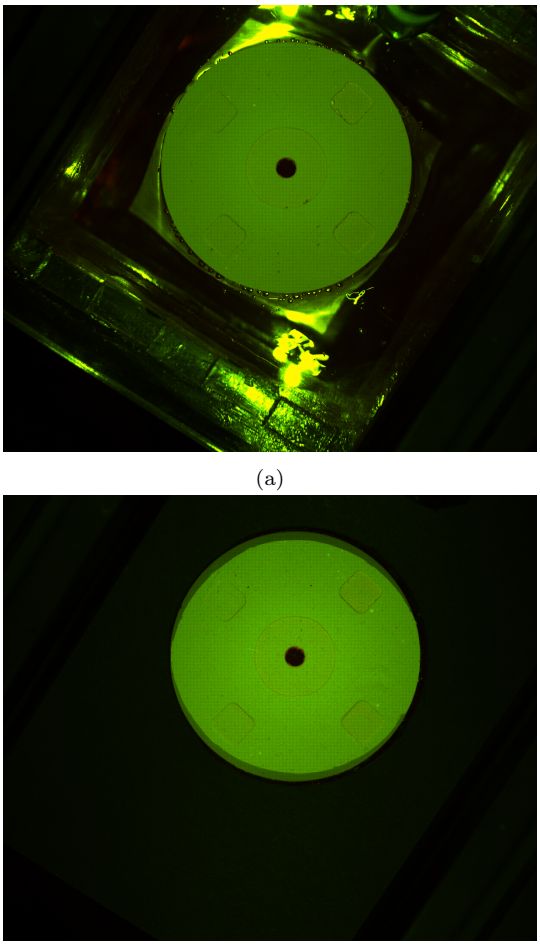

(a)

(b)

Fig. 9: (a) The bearing surface exposed to the LED without a mask. (b) The bearing surface exposed to the LED with a mask.

2.4 Setup B

In measurement setup B a compliant bearing is being implemented. This means the setup needs some adaptations. To apply multiple load condition in order to see the increase in recess height a pneumatic cylinder is added. Furthermore, to measure the force applied to the bearing a force sensor is added to the setup. Setup B is shown schematically in figure 10. During the measurement the setup will be placed in a box. This ensures the measurement will not be influenced by external light. The same solution of water and fluorescent dye utilized in setup A is used in this setup as well. In setup B the camera and the LED used are the same as setup A. To measure the force applied to the bearing a OPTOFORCE HEX-70-XH-200N force/torque sensor is used. Also a force needs to be applied, this force is created by a pneumatic cylinder. The cylinder used is a SMC C55 with bore diameter of 25 mm^2 and a stroke of 80 mm.

The compliant bearing is made using silicon

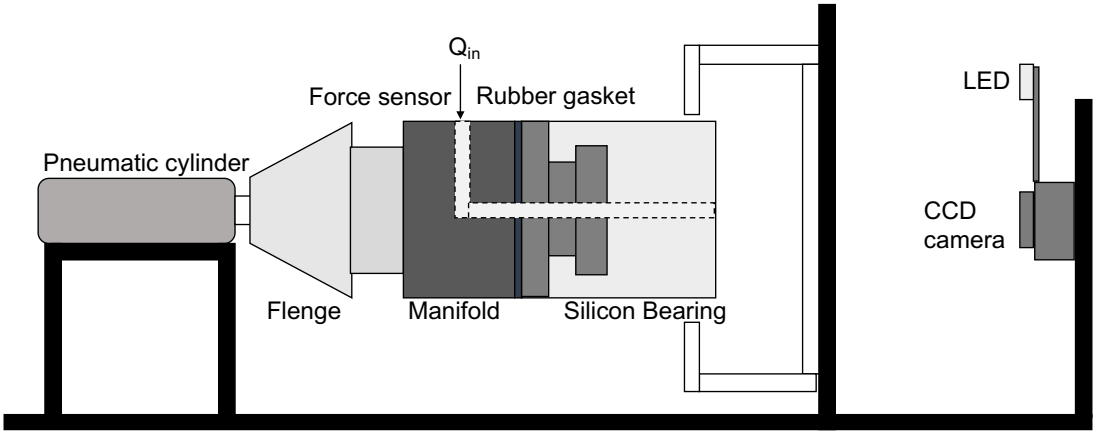

Fig. 10: schematic side view of measurement setup B.

rubber, which was casted using a 3D printed mold. To make sure the bearing can be connected to the manifold, an aluminum part is made which is used as top part where the silicon rubber is form enclosed. The silicon rubber has been tested in a tensile test to obtain the Young's modulus. This silicon rubber has an effective Youngs modulus for small strains equal to E = 0.3 MPa, which will be used for a finite element method comparison. Due to small deformations of the compliant bearing, assumptions can be made to model this bearing linear elastic [1].

Because the silicon is unable to be spray painted, a PLA 3D printed plate is introduced to ensure a similar reflection from the compliant hydrostatic bearing as from the classic bearing. This plate has a thickness of 0.5 mm and is therefore flexible enough to follow the deformation of the compliant bearing. The plate can be painted matt white and therefore resulting in a similar reflection of the incident light. The plate has been printed with a tube in the middle, ensuring water to be able to flow underneath the PLA plate. This tube can be placed in the outlet of the compliant bearing, shown in Figure 11.

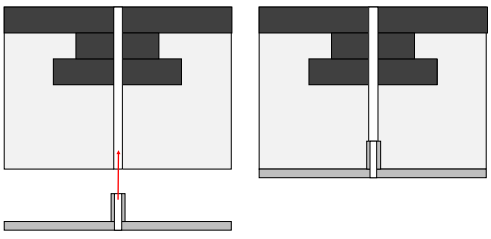

Fig. 11: Schematic overview of the PLA plate placed in the compliant bearing

2.5 Finite element analysis

To validate the measured film height of the compliant bearing, a FEM model has been made using COMSOL multiphysics. A 2D axisymmetric model has been created using the actual bearing dimensions. Furthermore, flow boundary equations have been applied on the surface of the bearing and a coupling has been made between the pressure calculated by the flow equations and the solid mechanics boundary load. The flow equations used for this model are as follows [4]:

$$Q = \frac{-h^3}{12\eta} r \frac{dP}{dr} \tag{9}$$

with Q being the flow in $[\frac{\mathrm{m}^3}{\mathrm{s}}]$, h being the film height in m, η being the dynamic viscosity in [Pa·s] and r is the radius in m. The pressure solved by the flow equation can be applied to the bearing resulting in a deformation. The deformation determines the film height and thus the flow. This process iterates to an equilibrium.

3 Results

Calibration needs to be carried out to plot the fluorescence intensity given a known film thickness. Figure 12 gives the schematic diagram. A feeler is placed on one side under the rigid hydrostatic bearing [18] of setup A, that has a thickness of 500 μm. This means a linearly decreasing gap is formed and by filling the tray with the solution the gap will be filled as well. During calibration the water is no operative, thus the is no lubrication effects present. The weight of the bearing and the manifold will make sure the bearing is in contact with the feeler and the surface. By mapping the result from the created gap and the fluorescence intensity, the film thickness can be obtained.

Figure 13 shows the result of the film thickness calibration. It was found that the scaling factor, as seen in equation 6, of the measurement needs to be 5714. Another observation made was the need for an offset. The film height where the bearing

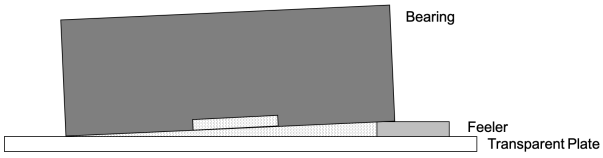

Fig. 12: schematic calibration setup.

	Confidence interval	Accuracy
Feature 1	206 μm $\pm$ 13.4 μm	1.9%
Feature 2	225 μm $\pm$ 14.7 μm	19.6%
Feature 3	401 μm $\pm$ 17.1 μm	4.2%
Feature 4	467 μm $\pm$ 15.4 μm	4.9%

Table 1: Confidence interval and accuracy for the four features on the bearing surface

was standing on the transparent plate was not been found to be zero and therefore equation 6 needed to be adjusted.

$$h = aR - b_{\text{offset}} \tag{10}$$

This offset occurs because the white primer paint on the aluminum also absorbs some of the Rhodamine B particles which led to a slightly red colored surface. This effect happens once and will not increase over time. After first scaling the measurement, the offset was found to be 450 μm.

3.1 Setup A

Figure 14 gives the film height map and also gives the film height at a cutline in the middle just above the inlet, at a distance 1.1 times the radius from the middle. All measurements have been repeated four times and are being presented in this work as a representation of the repeatability of this method. To investigate the accuracy of the method used, the film height is also measured by a laser distance sensor and the surface is measured by a whitelight interferometer. The height and tilt were measured with the laser sensor, resulting in a film height 115 μm and a negligible tilt. From the four measurements a 95% confidence interval is taken, resulting in a mean film height of 122 μm $\pm$ 14.4 μm. This results in a accuracy of 6.1%. For the recess this resulted in a mean recess height of 462 μm $\pm$ 10.7 μm with a accuracy of 1.7%. The results for the features are shown in Table 1.

3.2 Setup B

The results for the compliant hydrostatic bearing are shown in Figure 15. With these measurements a supply pressure of 0.8 bar is used and three load cases are applied: 50 N, 100 N and 150 N respectively. The result is that the elastic material will deform more creating a larger pocket so the bearing can carry the higher load. Figure 16 shows the deformation measured using fluorescence and the FEM modeled film height. The fluorescent measurement is first being calibrated in a similar way as setup A, but due to the alignment of the setup being horizontally, a calibration ring is added. This calibration ring has an increasing known thickness from 500 μm to 1000 μm. It was found that the scaling factor is 6666 and a offset value of 450 μm. An identified issue with measuring the film height of a compliant hydrostatic bearing is caused by the stickiness of the silicon. This causes fluorescent particles to remain on the silicon, causing a saturation effect on the surface and a discoloration of the surface from white to pink. This results in a measurement which has no reference. To resolve this problem, a 500 μm tick matt white painted PLA piece has been added to the bottom of the compliant bearing. On this new surface, this particle sticking occurs in a similar way to the previously presented rigid bearing. This plate is also taken into account in the FEM model. As seen from Figure 16 the error, compared to the FEM, in deformation is the largest with the 150 N measurement. Although giving the same film height at the edges, the rounded maximum error is found to be 300 μm. The 100 N measurement gives a similar shape with a rounded maximum error of 200 μm. The measurement with a load of 50 N gives a lower film height than predicted by the FEM model, with a rounded maximum error of 100 μm.

In the figure it is clearly shown that the higher force applied, the larger the recess it creates. This happens due to the fact that the pressure underneath the bearing increases when the load becomes higher. The result is that the elastic material will deform more creating a larger pocket so the bearing can carry the higher load

4 Discussion

This work presents a measurement setup that can be utilized to determine large deformation effects in the fluid film of compliant hydrostatic bearings. A number of limitations have been observed in the setup and approach. Because the area of interest is large (80x80 mm^2), not all the fluorescent light is captured by the camera. This means small fluctuation are not well captured resulting in a somewhat high maximum deviation. To improve this the setup could be altered to capture the all the fluorescent light. Furthermore, the PMMA counter surface is assumed to be perfect transparent but due to small scratches and dents this is not the case. These scratches on the plate can cause noise in the measurement. To improve a measurement the PMMA could be polished to remove the

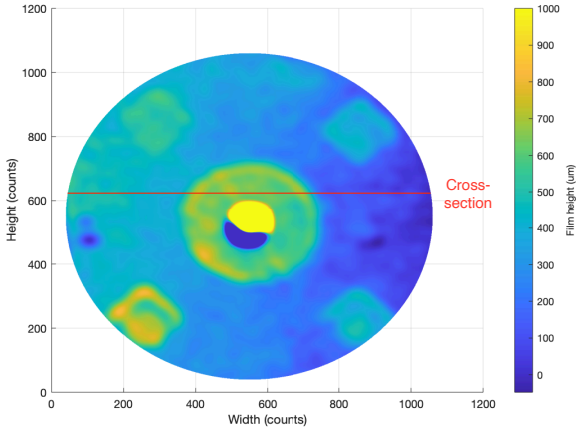

(a) Height map of the bearing placed on a feeler.

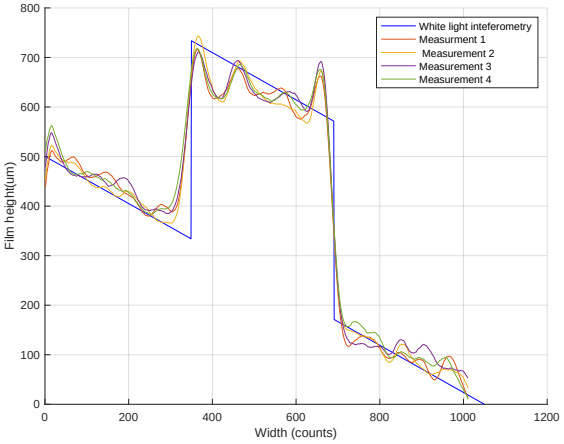

(b) The film thickness in the middle of the bearing at cross-section.

Fig. 13: Film thickness calibration method.

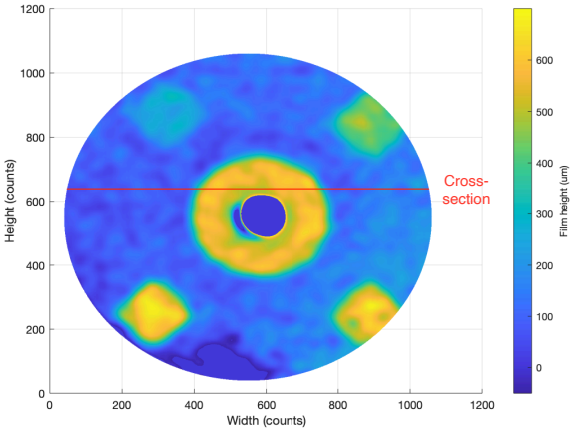

(a) Height map of the bearing placed.

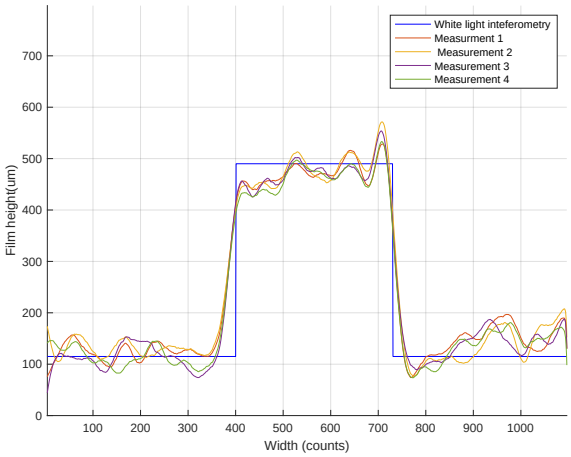

(b) The film thickness in the middle of the bearing at a cross-section for multiple measurements.

Fig. 14: Film thickness map using fluorescence.

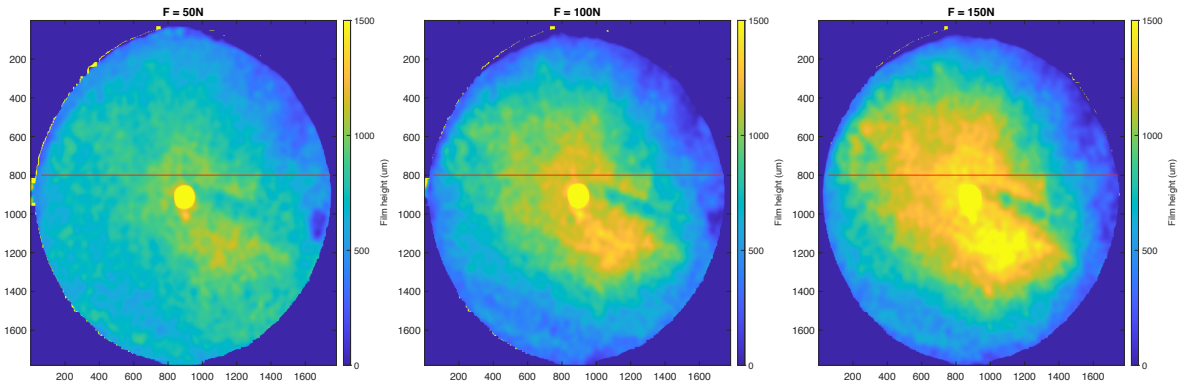

Fig. 15: The film height map of the compliant bearing for 50 N, 100 N and 150 N respectively

scratches. The limitation of this setup is measuring small film heights (under 15 μm). This is because the fluorescent wavelength(570 nm) intensity is too small compared to the LED intensity (570nm). For

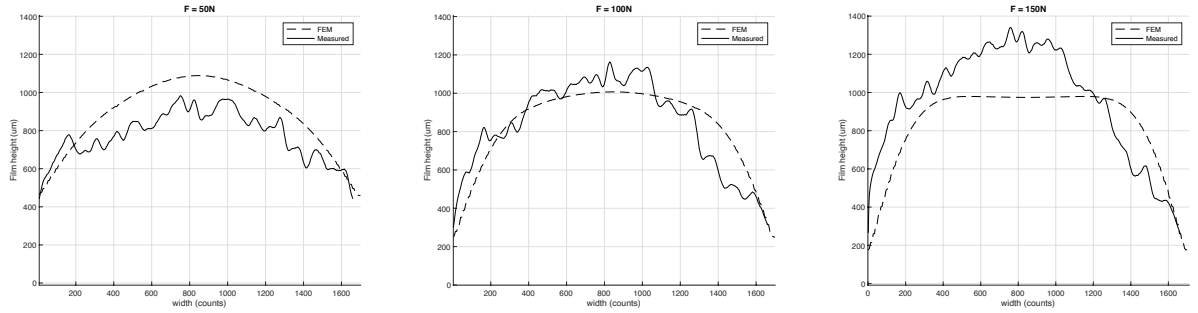

Fig. 16: The fluorescent film height of cross-section of the compliant bearing and the FEM for 50 N, 100 N and 150 N respectively

measuring smaller film height adaptation to this setup need to be made, such as a light source with a small bandwidth wavelength.

Setup A

For the measurement method calibration it was found an offset is needed. This offset can be explained by sticking of Rhodamine B particles to the surface. The surface of the Aluminum bearing has been painted with a matt white prime. This layer of paint has some roughness where the Rhodamine B particles can get stuck behind. This results in a slight red coloring of the surface and therefore a offset is needed to counter this. This means the when the fluorescent signal is compared to the $R_{h=0}$ value it created an error, due to the 'red' light of the fluorescence adds up to the 'red' light reflected from the surface with Rhodamine B particles, and this needs to be compensated in the calibration by an offset. This effect does not change over time and therefore the offset value can be assumed constant. The noise of the results observed in Figure 14 can be explained by the ratio in equation 5 that needs to be taken. Small perturbations in the raw image signal seen in the red channel and the green channel will lead to a large perturbations of the film height signal. Moreover, the light emitted from the Rhodamine particles compared to the LED light emitted in the same wavelength of the Rhodamine particles is small. This means that small changes in film height are complex to measure due to this leakage effect. To minimize this leakage effect a light source can be chosen which has a small bandwidth around the dominant wavelength. Moreover, the use of a two optical filters and a monochrome camera will reduce the leakage even further, although this comes at the cost of lower intensity and thus more difficult to measure signals. The observed features accuracy for feature 2 differs from the other features. A reason for this can be due to the cleaning process. When cleaning the surface of the bearing with isopropanyl, the Rhodamine particles will be removes. When not properly cleaned some particles will remain in the feature and therefore resulting in a lower accuracy. Furthermore, comparing the accuracy of the measurement to other fluorescent measurement methods [18] [15]. It is found that this method is in between the accuracy found in literature, 1 % from [15] and 20% from [18] respectively. Where in the case of [15] an optically thick solution is used, where, to obtain a usable height map, two fluorescent dyes need to be dissolved. In the case op [18] the method obtaining the height map does not include a ratio to be taken. This ratio does remove an error due to spatial variance of the light source.

Setup B

The FEM model of the compliant hydrostatic bearing uses a isotropic uniform silicon part with a modulus of elasticity of 0.3 MPa. In the actual bearing the method of fabrication does not include the use of a vacuum pump to remove air from the silicon. This result in a non uniform stiffness of the material. Furthermore, the FEM model has been used to validate multiple modulus of elasticity. Those different Young's modulus have a small effect on the deformability of the silicon in the finite element analysis. This does not explain the the difference in measurement compared to the FEM. The tube of the PLA plate has been designed to be greater than the diameter of the compliant outlet. This results in a certain stiffness between the PLA plate and the compliant bearing. This effect has not been included in the FEM model. Moreover, because the PLA plate is not included in the design of the complaint bearing and is later added, the plate is able to freely relative to the bearing surface. This could result in different film heights compared to the FEM model.

5 Conclusion

A LED induced fluorescence technique is used to measure the water film thickness of a classic hydrostatic bearing and a compliant hydrostatic bearing. The current work demonstrates a measurement system with an operating range of 15 - 1400 μm and

95% average confidence interval of 15.2 μm and an average measurement accuracy of 6.4% for the classic hydrostatic bearing. To obtain a height map, calibration must be performed using a calibration ring or a feeler with known dimensions. Limitations using this method are at the bottom of the operating range, due to the low fluorescent signal compared to the incident light. This can be resolved using a light source with a smaller bandwidth and the use of a monochrome camera. Furthermore, at the top of the range, limitations occur due to the optical thickness of the measurement. By changing the concentration the range can be extended to larger or smaller film heights. Further improvements that can be made by using a fluorescent dye that has a larger stokeshift, this would minimize the leakage. This method is developed for hydrostatic bearings, but can be used for the measurements of other lubricating films or boundary films where other measurement techniques are not easily implemented.

References

[1] Ron A.J. Van Ostayen, Anton Van Beek, and Mink Ros. "A parametric study of the hydrosupport." In: *Tribology International* (2004). ISSN: 0301679X. DOI: 10.1016/j.triboint.2004.01.009.

[2] Joep P. A. Nijssen and Ron A. J. van Ostayen. "Compliant Hydrostatic Bearings Utilizing Functionally Graded Materials." In: *Journal of Tribology* (2020). ISSN: 0742-4787. DOI: 10.1115/1.4047299.

[3] J. Nijssen, A. Kempenaar, and N. Diepenveen. "Development of an interface between a plunger and an eccentric running track for a low-speed seawater pump." In: *Fluid Power Networks* (2018).

[4] T. A. Osman et al. "Experimental assessment of hydrostatic thrust bearing performance." In: *Tribology International* (1996). ISSN: 0301679X. DOI: 10.1016/0301-679X(95)00078-I.

[5] R. Cameron and R. W. Gregory. "Paper 4: Measurement of Oil Film Thickness between Rolling Discs Using a Variable Reluctance Technique." In: *Proceedings of the Institution of Mechanical Engineers, Conference Proceedings* (1967). ISSN: 0367-8849. DOI: 10.1243/pime_conf_1967_182_403_02.

[6] Ziqiang Cui et al. *Liquid film thickness estimation using electrical capacitance tomography.* 2014. DOI: 10.2478/msr-2014-0002.

[7] A. Dyson, H. Naylor, and A. R. Wilson. "Paper 10: The Measurement of Oil-Film Thickness in Elastohydrodynamic Contacts." In: *Proceedings of the Institution of Mechanical Engineers, Conference Proceedings* (1965). ISSN: 0367-8849. DOI: 10.1243/pime_conf_1965_180_072_02.

[8] Tom Reddyhoff, Rob Dwyer-Joyce, and Phil Harper. "Ultrasonic measurement of film thickness in mechanical seals." In: *Sealing Technology* (2006). ISSN: 13504789. DOI: 10.1016/S1350-4789(06)71260-0.

[9] R. S. Dwyer-Joyce, B. W. Drinkwater, and C. J. Donohoe. "The measurement of lubricant-film thickness using ultrasound." In: *Proceedings of the Royal Society A: Mathematical, Physical and Engineering Sciences* (2003). ISSN: 14712946. DOI: 10.1098/rspa.2002.1018.

[10] I. K. Kabardin et al. "Optical measurement of instantaneous liquid film thickness based on total internal reflection." In: *Journal of Engineering Thermophysics* (2011). ISSN: 18102328. DOI: 10.1134/S1810232811040072.

[11] Seung-Woo Kim and Gee-Hong Kim. "Thickness-profile measurement of transparent thin-film layers by white-light scanning interferometry." In: *Applied Optics* (1999). ISSN: 0003-6935. DOI: 10.1364/ao.38.005968.

[12] P. A. Flournoy, R. W. McClure, and G. Wyntjes. "White-Light Interferometric Thickness Gauge." In: *Applied Optics* (1972). ISSN: 0003-6935. DOI: 10.1364/ao.11.001907.

[13] A. A. Mouza et al. "Measurement of liquid film thickness using a laser light absorption method." In: *Experiments in Fluids* (2000). ISSN: 07234864. DOI: 10.1007/s003480050394.

[14] Yoshio Utaka and Tetsuji Nishikawa. "An investigation of liquid film thickness during solutal Marangoni condensation using a laser absorption method: Absorption property and examination of measuring method." In: *Heat Transfer - Asian Research* (2003). ISSN: 10992871. DOI: 10.1002/htj.10124.

[15] Carlos H. Hidrovo and Douglas P. Hart. "Emission reabsorption laser induced fluorescence (ERLIF) film thickness measurement." In: *Measurement Science and Technology* (2001). ISSN: 13616501. DOI: 10.1088/0957-0233/12/4/310.

[16] T. Reddyhoff et al. "Lubricant flow in an elastohydrodynamic contact using fluorescence." In: *Tribology Letters* (2010). ISSN: 10238883. DOI: 10.1007/s11249-010-9592-6.

[17] Nicholas M. Husen, Tianshu Liu, and John P. Sullivan. "The ratioed image film thickness meter." In: *Measurement Science and Technology* (2018). ISSN: 13616501. DOI: 10.1088/1361-6501/aabd27.

[18] Xingxin Liang et al. "Comparison of measured and calculated water film thickness of a water-lubricated elastically supported tilting pad thrust bearing." In: *Surface Topography: Metrology and Properties* 7.4 (2019). ISSN: 2051672X. DOI: 10.1088/2051-672X/ab47a6.

[19] Alexander P. Demchenko. *Introduction to fluorescence sensing*. 2009. ISBN: 9781402090035. DOI: 10.1007/978-1-4020-9003-5.

[20] D. F. Swinehart. *The Beer-Lambert law*. 1962. DOI: 10.1021/ed039p333.

[21] Husen. "Skin friction measurements using luminescent oil fims." In: *Measurement Science and Technology* (2017).

5

Measurement Analysis

This chapter will elaborate on the measurement system. In order to achieve a representative result multiple settings had to be analysed as well as the measurement itself. To achieve the most accurate result, the measurement method has been analysed. In this analysis multiple camera settings have been tested, as well as multiple LED's. Furthermore, time dependence has been investigated and the confidence interval has been determined. All these different settings and variable led to a result that has the least signal noise.

5.1. Measurement system A

Measurement setup A was used to determine the performance of the measurement. To do this all the settings and variables need to be analysed to come up with the best result. In this section multiple settings have been tested and the results are discussed.

5.1.1. Laser sensor measurement

To determine the actual height of the bearing a laser sensor is used. This laser sensor has an operating range of 0-500 μm with an accuracy of 0.2 μm. Using this sensor on three location on the manifold the height and tilt can be determined. Figure 5.1 shows schematically what this looks like. The results of this laser sensor measurement are shown in table 5.1. In this work the film height will be assumed to be uniform at 115 μm. The reason is that the noise of the fluorescent measurement prevents to measure deviations < 1 μm.

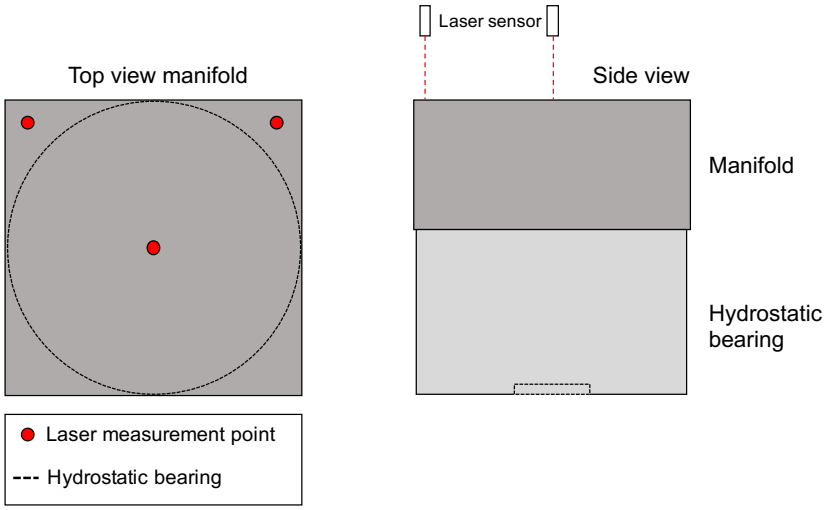

Figure 5.1: Schematical overview of triangulate film height of the bearing

Position	Height measured (μm)
Top left	114
Top right	116
Middle	115

Table 5.1: Laser sensor measured results for three locations on the bearing

5.1.2. Camera settings

A Pixelink CCD camera was used in combination with additional software. This software is useful for adjusting settings of the camera. The camera itself lets you adjust the aperture and the focal point. Within the camera a SONY IMX264 sensor [2] captures the image. This sensor has a spectral response shown in figure 5.2, where the emission wavelength of the LED (530-540 nm) and the emission wavelength of Rhodamine B (570 nm) are shown. The figure shows that the red and green channels of the image can be used as a filter. Although the dominant wavelength of the LED is between 530 and 540 nm, it also emits some some light in the 570 nm range, shown in figure 2.6. This 570 nm wavelength emission from the LED will interfere with the 570 nm emission from the Rhodamine B particles. The effect is called leakage and this is preferably minimized. A method of minimizing this is by taking a image where h=0. By taking the ratio of the h=0 image the intensity of the red channel relative to the green channel is determined, so a increase of the red channel relative to the green channel can be coupled to the film height.

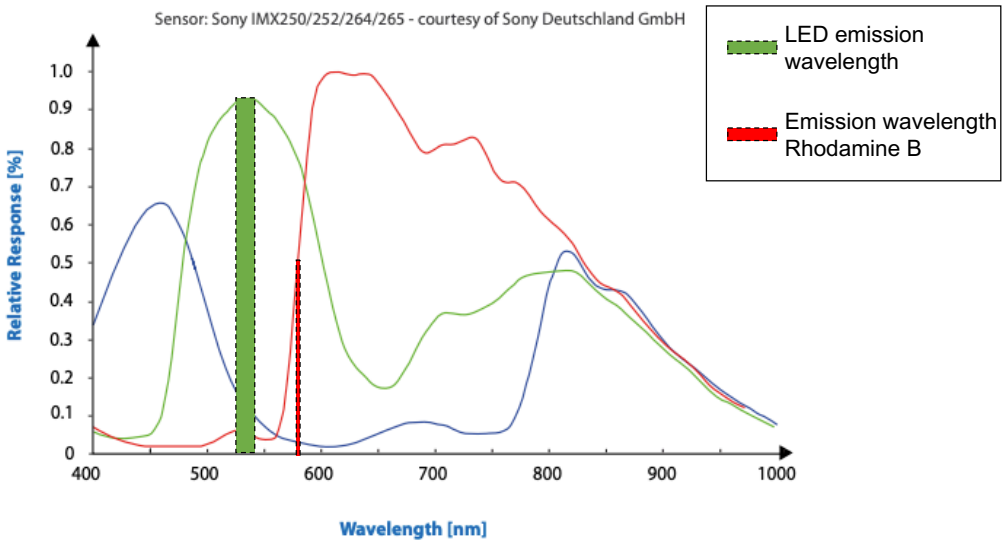

Figure 5.2: Spectral response of the camera sensor with LED emission wavelength and emission wavelength of Rhodamine B

The settings used for the aperture and focal point have been manually set. The aperture is set to completely 'open' and the focal point has been adjusted so the image is in focus. Next, the settings of the camera set by the Pixelink software have to be determined. Most settings have been set to default, but it was found that the setting of the white-balance play a crucial roll. First, the button AUTO needs to be pressed so the mosiac image will become a demosiac image. The white balance setting can be manually adjusted, this means the individual channels can be changed to obtain a image to your own preference. They can be set to a value between 0-8. Because the signal the red channel receives is low this is set to a value of 8. The blue channel does not play a role in the image process, so this is set to zero. Now the green channel needs to be determined. Multiple measurements have been done with different values of G-channel. Figure 5.3 shows the film height for multiple settings of the G-channel and figure 5.4 shows at the cross-section the film height. Although being Gaussian filtered, the noise differs between the different settings, and from these measurements it is found that $RGB = [8, 0.7, 0]$ results in the least amount of noise.

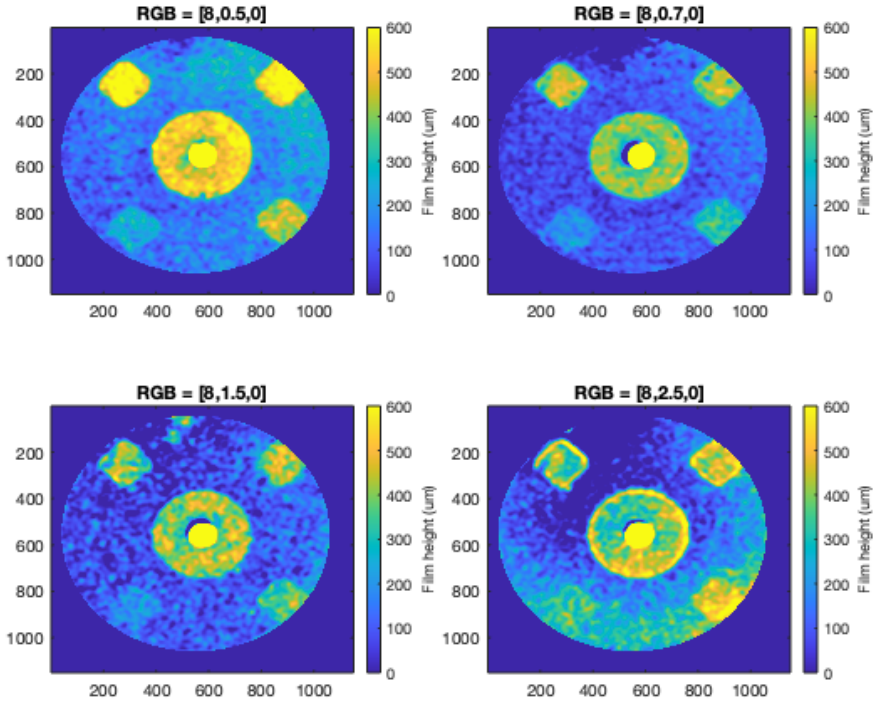

Figure 5.3: 4 Film height maps for with varying white-balance settings of the camera. With R=8 and B=0 and different values for the green channel have been used: 0.5, 0.7, 1.5 and 2.5 respectively.

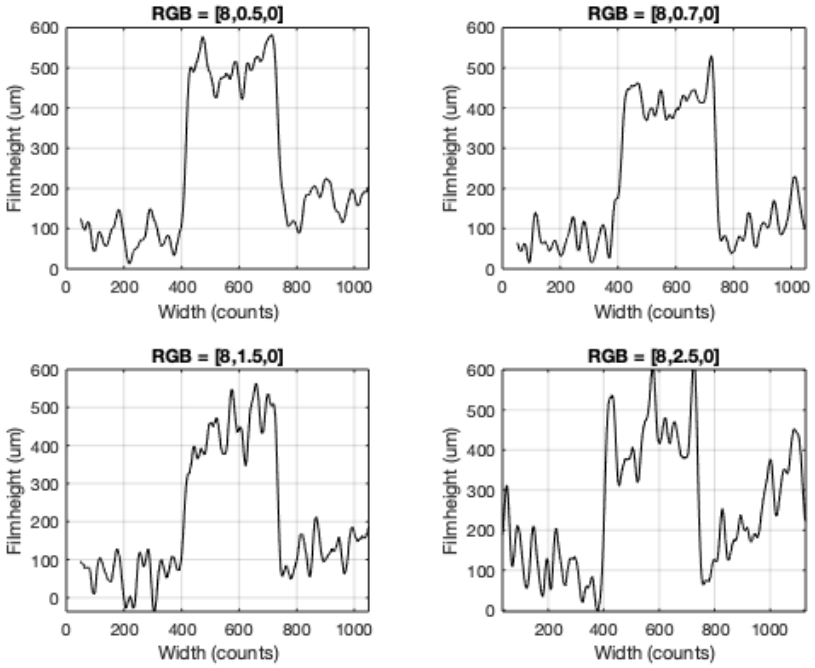

Figure 5.4: Film height at cross-section for different white-balance settings of the camera

5.1.3. Mask

While doing measurements it was found that applying a mask helps to reduce noise. This mask eliminates light from the LED to perpetrate the liquid which is not under the bearing. This also would exclude fluo-

rescent light from the liquid in the tray from influencing the the measurement. The mask is made of black cardboard in which a circle is cut out, such that the region of interest, the surface of the bearing, can be illuminated. Figure 5.5 shows two measurements, one with and one without a mask. What is shown in this figure is that the height map without a mask has a larger and more deviating film height. Furthermore, the offset for the measurement without a mask is 2.5 times larger than the measurement with a mask. The mask also makes sure the film height measurement is more accurate due to the resulting uniformity of the film height.

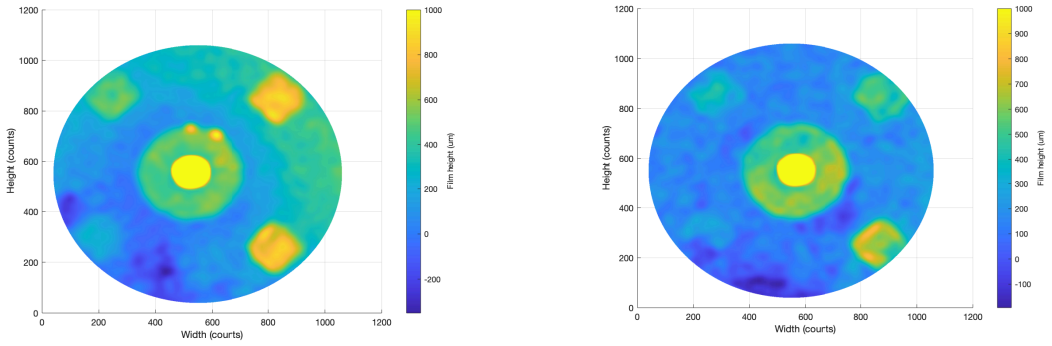

(a) Film height map of the bearing without a mask

(b) Film height map with a mask

Figure 5.5: Two measurements one with a mask and one without a mask

5.1.4. LED location

The position of the LED is insensitive to the incident angle [15] and it is demonstrated experimentally that it is very robust to varying incident light intensity and camera angle up to 70°. The effect of the light source location will therefore not be taken into account in the measurement setup. The only thing of importance is that the specular reflection will not reflect directly into camera resulting in a green spot. For both setups the LED is placed at a distance of 120 mm from the camera in the same plane. Both the camera and the LED are placed 210 mm from the bearing surface.

5.1.5. Multiple LEDs

Because the LED is placed on one side, it was thought that this has effect on the fluorescence. Therefore, measurements have been performed with 1, 2 and 3 LEDs. A LED mount has been placed on the camera lens, shown schematically in figure 5.6. The idea is that more LEDs will give a more uniform light distribution over the bearing surface.

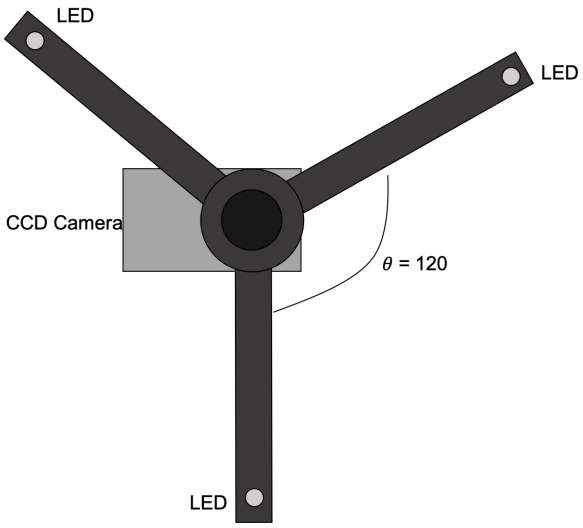

Figure 5.6: Schematically camera setup with mount for 3 LED's

Three measurements have been performed where 1,2 and 3 LEDs respectively have been switched on to obtain a result. Although a more uniform film height was expected, this was not observed in the results. The film height map of the three different conditions are shown in figure 5.7. In this figure it is clear that when adding more LED there arise spots where the film height is almost zero. For 1 LED this is not the case and the film height stays uniform. Except for the amount of LEDs the three measurements conditions are the same. This means for measuring film heights it is found 1 LED gives the most uniform result. This is probably due to slight changes in wavelengths from the different LED's. These different wavelengths can interfere with each other and with the fluorescent signal resulting in severe fluctuation per area.

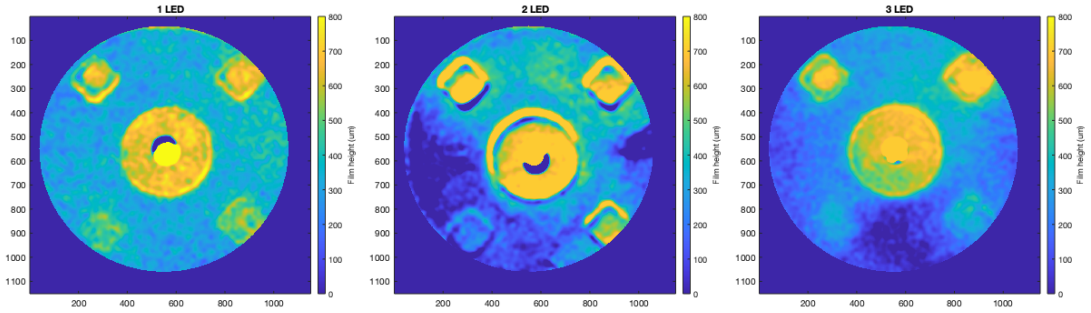

Figure 5.7: The film height map for multiple used LEDs.

5.1.6. Noise reduction

During image processing a smoothing is used to reduce independent pixel noise, necessary to obtain a usable result. Within the MATLAB environment this Gaussian smoothing can be implement by using the Gaussian filter command. The Gaussian filter blurs the image by a Gaussian function. This filter takes an normal distribution, with a self defined standard deviation, of the surrounding pixels, resulting in a reduced noise image and reduced detail. When a Gaussian filter is applied a trade-off must be made between the spatial resolution and the precision. This work applies a standard deviation of the Gaussian distribution of 15. Figure 5.11 show the red and green channel filtered and unfiltered as well as the ratioed film height filtered and unfiltered. It was found that for the result it does not matter whether the signal is first filtered and then the ratio is taken or vice versa. Both methods result in exactly the same result.

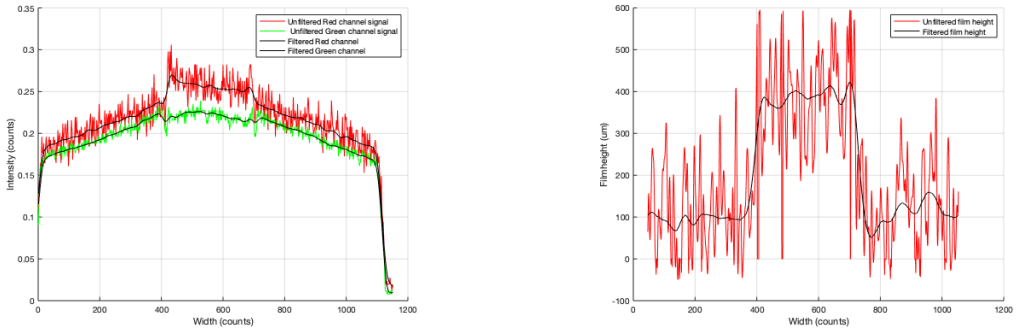

(a) Red and green channel unfiltered and filtered

(b) Ratioed film height filtered and unfiltered

Figure 5.8: Example of the use of a Gaussian filter

Furthermore, to obtain an even further reduction in image signal noise multiple images are taken which have been averaged. In this work this has not been used, but will be used as recommendation to obtain an more accurate result. Figure 5.9 shows the difference between one image taken and the average of 5 images taken. The latter demonstrates that most but not all of the noise is reduced.

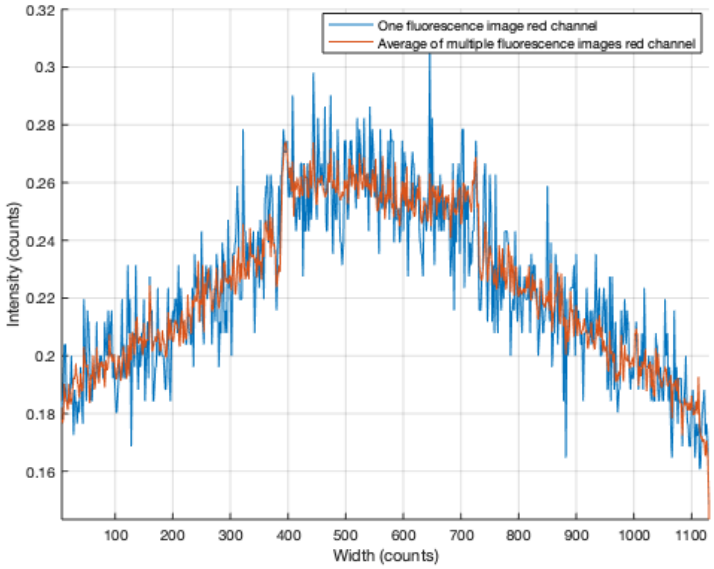

Figure 5.9: One image signal and the signal of the average of 5 images

5.1.7. Calibration

To use the fluorescent signal and couple it to a film height a calibration must be done. This has been done by placing the bearing on a feeler on one side and by placing the other side directly on the PMMA. The thickness of the feeler is 500 μm, with this known thickness the signal result can be coupled to an actual height. Figure 5.10 shows a schematic overview of the setup. This setup is used to find the scaling factor a, which is a value determined by the concentration, quantum efficiency, molar absorption and the lambertian surface reflection. These parameters are hard to determine precisely and therefore the calibration becomes valuable. Because the change in height is known it can be scaled. This is shown in figure **??**. The scaling factor can be determined by $a = \frac{500}{\mathrm{d}y} = \frac{500}{0.087} = 5714$. The scaling factor is applied and the result is shown in Figure **??**. It was found that on the side were the bearing was placed on the PMMA the fluorescence was not zero. So an offset needed to be subtracted from the film height result. Figure 5.12 shows the scaled and offset bearing film height, the offset was found to be 450μm.

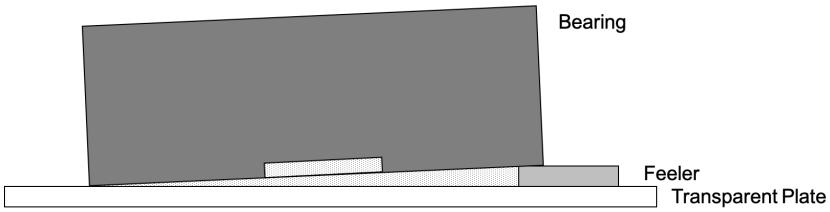

Figure 5.10: schematic overview of the feeler and the bearing

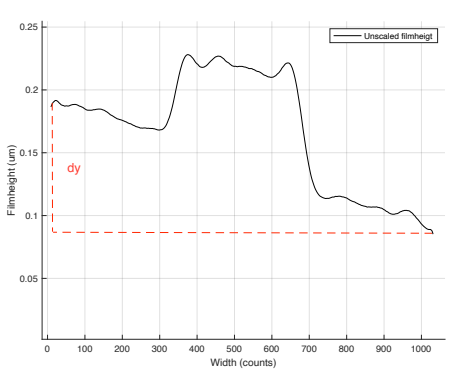

(a) Unscaled film height of the calibration of the bearing

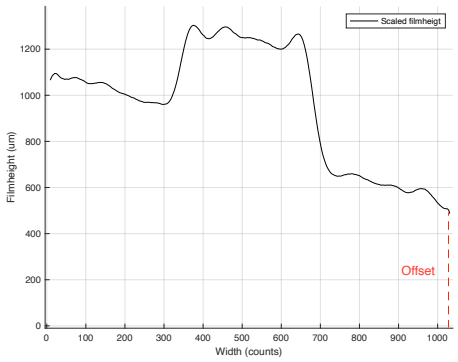

(b) Film height scaled using the calibration feeler

Figure 5.11: Determine the actual film height using a scaling factor and an offset

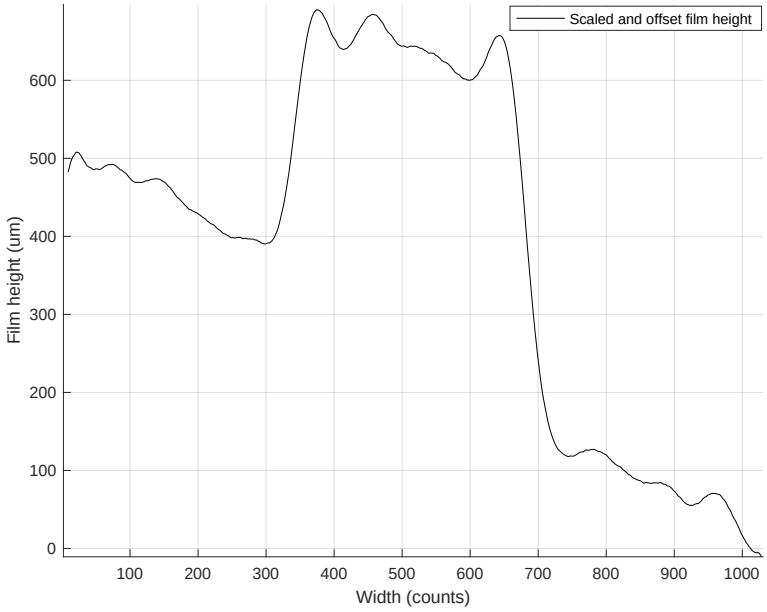

Figure 5.12: Film height scaled and offset

5.1.8. Confidence interval

To obtain the performance of this measurement method a confidence interval was used. This confidence interval uses the number of measurements and the standard deviation to obtain a result. A confidence interval can be describe as follows:

$$\text{Mean} \pm Z \cdot \frac{s}{\sqrt{N}} \tag{5.1}$$

Where the mean is the average of the measurement. Z is determined by the percentage of confidence, in the case of 95% this is 1.96. S is the standard deviation calculated with the following equation:

$$s = \sqrt{\frac{\sum |x_i - x_{\text{avg}}|^2}{n}} \tag{5.2}$$

With x_i the observed value. N in both formulas is the number of measurements taken. By applying these equations the confidence interval can be obtained. Figure 5.13 shows the mean of multiple measurements and the upper and lower confidence interval. This resulted in a mean film height of 98 μm $\pm$ 14.3μm. With this result also the accuracy can be obtained. This can be found by the following formula:

$$Accuracy = \frac{x_{\text{mean}} - x_{\text{laser}}}{x_{\text{laser}}} \tag{5.3}$$

The film height was measured to be 115 μm, this can be used to obtain the accuracy. The accuracy was found to be 14.7%.

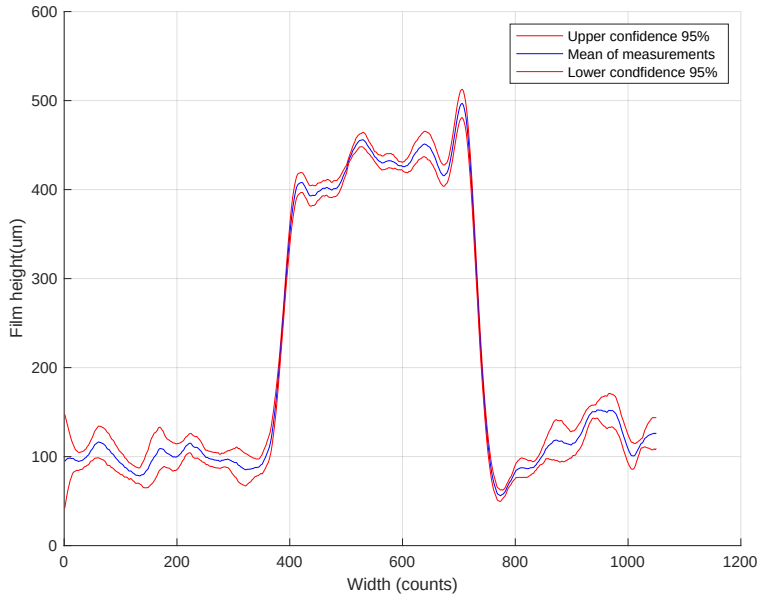

Figure 5.13: the mean of multiple measurement with 95% confidence interval

5.2. Measurement system B

Measurement setup B has multiple consideration regarding measuring. The silicon rubber was not sufficient in reflecting the incident light properly. This resulted in a adaptation of the bearing, described below.

5.2.1. Particle sticking

When performing the first measurements it was found that the bearing was changing in colour. This was caused by fluorescent particles sticking to the bearing surface which has a certain roughness. Figure 5.19 shows the change of colour. This effect slightly happens to the classic aluminum bearing, resulting in a offset in the calibration. For the compliant bearing this is different. The particle sticking keeps happening over time resulting in a increased film height. Where for the aluminum bearing this is effect happens once resulting is a constant offset, for the compliant the effect keeps increasing resulting in an increasing offset. To show this in an example six measurements have been done, each measurement 30 seconds in a row. Figure 5.15 shows the film height map over time and figure 5.16 shows at height = 600(counts) the film height over time. This very clearly shows that the film height increases over time, which is the result of increasing amount of particles sticking to the compliant bearing surface. Another observation made was the uneven increase of particle sticking throughout the surface of the bearing. This results in certain areas having a 'higher' film height then other areas. This is a problem because the film height cannot be calibrated due to the changing amount of particles which have stuck to the surface. To obtain a measurement method for compliant bearings a method has to be developed where this effect is neglected.

The idea arises that the $R_{h=0}$ image can be taken at the end of the measurement so the amount of red in the image without a fluorescent liquid can be compared to the red in the image with a fluorescent liquid. This has been done and resulted in film height being negative. This means the amount of fluorescent light with liquid is less than the amount of fluorescent light without the liquid. This cannot be the case. The reason why this happens is probably cause by the fact the amount of fluorescent light is so small compared to the 'red' light reflected from the bearing surface containing all does fluorescent particles that are stuck to it, the

(a) Compliant bearing before being used with the solution of water and Rhodamine B

(b) Pink coloured bearing surface as a result of the Rhodamine B particles sticking

Figure 5.14: Colouring of the bearing surface

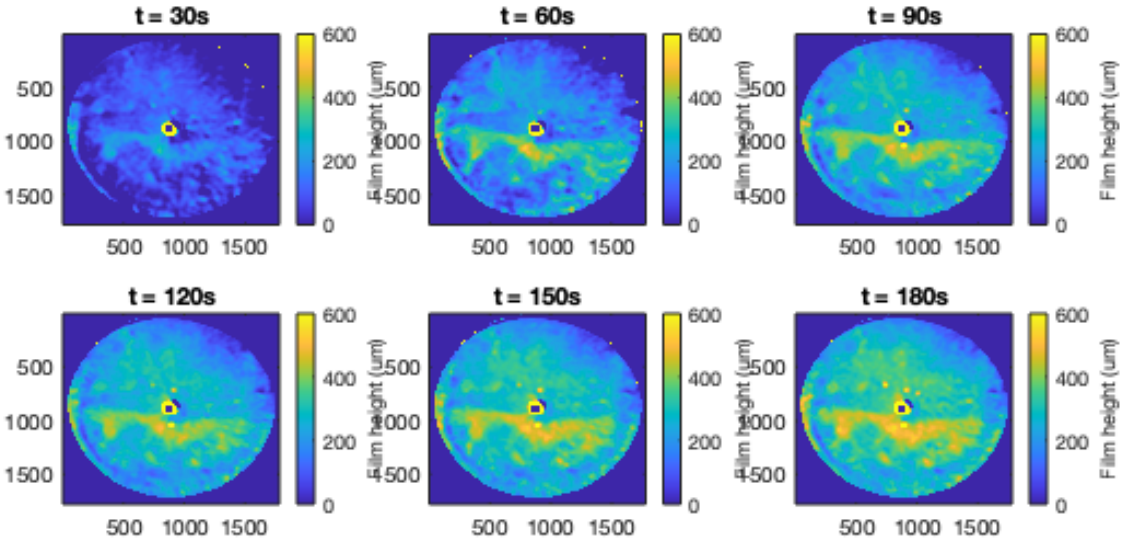

Figure 5.15: Film height map of the compliant hydrostatic bearing over time

difference in increase of fluorescent light is not noticeable.

To solve this problem a PLA piece is 3D printed. This PLA has a thickness of 500 μm and is therefore flexible enough to deform according to the compliant bearing. This piece has a mouth piece that can be placed inside the bearing outlet. Figure 5.17 shows schematically how this is done. This PLA piece is able to be painted with the matt white primer paint, used on the rigid bearing as well. By using this piece the fluorescent particles will not stick to the surface anymore and therefore it has no effect on the measurement of the film height. The addition of the PLA plate brings some extra stiffness to the bearing. Although being flexible enough to deform as much as the silicon, the stiffness does increase. This has been taken in to account in the FEM, using a Young's modulus for PLA of E = 3.5 GPa [10]. The tube of the PLA has some additional stiffness because it is being placed in the outlet of the silicon bearing. Between the tube of the plate and the outlet friction will occur. This fiction in combination with the elastic nature of the silicon will create additional stiffness to the plate. This effect has not been implemented in the FEM model.

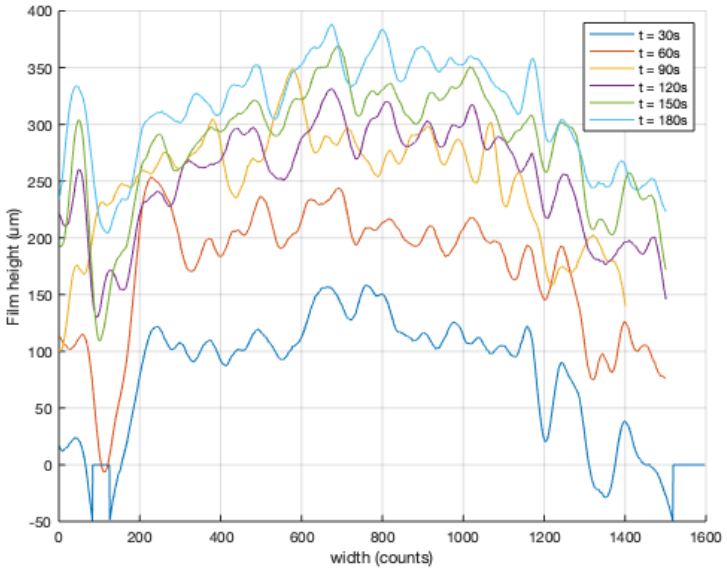

Figure 5.16: Film height at cross-section over time

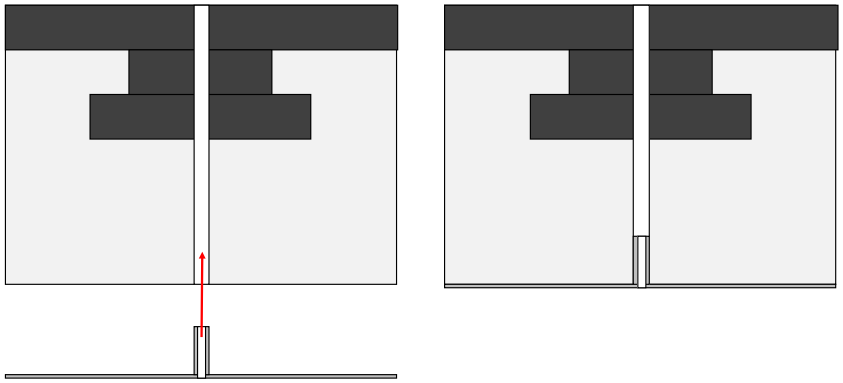

Figure 5.17: Schematic overview how the PLA piece is placed in the bearing

5.2.2. Calibration

To calibrate the compliant hydrostatic bearing a feeler is not good to use anymore. Due to compliance it is unknown where the film height is zero. Furthermore, the setup is placed horizontally so the tray cannot be filled with water. To still calibrate the setup a calibration ring is introduced. This calibration ring has an increasing thickness from 0.5 mm - 1 mm and therefore can be coupled to the fluorescent signal. Figure 5.18 shows schematically how this calibration ring looks like. The ring is not closed entirely because the solution needs to flow somewhere and it is not desired that a film height is created. With this calibration ring the same step can be repeated as used for setup A. The result for this calibration ring gave a scaling factor of $a = 6666$ and an offset value of $b = 400\mu$m. The film height map and the film height at a cross-section are shown in figure 5.19a and 5.19b respectively.

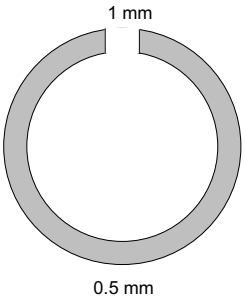

Figure 5.18: schematical calibration ring

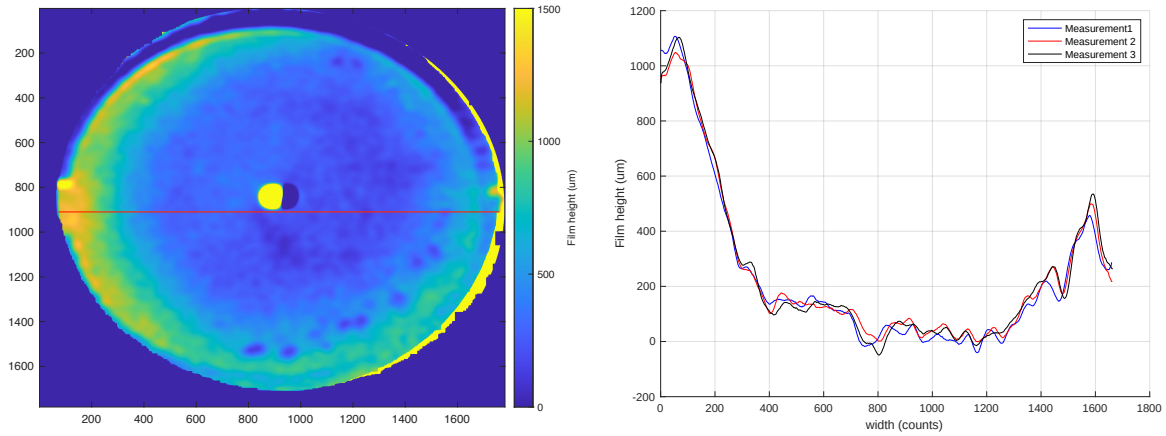

(a) Film height map of compliant bearing using a calibration ring

(b) Cross section film height of calibration ring for three measurements

Figure 5.19: Calibration ring film height map

6

Finite Element Analysis

6.1. Fluorescence simulation

A model using finite element analysis has been used to look at sensitivities regarding a fluorescent measurement. This analysis has been done by using COMSOL multiphysics [16]. In order to perform the analysis multiple effects have to be implemented in the model, as well as the influence of the transparent plate PMMA. All the assumptions that have been taken into account are described in this section. These assumptions are made next to the fluorescence equation described in chapter 2. The model uses the geometry as used in section 3, the measurement setup A.

6.1.1. LED

First up is the LED. For the LED we use a small circular Luxeon C LED [19] which can be seen as a point source. This LED has a certain excitation bandwidth but its dominant wavelength is 530 nm, the color is therefore green. The spectral power distribution of the LED is shown in figure 6.2, where we look a the green power distribution. Next to the spectral power distribution of the LED we also have to look at the polar radiation pattern, this is shown in figure 6.1. These two characteristics of the LED have been modelled accordingly.

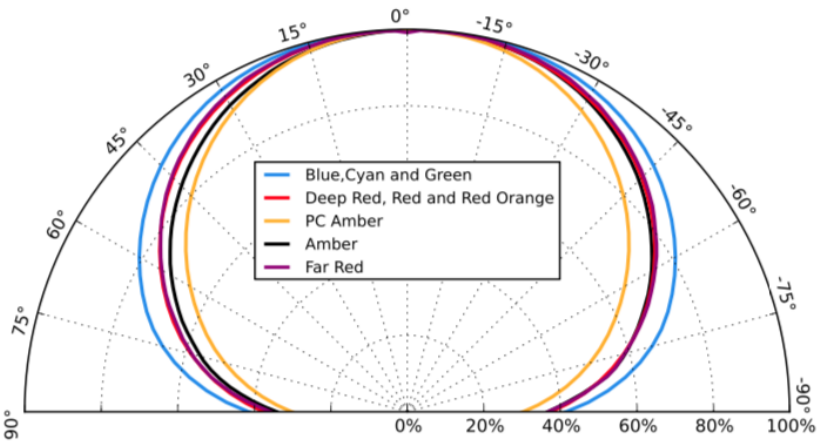

Figure 6.1: Polar radtion pattern of multiple colors from LUXEON C leds

6.1.2. Effect of point source

By assuming the LED behaves as a point source it affects the way the light rays enter the fluid of the hydrostatic bearing. This means the light rays will not enter the fluid parallel, but will expand from the source. Resulting in an increasing distance a light beam travels through the fluid along the surface of the bearing. An example

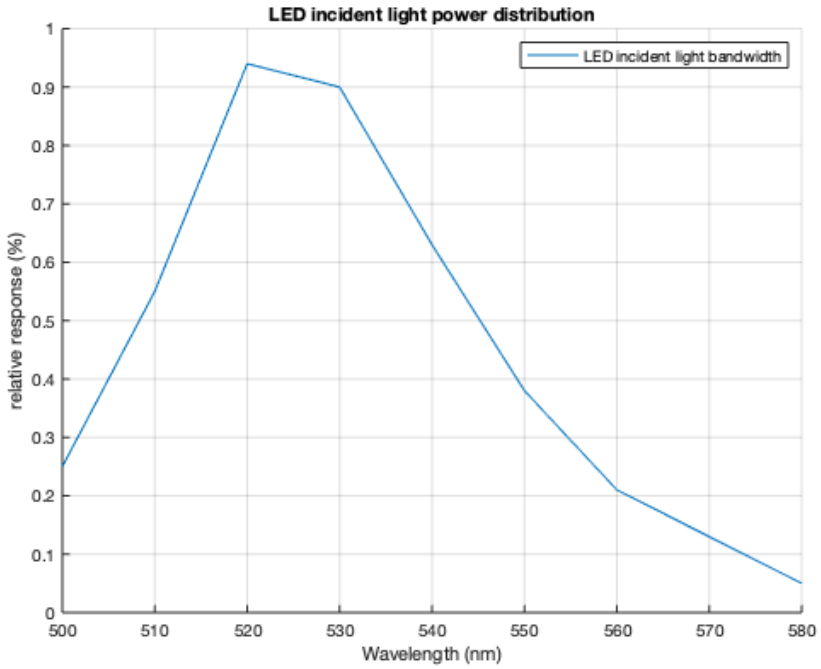

Figure 6.2: Power distribution of the LED used in the measurement setup

of this effect is shown in figure 6.3. So we have to implement this effect in the model. The way this is done is by calculating, with the use of geometric equations, the distance at every point on the surface of the bearing. This distance is then used to scale the model appropriately.

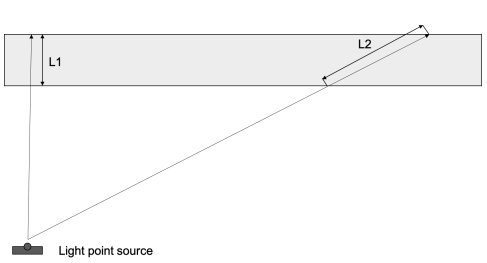

(a) A point source with its light rays

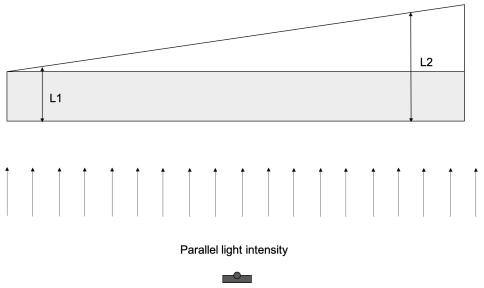

(b) modeled light intensity as parallel light rays

Figure 6.3: How a point source is modeled as if it were parallel light rays

6.1.3. Lambertian reflection

In the model the assumption is made that the reflection surface of the hydrostatic bearing is a lambertian surface. This means no matter what the angle of incident is it will always reflect back according to lambertian cosine law [3]. The lambertian law says the following:

$$I_{\text{reflected}=I_{\text{inc}}\cos(\theta)} \quad (6.1)$$

This is shown schematically in figure 6.4. This means the reflection of the reflected light of the incident light at the two sides of the bearing is less then in the middle of the bearing. This effect is also used in the model.

6.1.4. Inverse square law

Because we make use of a LED where we model it as a point source we have to implement the inverse square law to model the intensity arriving at the bearing surface. The intensity of light radiating from a point source

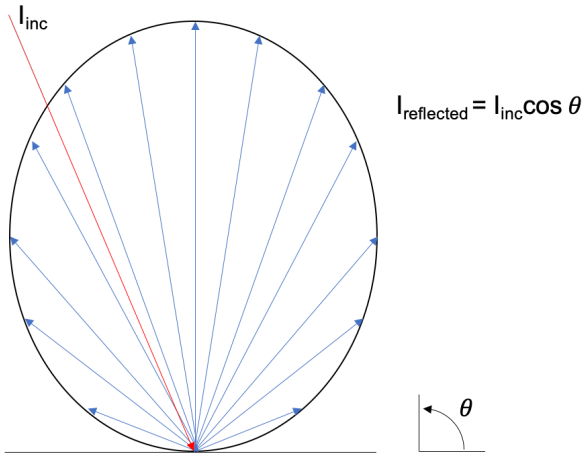

Figure 6.4: schematic overview of the Lambertian cosine law

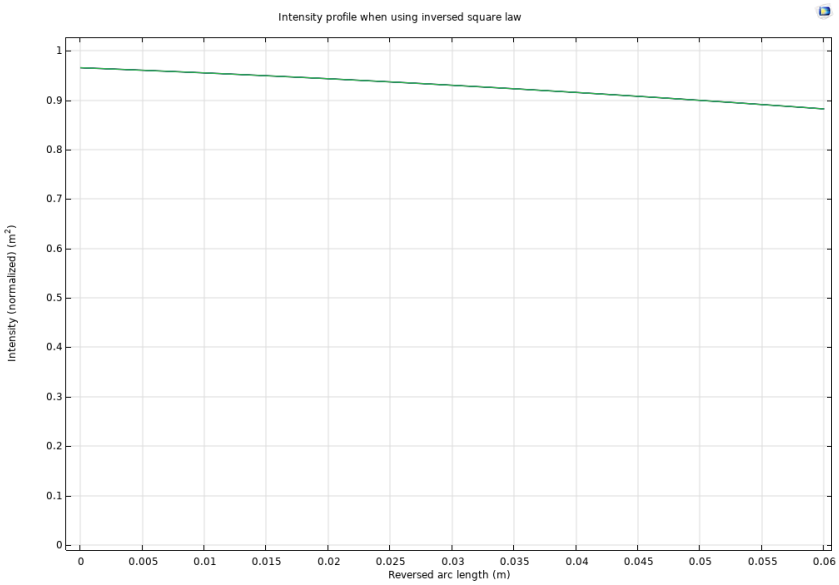

Figure 6.5: Intensity profile on the surface of the bearing due to inverse square law

is inversely proportional to the distance squared.

$$I \propto \frac{1}{r^2} \tag{6.2}$$

So if we implement this to our model this means we get an intensity profile that is quadratic. If the distances used in setup A would be implemented in the model, the intensity profile would look like something shown in figure 6.5

6.1.5. Reflection and transmittance

For the model it is also important to look at the effect of reflection and transmittance. Furthermore, the refraction of the light beam should not exceed the critical angle. How reflection, transmittance and refraction schematically looks like is shown in figure 6.6. With Fresnel equation the transmittance can be calculated per layer the light travel trough. To do so it is important to know the different refractive index of the material. This is shown in tabel 6.1.

By using derived Fresnel's equation [3], the reflection and transmission through the medium can be calculated. The equation is for reflection R and transmission T is shown below.

Material	Refractive index
Air	n = 1
PMMA	n = 1.49
Water	n = 1.3

Table 6.1: Refractive index of multiple materials

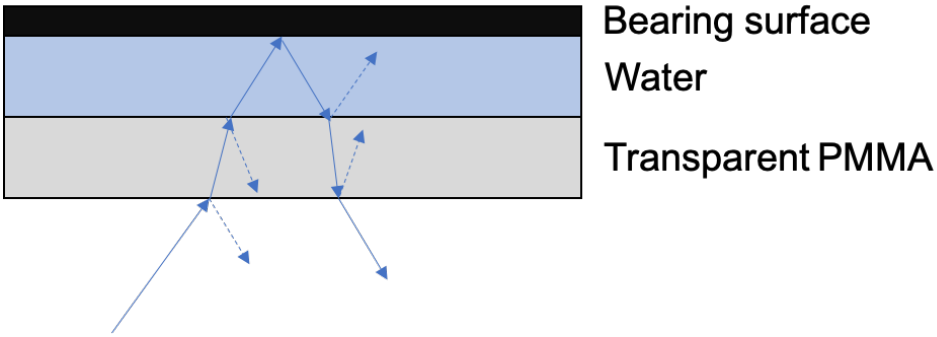

Figure 6.6: The reflection and transmittance of light trough different mediums with refraction

$$R = r^2 = |\frac{n_1 - n_2}{n_1 + n_2}|^2 \tag{6.3}$$

$$T = 1 - R \tag{6.4}$$

This means that the reflectance per layer transition can be determine. This is for $R_{a-p} = 0.04$ and for $R_{p-w} = 0.0055$. The reflectivity of the bearing is assumed to be 1. So if this is combined to determine the light intensity that is incident on the water layer, the incident light intensity becomes $I_{\text{inc}} = T_{a-p}T_{p-w} = 0.96 \cdot 0.995 = 0.955$. This means that the light recorded at the camera is 95.5% of the light that is imposed at the layer of water. The fluorescence light emitted from the water will also transmit 95.5% of the total light it emits. This is because both these signals go through the same layers. The ratio remains the same and therefore this effect can be neglected. For the case when $R_{h=0}$ the light also has the same layer it has to go through making the ratio effective to use.
The part reflected from the layer should effectively also be added to light intenisty signal received by the camera. Because this only applies for lightbeams that are specular reflected this does not have to be taken into account. The specular reflected light beam will not shine upon the camera, because the camera is positioned directly underneath the region of interest and the light source is placed at a distance from the camera, such that the light beams will hit the region of interest with an angle.

6.1.6. Wavelength analysis

For the analysis there has been looked per wavelength what the effect is of excitation, absorbance and emission. This has been done for the wavelength 500 till 580 nm with incremental steps of 10 nm. Per wavelength the LED has a certain relative intensity, this intensity is being absorbed by the liquid for a certain amount, from this absorption the light is being emitted according to the emission bandwith of the fluorescent particle. Furthermore, the bandwith is being measured by the RGB-camera. Each channel absorbs some amount of this light, which is taken into account. By summing all the fluorescent en reflected light per channel the total excitation and emission can be determined. This is being used in the results for the COMSOL analysis

6.1.7. Model

All the effects explain above have been implemented to determine the light intensity as function of width of the bearing. By using the equations explained in chapter 2, the fluorescent signal can be obtained. To obtain the results, the liquid film is modeled according to the dimension of the actual bearing with a film height of 100 μm. By using the the partial derivation equations, as a 'physics' in COMSOL, the simulated signal can be obtained.

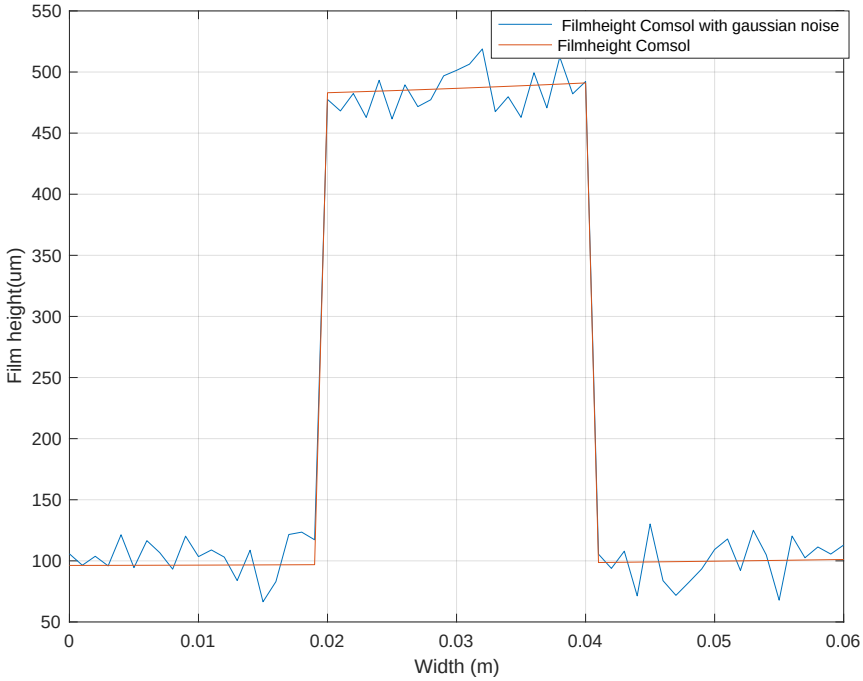

Figure 6.7: Film height modeled analytically with and without added Gaussian noise

6.1.8. Results of the COMSOL analysis

Figure 6.7 contains the film height determined analytically. Also a noise is added to the independent signals to obtain a results that is comparable to the measurement. The result from this figure is that when applying a small Gaussian noise the result also deviates from the mean. Figure 6.8 shows the different channels for the $R_{h=0}$ measurement and the fluorescent measurement, for both the analytical and the measured one. For the analytical channels a Gaussian white noise is added, which is not clearly visible. This resulted in the film height in figure 6.7. If the figures are compared it is clear that the lines do follow the same shape. However, for the fluorescent signal the green and red signals are of lower intensity. Due to the layer of liquid the intensity decreases, even if only water is used as liquid. Because only the ratio is of importance and both the green and red channels are decreased with the same amount in light intensity the ratio will remain the same. Therefore, this will not effect the measurement.

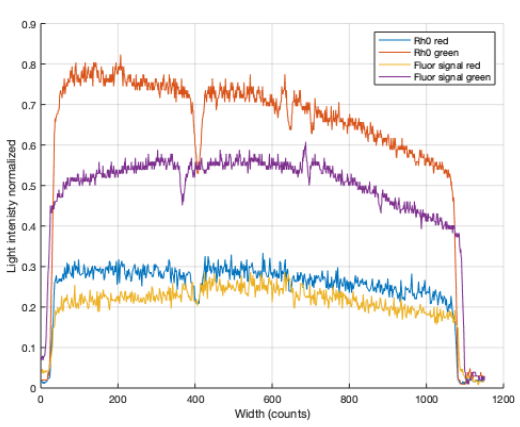

(a) Green and red channels measurement

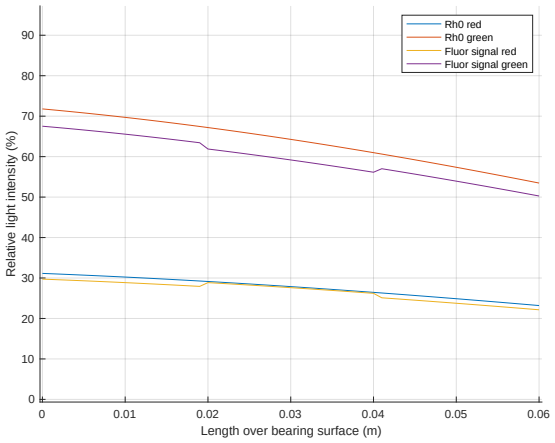

(b) Green and red channels analytically determined

Figure 6.8: Comparison of the measurement signals and the analytically determined

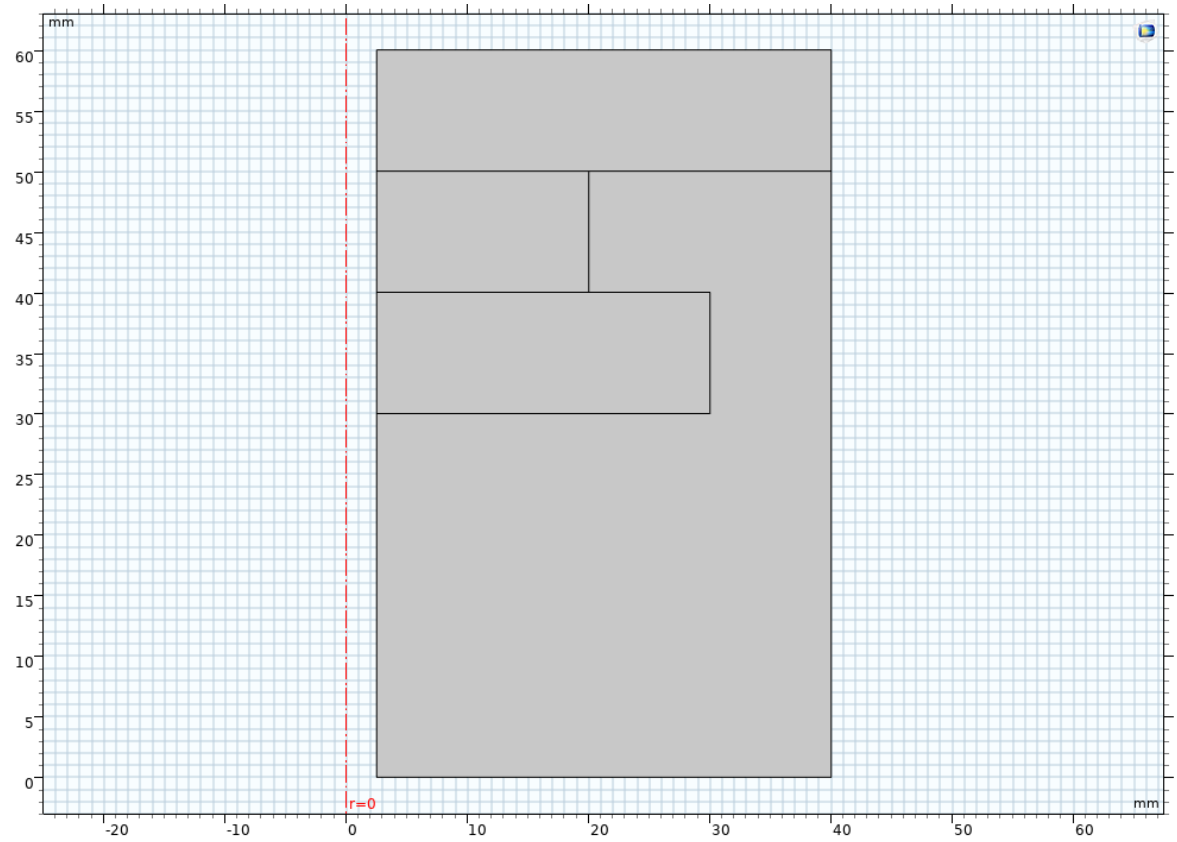

Figure 6.9: Geometry of compliant bearing used in COMSOL

6.2. Structural simulation

In order to compare the measured thickness profile with the simulated one, a FEM model has been build using COMSOL multiphysics. By analysing the outcomes of the Reynolds equations applied to the bearing surface, a pressure profile can be made. The pressure profile can than be used to apply as a boundary load of the silicone rubber. This process keeps iteration until a solution is found. In order to perform all these steps a model has to be build first.

6.2.1. Building a compliant hydrostatic bearing using COMSOL

First, we start by using 2D axissymmetric design plane. Now it becomes easier to apply Reynolds equations to a certain boundary. The bearing shape can be modeled as only a half of the cross section, this is shown in figure 6.9. The top part given the material properties of aluminum and the lower part is given self defined material properties shown in table 6.2

Property	Value
E	0.3 Mpa
Poisson ratio	0.49
Density	1 $\frac{kg}{m^3}$

Table 6.2: Material properties of self defined silicone rubber

Next up is to determine which multiphysics are needed for the analysis. To apply Reynolds boundary equation we are using 'General form boundary PDE'. Furthermore, to use the outcome of this Reynolds equation regarding the boundary imposing the pressure onto the bearing surface, the physics 'Solid Mechanics' was used. The last physics/mathematics is the 'Global ODE and DAE', this tool can solve the equation for a given certain load, which is useful when we want to determine it for multiple load cases.

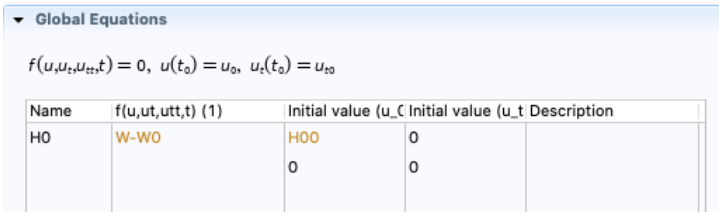

Figure 6.10: Settings for the Global ODE in COMSOL

Parameter	Value	Description
ν	8.9e-4 [Pa·s]	Dynamic viscosity water
H00	50e-6 [m]	Film height from which it start iterating
W0	50 - 150 [N]	Applied to load to the bearing
Ps	0.8e5 [Pa]	Supply pressure
Qc	9.3e-11 [$\frac{m^4 \cdot s}{kg}$]	The resistance of the capillary restrictor, determined in chapter 3

Table 6.3: Parameters used in COMSOL

For the 'General form boundary PDE' the first thing to do is to set the dependant variable to P. Next, the the general form PDE1 should be selected and the Reynolds equation can be filled in for the conservative flux at r. The bottom line should be selected and the equation corresponding to the Reynolds equation is:

$$T = \frac{-H^3}{12\nu} \cdot r \cdot PTr \tag{6.5}$$

Next up, a Flux/source should be added. Therefore the point at the bottom closest to the red axissymetric line should be selected. Here the Flux/source can be set to $Qc \cdot (Ps - P)$. And lastly the boundary Dirichlet condition needs to be added. by selecting the outside point at the bottom, and by setting the value to zero.
To use the solid mechanics three extras needs to be added. That are, a fixed constraint, a boundary load and a prescribed displacement. For the fixed constraint the top line should be selected. For the boundary load the bottom line needs to be selected and the load type set to pressure. For the pressurs P should be filled in. The prescribed displacement can be set to zero in r direction when the bottom line is selected.
At last the global ODE and DAE should be filled in accordingly to figure 6.10.

The following step is to fill in all the parameters. These parameters can be found in table 6.3

Two last things need to be adjusted before the simulation can run. In component-definitions-variable a variable needs to be implemented. That is total film height H and this should equal $H = H0 + w$. This consists of the H0, the calculated film height for the applied load and the deformations of the silicon due to the imposed pressure profile w. The last thing is a integration needs to be added over the boundary layer. This is the integration of the pressure over the bearing surface resulting in a load. This can be done using the command $intop1$. The calculated load W is compared to the self defined load $W0$. The model will iterate to a load which is equal to the self defined load, see Figure 6.10.

6.2.2. Results of COMSOL simulations

The results coming from the COMSOL simulations can be chosen properly. The film height, pressure distribution, flow and deformations of the bearing can be plotted in 2D and 3D. Figure 6.12 shows the film height of the hydrostatic bearing for 4 load cases. This is for 50 N, 75 N, 100 N, 150 N.

And if we look at the film height corresponding to the different load cases at a cross-section through the middle, we can see the results plotted in figure 6.11. What can be noticed is that the film height in the middle of the bearing does not change that much, but it is clearly shown how the bearing creates a pocket. By creating this pocket, the pressure distribution changes resulting in a higher load capacity. Furthermore, although the film height in the middle does not change a lot. The film height at the edges does becomes smaller. Between the 50 N and the 150 N this difference becomes 300 μm.

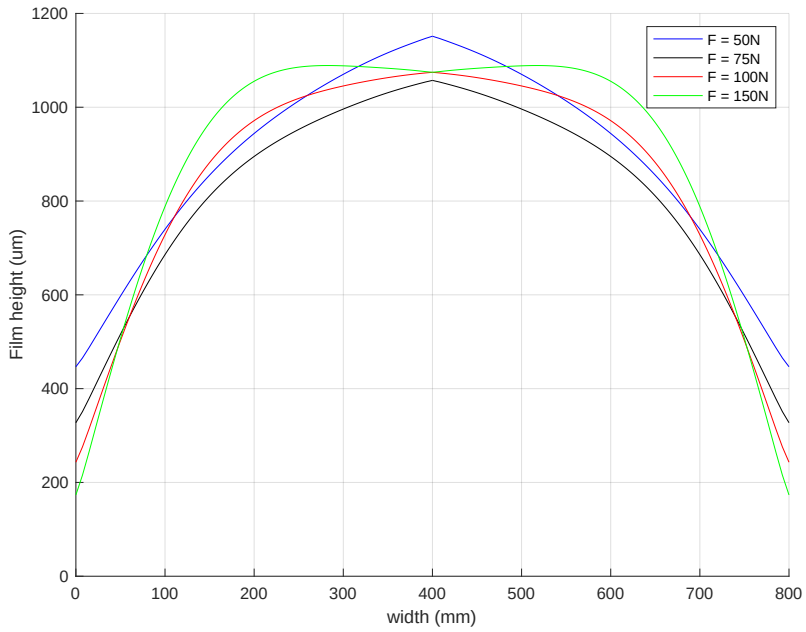

Figure 6.11: Film thickness of the compliant hydrostatic bearing for four loadcases at cross-section

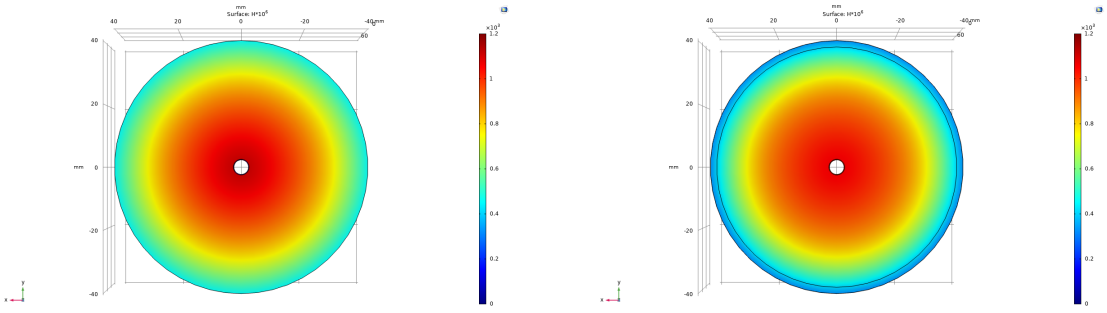

(a) F = 50N

(b) F = 75N

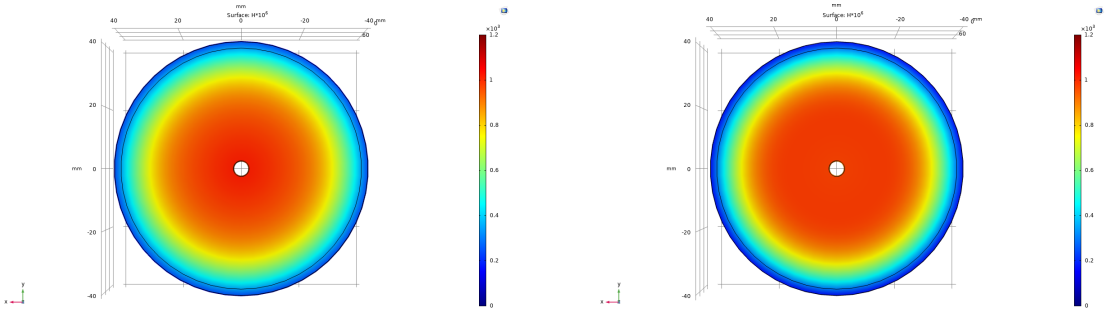

(c) F = 100N

(d) F = 150N

Figure 6.12: Film height of the compliant hydrostatic bearing for different load cases

7

Discussion

This chapter will discuss the main results of this study. First, the fluorescent measurement of setup A will be discussed, and thereafter that of setup B. Then, the COMSOL simulated results will be discussed

7.1. Measurement setup A

7.1.1. Fluorescence

By using fluorescent particles dissolved in water a fluorescent liquid can be achieved. In this measurement a trade-off has to be made by the concentration dissolved in water. The more fluorescent dye is added the more clear the fluorescent signal will becomes. However, the incident light reflected from the surface of the bearing would be less due to Beer-Lambert's law and therefore the measured reflected incident light cannot be used as comparison signal. For small film heights (>15 μm) a higher concentration is desired to obtain a signal which is useable. Another aspect of using these fluorescent particles is that they stick to certain bearing surfaces. This means that when taking an image these particles sticking to the surface will create an error in the measurement, therefore a offset value is introduced. The offset value is found to be constant and does not change over time, therefore it does not form a problem

7.1.2. Image noise

The noise of the image is around 10 % of the mean signal. This noise can inflict large deviation, which is unwanted. To reduce or minimize the noise multiple measurements (read: images) can be taken to average the signal and therefore creating a better resolution result. An alternative method is taking a movie, consisting of multiple images. The downside of taking a movie is that the resolution of each image is lower and therefore make the measurement less precise.

7.1.3. Fluorescent dye

In this work there has been chosen to use Rhodamine B as fluorescent dye. This dye has an excitation and emission wavelength of 535 nm and 570 nm respectively. The results in a stoke shift of 35 nm. Perhaps one could improve the measurement by choosing a dye that has a larger stoke shift, such that the emitted bandwidth of the fluorescence is not again absorbed by the the fluorescent dye resulting in a lower fluorescent signal. By using another fluorescent dye with a greater stoke shift, this could mean it is not soluble in water. Another disadvantage could be that the excitation and emission wavelengths are not in the visible spectrum and therefore a more complex camera system is needed. Furthermore, A light source can be chosen that has a smaller wavelength bandwidth and therefore only emitting light at the excitation wavelength of the fluorescent dye and therefore minimizing leakage. This could be achieved by for instance using a laser, but due to the small area that is being illuminated, multiple lenses should be used to illuminate the whole surface of the bearing. This would make the setup more complex.

7.2. Measurement setup B

7.2.1. Alignment

In this measurement setup a pneumatic cylinder is used which actuates the compliant bearing. This means it only has one degree of freedom and the bearing is only suspended by the cylinder piston. The piston of the cylinder has a wiggle and therefore the alignment of the bearing to the plate becomes complex. The compliant bearing can absorb some of that misalignment, but to improve the measurement validation of the measurement a new setup could be designed which eliminates the small tilt.

7.2.2. Repeatability

Due to the PLA plate underneath the compliant bearing, it was possible to measure the film height of the bearing. But it was found that repeatability is small. The reason for this is that the PLA is not rigid connected to the bearing itself, therefore it is able to move independently. Furthermore the middle of the PLA piece, the tube, sticks out the bearing with a small distance (1 mm). This results in that when the solution flow underneath the bearing, the bearing reacts as a diffuser and therefore the PLA plate creates a vacuum between the plat and the counter surface. Therefore measuring with this configuration is complex and most results show a film height near zero. A new compliant design could solve this problem, where the total compliant bearing and the PLA piece are one solid component.

7.3. COMSOL results

7.3.1. Fluorescence

The fluorescence result in COMSOL shows that the final ratioed signal does contain noise inflicted by the red and green channel noise. Due to the ratio the smaller perturbations of the red and green channel result therefore in larger perturbations in the ratioed result. This means that obtain a result with less noise can become complex. This can however be improve by not using the ratioed technique and only use the fluorescent signal as the film height. But by not using the incident light signal as a reference, the spatial information of the incident is lost and therefore the film height does contain other errors.

7.3.2. Compliant bearing model

Because the bearing is modelled as an isotropic uniform silicon rubber part, the model deviates from the actual bearing. Due to small air bubbles in the silicon, the stiffness throughout the compliant material can differ. Another reason for this could be due to the fact that the material is modeled as linear elastic, while the material could suffer from non linear effects. Furthermore, the silicon rubber consist of two components that need to be mixed. This is mixed with a one on one ratio. Due to non optimal mixing, this results in different moduli of elasticity throughout the bearing. To improve this perhaps a vacuum chamber can be used to get rid of the majority of air bubbles.

7.3.3. Fluorescent sensitivity

The COMSOL results show that small perturbations in a received signal can give larger noise in the result. The reason for this is that the signal are being ratioed and therefore lead to a greater noise. This can be reduced by taking multiple measurements such that those perturbations becomes even smaller. Furthermore, the use of a monochrome camera with bandfilter and a light source which emits light from only small bandwidth wavelength. This could result in a smaller signal-to-noise, because the leakage effect is minimized. This should also improve the range of the measurement.

8

Conclusion

In this work, a fluorescence based measurement technique to obtain film height regarding compliant hydrostatic bearings has been presented. This has been validated using setup A, which has a rigid hydrostatic bearing with known features. The performance of the method is limited by its optical thickness at the top of the operating range and at the bottom limited by the weak fluorescent signal compared to the incident light. Both these limitations can be improved upon by using a concentration of fluorescent particles suited for the application. Another method of increasing the lower limit is by decreasing the amount of leakage by using a smaller bandwidth light source. Furthermore, calibration of this method has been presented by using a feeler or calibration ring with known dimensions, resulting in a offset and a scaling factor to obtain the actual film height. Due to the offset being constant this does not affect the result. The results of the paper show that the measurement technique is able to measure the film height over the whole surface of a compliant hydrostatic bearing. Because the compliant bearing has large deformations the standard deviation of the measurement method will fall within the accuracy bound. Following, the most important conclusions of this work are summarized.

- The measurement method has a operating range of 15 - 1400 μm, limited by its optical thickness and the fluorescent signal compared to the incident light signal.
- A calibration tool needs to be introduced to couple the measured signal to film height, in the form of a feeler or a calibration ring.
- The method could measure with a an average accuracy of 6.4% and a 95% average confidence interval of 15.2 μm. This can be improved by minimizing the leakage effect.
- The compliant hydrostatic bearing has a comparable shape and film height predicted by COMSOL and therefore COMSOL can be used to check the deformations and film height of the compliant bearing.

9

Recommendations

This chapter provides some recommendations for further research. The use of a fluorescent measurement system for compliant hydrostatic bearings shows great potential as presented in this work. To do more research in the field of compliant hydrostatic bearing and a fluorescent measurement method a list of recommendations is given:

- To improve the fluorescent measurement a monochrome camera with optical filter can be used to better separate the excitation and emission wavelength. Although the use of optical filter would decrease the amount of intensity, a difference in both the excitation wavelength and emission wavelength will be better noticeable.
- Search for a fluorescent dye with a greater stoke-shift. This would minimize the leakage and a more clear fluorescent signal would be obtained
- Investigate the concentration of fluorescent dye. The fluorescent signal will be greater with a higher concentration. This will result in a brighter intensity of the fluorescence. Investigate the effect of optical thickness and its limitations
- Investigate the background noise, such as reflections from the frame. Only a mask has been introduced in this work. Perhaps the frame does influence the measurement.
- Use a light source with a small bandwidth wavelength, preferably no leakage occurs.
- Redesign a compliant hydrostatic bearing such that a PLA plate is connected to the rest of the compliant material. An improved bearing design could be tested and compared to a FEM model resulting in a better comparison
- Improve methods of casting the silicon, better mixing and remove the air bubble forming in the material. This would result in a uniform material and therefore the FEM model will be more accurate to the actual bearing.

A

Matlab code

Film height determinitaion

```
close all
clc
clear all

format long

% parameters
a = 500/0.0875;   %Scaling factor
b = 450;    %offset value


%Import images
Rh0 = imread('Test_30_7/rh0_80.70_4.bmp');
Im1 = imread('Test_30_7/80.70_8.bmp');
Im2 = imread('Test_30_7/80.70_9.bmp');
Im3 = imread('Test_30_7/80.70_10.bmp');
lenscap = imread('Test_30_7/lenscap.bmp');



%convert 0-255 to double value between 0-1
Rh0 = im2double(Rh0);
Im1 = im2double(Im1);
Im2 = im2double(Im2);
Im3 = im2double(Im3);
lenscap = im2double(lenscap);


%Determine region of interest [x,y,dx,dy]
rect = [716,200,1150,1150];

%Crop image to region of interest
Rh0 = imcrop(Rh0,rect);
Im1 = imcrop(Im1,rect);
Im2 = imcrop(Im2,rect);
Im3 = imcrop(Im3,rect);
lenscap = imcrop(lenscap,rect);

%Green channel lenscap and red channel lenscap
lenscapR = lenscap(:,:,1);
lenscapG = lenscap(:,:,2);

%Determine ratio of signal and R_h=0
R_0 = (Rh0(:,:,1)-lenscapR)./(Rh0(:,:,2)-lenscapG);
R1 = (((Im1(:,:,1)-lenscapR)./(Im1(:,:,2)-lenscapG))-R_0).*a - b;
R2 = (((Im2(:,:,1)-lenscapR)./(Im2(:,:,2)-lenscapG))-R_0).*a - b;
R3 = (((Im3(:,:,1)-lenscapR)./(Im3(:,:,2)-lenscapG))-R_0).*a - b;

%Use gaussianfilter to filter result
R1 = imgaussfilt(R1,15);
```

```
R2 = imgaussfilt(R2,15);
R3 = imgaussfilt(R3,15);

% Give NaN to signal outside the diameter where you look at
for i=1:1151;
    for j = 1:1151;
        if (i-550)^2 + (j-550)^2 > (0.5*1020)^2
            R1(i,j) = NaN;
            R2(i,j) = NaN;
            R3(i,j) = NaN;
        end
        if R1(i,j) >1000
            R1(i,j) = 1000;
        end
        if R1(i,j) < -50
            R1(i,j)=0;
        end
        if R2(i,j) >1000
            R2(i,j) = 0;
        end
        if R2(i,j) < -50
            R2(i,j) = 0;
        end
        if R3(i,j) >1000
            R3(i,j) = 1000;
        end
        if R3(i,j) < -50
            R3(i,j) = 0;
        end
    end
end


%Reference signal line cross-section
B = ones(1,1100);
B(1:400) = B(1:400)*115;
B(401:730)=B(401:730)*490;
B(731:1100) = B(731:1100)*115;

%Reference signal line features
A = ones(1,1100);
A(1:230) = A(1:230)*115;
A(231:361)=A(231:361)*460; %250 voor yhoogte800
A(362:785) = A(362:785)*115;
A(786:960) = A(786:960)*410; %350 voor yhoogte800
A(961:1100) = A(961:1100)*115;


%plot results in figure
figure
hold on
grid on
plot(R1(630,40:1070),'k')
plot(R2(630,40:1070),'r')
```

```
plot(R3(630,40:1070),'b')
legend('measurement 1','measurement 2','measurement 3')
ylabel('Film height (um)')
xlabel('Width (counts)')

%Plot result in height map
figure
mesh(R2)
xlabel('Width (counts)')
ylabel('Height (counts)')
c=colorbar
c.Label.String = 'Film height (um)';
```

```
c =

  ColorBar with properties:

    Location: 'eastoutside'
      Limits: [-49.902141672122561 9.999434060940740e+02]
    FontSize: 9
    Position: [1×4 double]
       Units: 'normalized'

  Use GET to show all properties
```

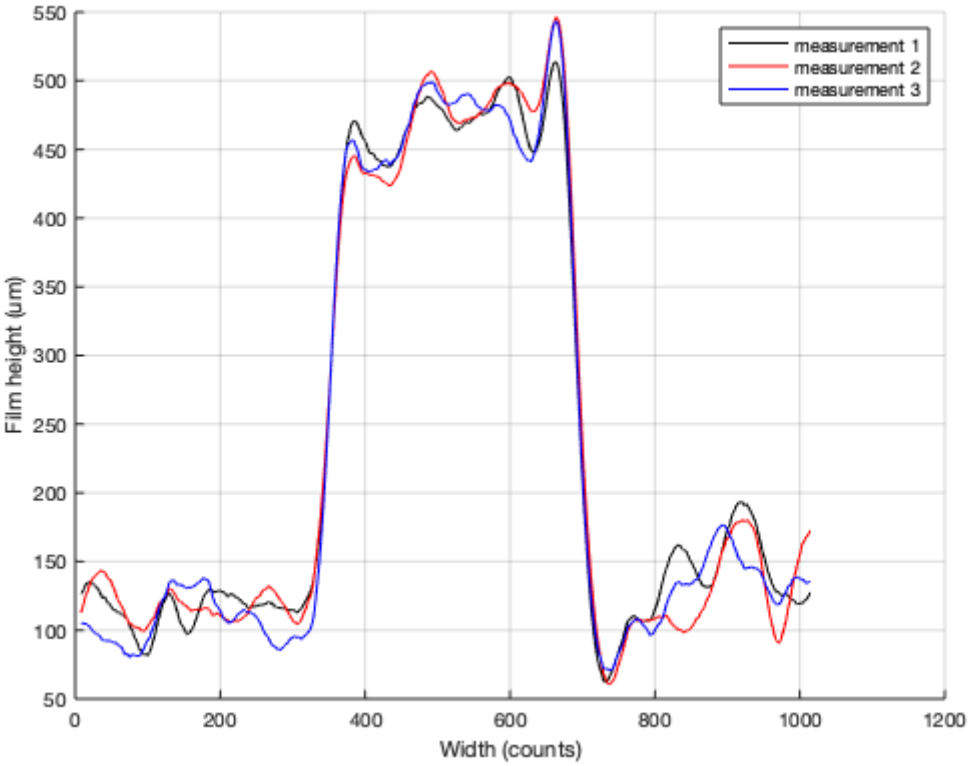

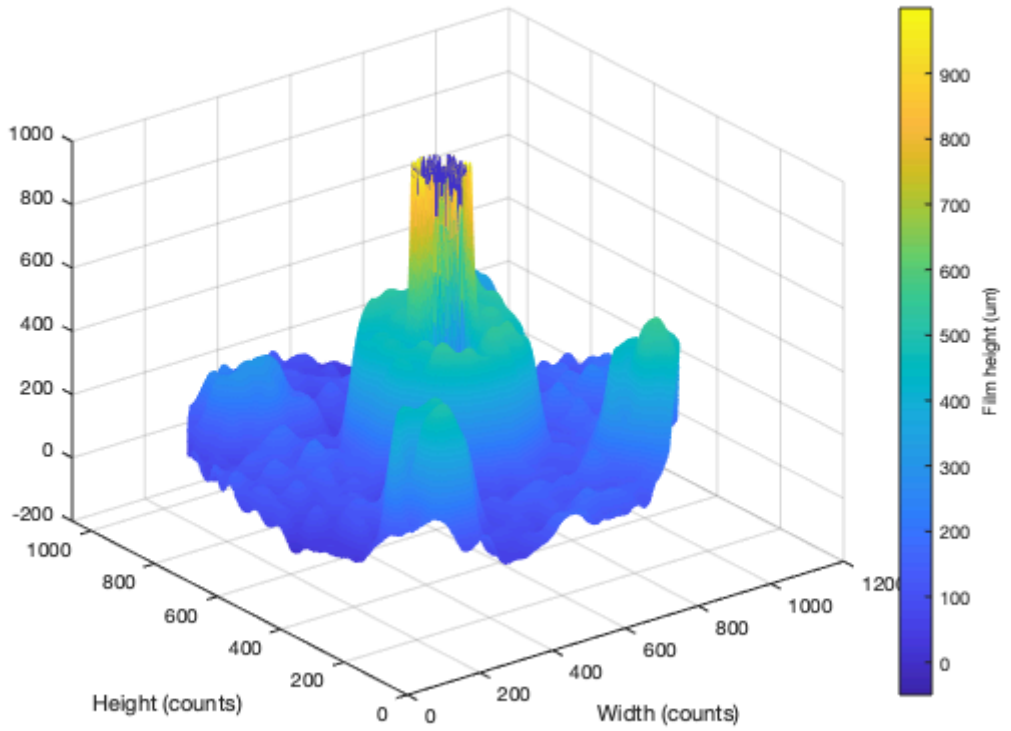

standard deviation and confidence

```
%define empty matrix
M_all = zeros(3,1151);

% Insert ratios into empty matrix
M_all(1,:) =R1(625,:);
M_all(2,:) =R2(625,:);
M_all(3,:) =R3(625,:);

%Determine the mean and standard deviation
M_mean = mean(M_all);
M_std  = std(M_all);

%Determine the confidence interval and variance
M_interval = (1.96/sqrt(3)).*M_std;
M_upper = M_mean+M_interval;
M_lower = M_mean-M_interval;
var = M_interval./M_mean;

%Determine the filmheight at different positions
mean_flyheight1 = mean(M_mean([1:360 750:1050]));
mean_flyheightpocket = mean(M_mean(400:740));
mean_interval = mean(M_interval([1:360 750:1050]));
mean_intervalpocket = mean(M_interval(400:740));
```

```
%Plot figure with upper and lower condfidence interval
figure
grid on
hold on
plot(M_upper(1:1050),'r')
plot(M_mean(1:1050),'b')
plot(M_lower(1:1050),'r')
xlabel('Width (counts)')
ylabel('Film height(um)')
legend('Upper confidence 95%','Mean of measurements', 'Lower
 condfidence 95%')
```

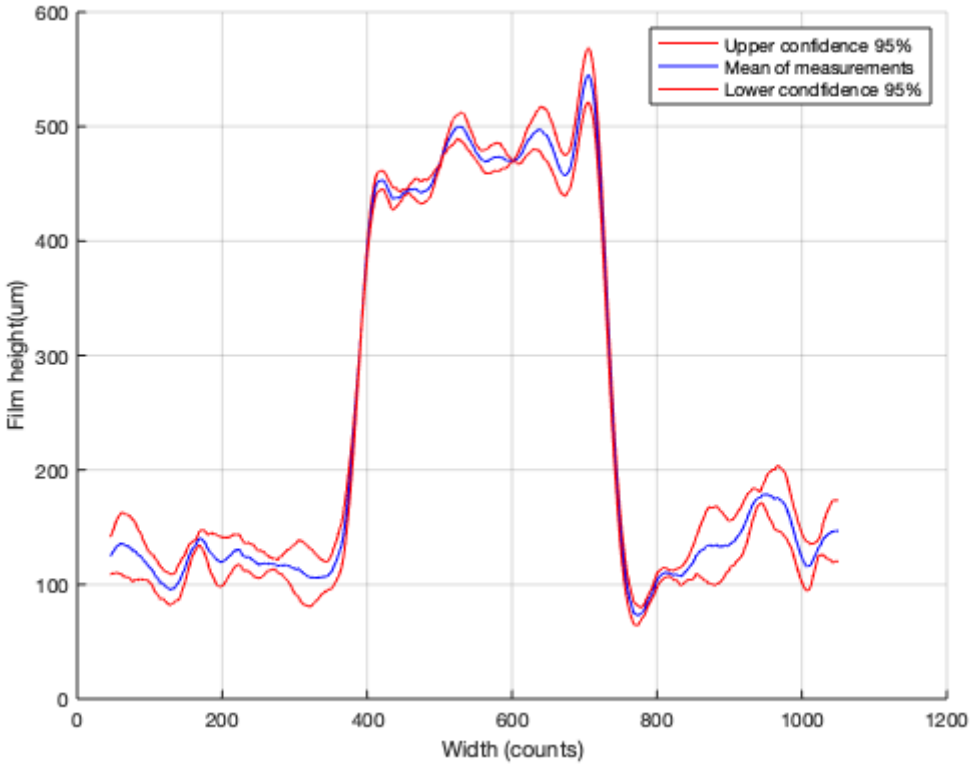

Published with MATLAB® R2019b

Intensity plot Linearization of the absorbtion

```
close all
clc
clear all

%parameters
x = 10:10:6000;
x=x.*10^-6;
C = 4e-6;        %Concentration
E = 10800000;    %extinction in m-1 M-1
o = 0.7;         %quantum efficiency

for i = 1:600

    f(i) = 100*exp(-C*x(i)*E)*o*x(i)*C*E;
    Lin = (0.27087/9e-5)*x+ 0.00013;

end


plot(x.*1000,f,x.*1000,Lin)
grid on
legend('fluorescent light intensity as function of
 thickness', 'Linearization of fluorescent light intensity')
xlabel('Film tickness (mm)')
ylabel('Fluorescent light intensity (counts)')
```

Comsol data processing

```
clear all
clc
close all

%import text data from comsol
I = importdata('I_400mu60.txt');
If=importdata('If_I_400mu60.txt');

%write string to double
I = str2double(I);
If = str2double(If);

%Wavelengths used and corresponding power distribution from LED
lambda = [500 510 520 530 540 550 560 570 580];
LED =[0.25 0.55 0.94 0.9 0.63 0.38 0.21 0.13 0.05];

%Writing relative power distribution to absolute power distribution
 for i=1:length(LED)
LED_partialpower(i) = LED(i)/sum(LED);
 end


%Preparing data for analysis, removing text from file
I=I(4:end,5);
I_rh0= If(4:end,6);
If=If(4:end,5);
Size=size(If);
num_of_cutline = Size(1)/9;
x=linspace(0,0.06,num_of_cutline);


%Determine how many cutlines used in comsol
for j=1:9
    for i=0:num_of_cutline-1
    I2(j,i+1) = I(i*9+j);
    If2(j,i+1) = If(i*9+j);
    I_rh02(j,i+1) = I_rh0(i*9+j);
    end
end

%relative respons of camera sensor for RGB
green = [0.81 0.88 0.92 0.93 0.91 0.9 0.85 0.8 0.75];
red = [0.01 0.02 0.07 0.07 0.03 0.04 0.075 0.31 0.58];


%Emission intensity relative of the rhodamine B particles
emission=[0.18; 0.30; 0.29; 0.21]; %[550 560 570 580] nm

%Multipline data from comsol with the camera response for RG
for i = 1:9
```

```
    I_green_out(i,:) = I2(i,:)*green(i);
    I_red_out(i,:) = I2(i,:)*red(i);
    I_rh0_green(i,:) = I_rh02(i,:)*green(i);
    I_rh0_red(i,:) = I_rh02(i,:)*red(i);
end

% Determining the total amount absorbed by camera
If2 = sum(If2);
If_spectral = If2.*emission;
If_spectral = If_spectral.*[0.04; 0.075; 0.31; 0.58]; %absorption of
 red of camera sensor
If_total_red = sum(If_spectral);
I_green_out = sum(I_green_out);
I_red_out = sum(I_red_out);
I_rh0_red = sum(I_rh0_red);
I_rh0_green = sum(I_rh0_green);



% Add signal nois to data
R0 = awgn(I_rh0_red,41);
R = awgn(I_red_out,41);
G0 = awgn(I_rh0_green,41);
G = awgn(I_green_out,41);

%determin the ratio for film height
I_green_out2 = I_green_out.*0.95;
ratio = (If_total_red+I_red_out)./(I_green_out) - I_rh0_red./
I_rh0_green;
ratio2 = (If_total_red + R)./G - R0./G0;

%plot individual R,G channels
figure
hold on
grid on
plot(x,I_green_out2)
plot(x,I_rh0_green)
plot(x,(If_total_red+I_red_out)*6*0.95)
plot(x,I_rh0_red*6)
plot(x,G*0.95)
plot(x,G0)
plot(x,(If_total_red+R)*6*0.95)
plot(x,R0*6)
legend('Green','rh0 Green', 'Fluorescent Red', 'rh0 Red')
xlabel('Length over bearing surface (m)')
ylabel('Relative light intensity (%)')


%Plot ratio found
figure
plot(x,ratio2*(800/0.009),x,ratio*(800/0.009))
legend(' Filmheight Comsol with gaussian noise','Filmheight Comsol')
xlabel('Width (m)')
ylabel('Film height(um)')
```

```
grid on

%Plot power distribution of LED and response of camera
figure
hold on
grid on
title('LED incident light power distribution')
xlabel('Wavelength (nm)')
ylabel('relative response (%)')
plot(lambda,red,'r')
plot(lambda,green,'g')
plot(lambda,LED)
legend('LED incident light bandwidth')
```

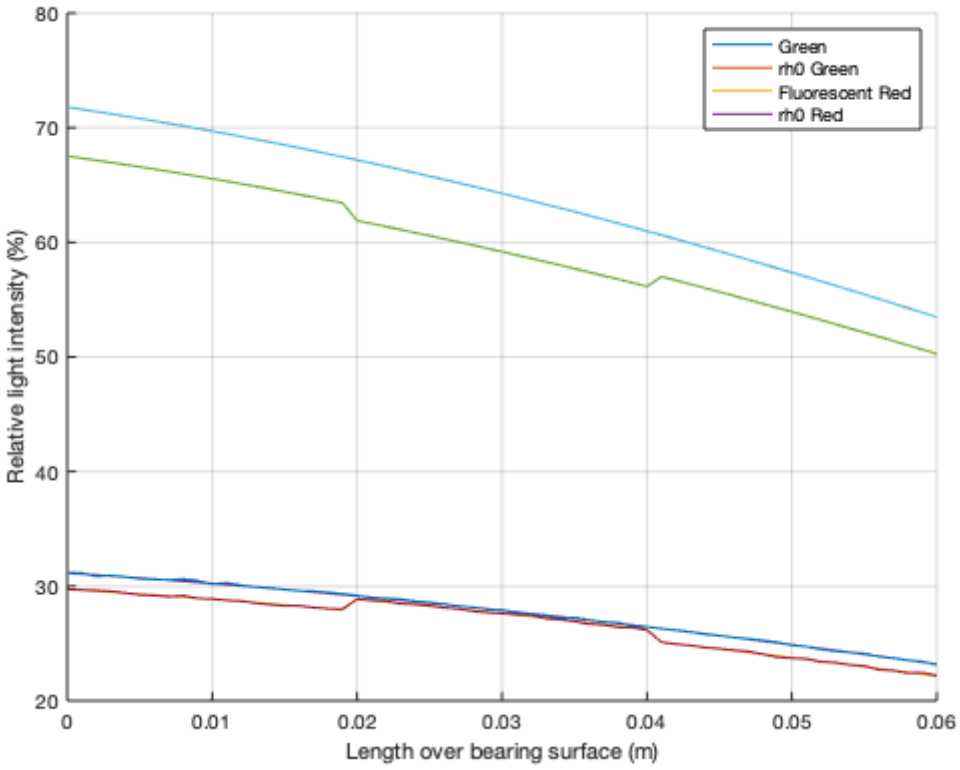

B

Manual for measuring

This manual helps to repeat the measurements. This manual will show all the step I took to do a measurement.

B.1. Preparation software

First, it is useful to make sure your computer is connected to a power supply and the cables of the LED and the camera are disentangled. Then we can start the PIXELINK software, it will probably say that there are no cameras attached. Then we can attach the camera USB cable to your computer. It is important that the USB cable is attached to a USB port that can deliver some power to the camera. If all goes accordingly, the screen shown in figure B.1 will appear. In the left window at the 'Control' tab, you can scroll down to the white balance settings. It is important to first click on 'AUTO' before you enter the values for RGB. The values to set for RGB should be: [R,G,B] = [8, 0.7, 0], this is shown in Figure B.2. Next, click on the 'Capture' tab to fill in the location of the image and the filename of the image in the left top corner, see Figure B.3. If this is done properly a test image can be taken by pressing the camera button on the bottom of the screen, see Figure B.3

B.2. Preparing hardware

For the preparation of the hardware a few steps need to be taken. The pressurized needs to be attached (figure B.4) and the power supply of the water pump needs to be attached. For the air it is important to make sure the pressure is set to zero. This can be seen on the pressure gauge connected to the air tube. Next, the bearing surface needs to be cleaned. This can be done by using a cloth and spraying some isopropanyl onto it. With this cloth you can clean the bearing surface, see Figure B.5. It is also usefull to clean the PMMA. The box

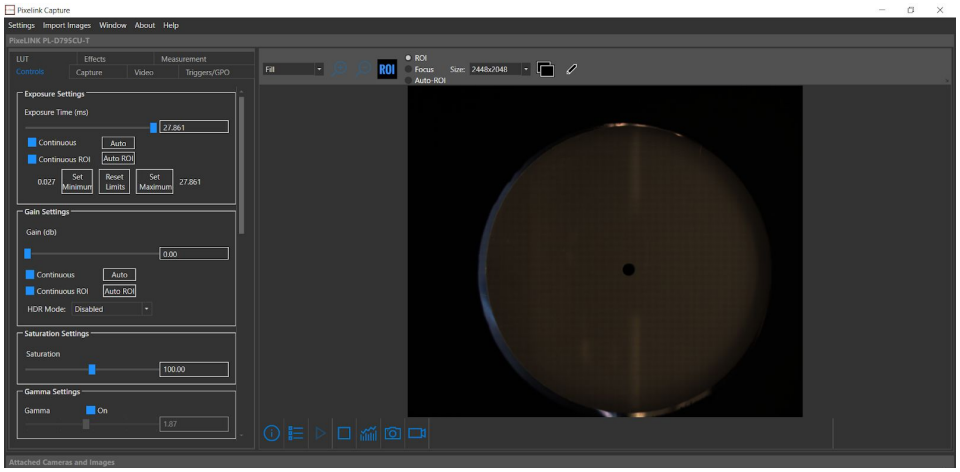

Figure B.1

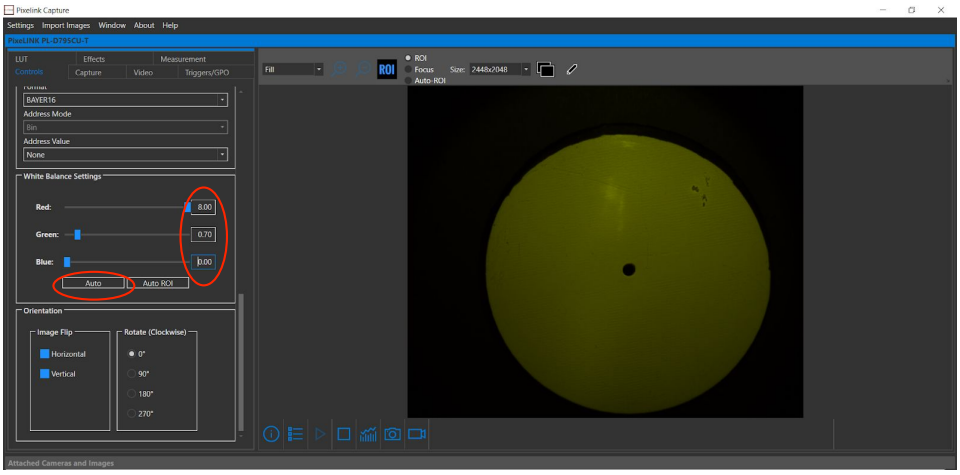

Figure B.2

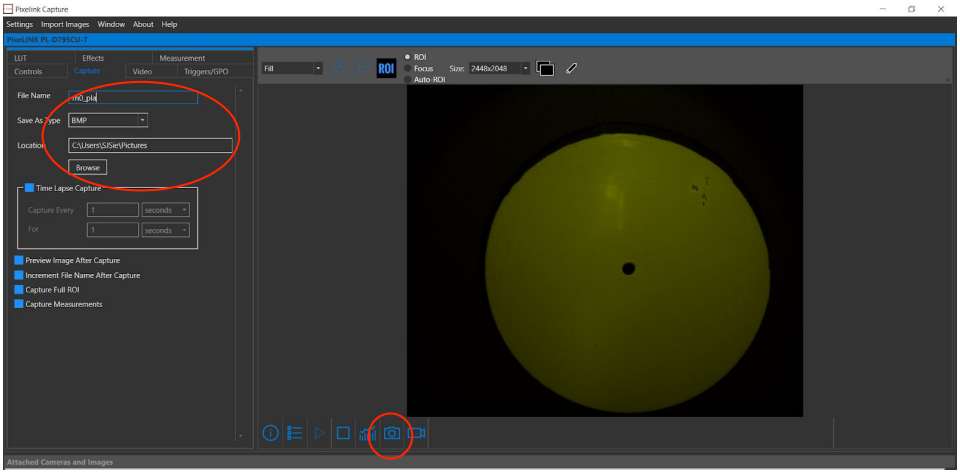

Figure B.3

Figure B.4

containing the fluorescent solution needs to be placed at three other boxes. This is to make sure the drainage can flow back in the water box, see Figure B.6

B.3. Measuring

To start first place the bearing and manifold onto the pneumatic piston coupling piece. This is shown in Figure B.7a. Next, a image needs to be taken for the $R_{h=0}$. This can be done via the PIXELINK software, make sure the LED USB is connected to your computer and The bearing needs to be touching the PMMA. Furthermore, The lit of the box needs placed on top. It can be that the USB cable holes in the box let some light trough, therefore a cloth is placed over it to minimize the influence of external light. The following step is to measure with a film. To then do a measurement I always first put the water pump on. This can be done by placing the banana plugs of the water pump to the power supply, see figure B.8a. Next, it is very important to look at the tray and check if it overflows, see Figure B.8b. Sometimes the drainage tube leading back to the water box cannot flow. You then have to wiggle the tube a little bit around and make sure the drainage point is the 'highest' such that the water flow 'down'. If this is successful, you can apply force to the bearing by adjusting the top knob of the pressure gauge connected to the air tube. The relation of pressure to force is 1 bar is equal to 50N. Before a image is taken check the bearing surface whether a full film is achieved. Some air bubbles can be eliminated by rotating/pushing on the bearing. Finally, take a image with the PIXELINK software, with a changed filename, as explained before.

(a) place some isopropanyl on cloth

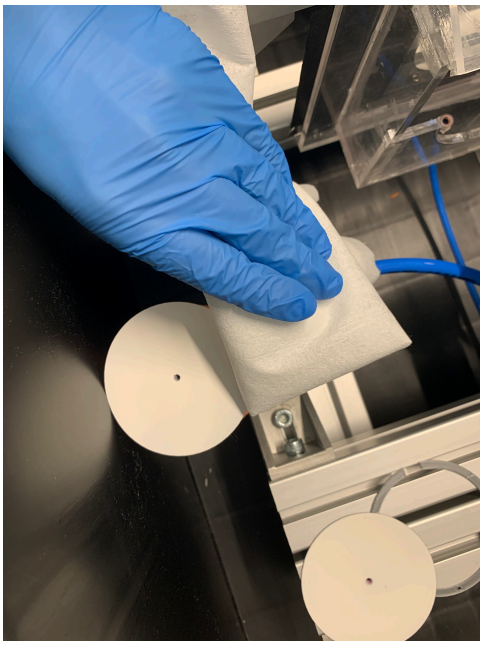

(b) Clean the bearing surface with the cloth

Figure B.5

(a) box on the counter

(b) box in the right position

Figure B.6

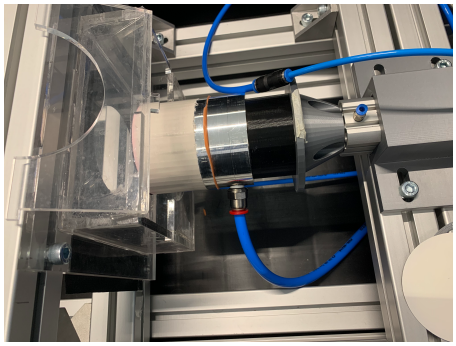

(a) Attached the bearing to the pneumatic piston

(b) Cloth placed over the USB hole

Figure B.7

(a) Attaching the power supply

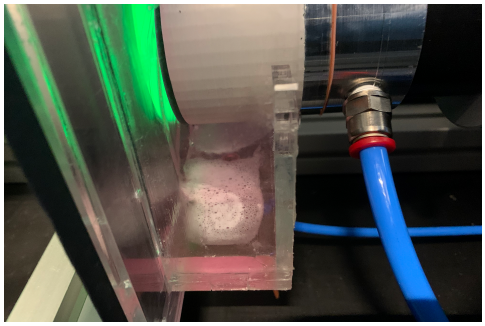

(b) Check if the tray fill with liquid, in this picture it is to full

Figure B.8

B.4. Summary of steps

This gives a summary of steps need to be taken to do a measurement

- clean bearing surface and the PMMA
- Place the bearing back on the piston
- Push by hand the bearing against the PMMA
- Make sure the LED is turned on
- Take the $R_{h=0}$ image
- Turn the water pump on
- Apply air pressure to the pneumatic cylinder
- Take the fluorescent image
- Remove air pressure and turn the water pump off
- Remove the bearing from the piston
- Clean the bearing surface and the PMMA

TO do another measurement follow again the steps perfomer above.

C

Drawings Solidworks

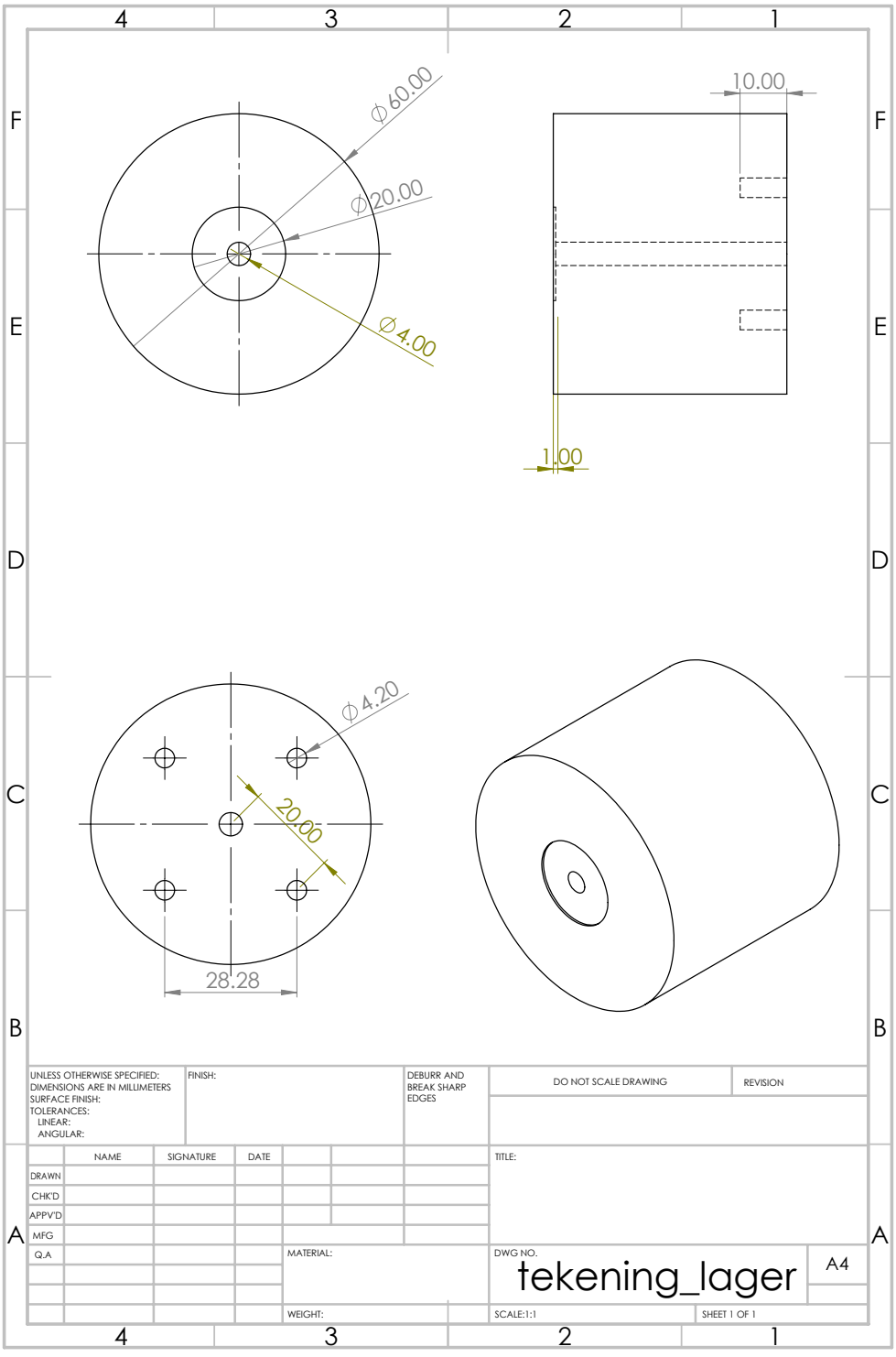

UNLESS OTHERWISE SPECIFIED: DIMENSIONS ARE IN MILLIMETERS SURFACE FINISH: TOLERANCES: LINEAR: ANGULAR:		FINISH:		DEBURR AND BREAK SHARP EDGES		DO NOT SCALE DRAWING		REVISION
	NAME	SIGNATURE	DATE				TITLE:	
DRAWN								
CHK'D								
APPV'D								
MFG								
Q.A				MATERIAL:		DWG NO.		A4
						tekening_lager		
				WEIGHT:		SCALE:1:1	SHEET 1 OF 1	

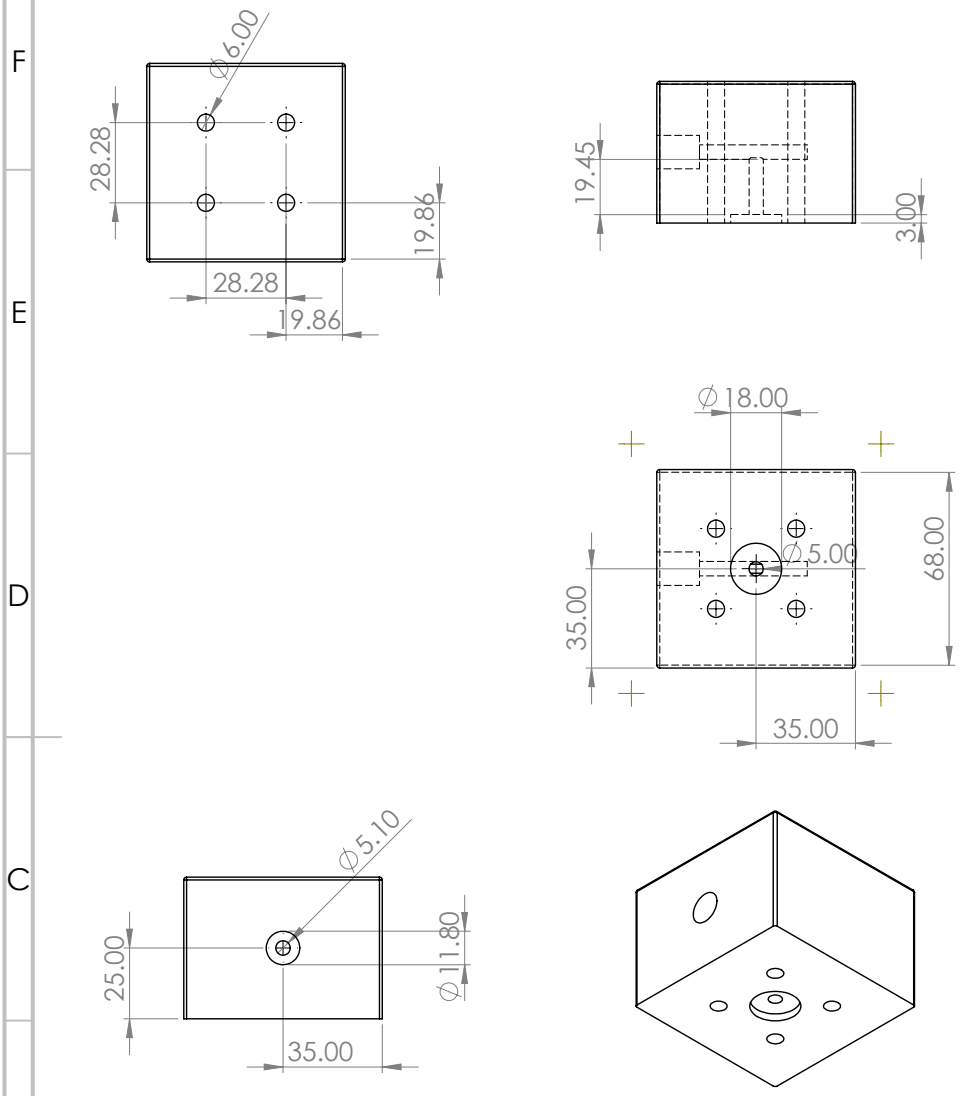

UNLESS OTHERWISE SPECIFIED: DIMENSIONS ARE IN MILLIMETERS SURFACE FINISH: TOLERANCES: LINEAR: ANGULAR:	FINISH:		DEBURR AND BREAK SHARP EDGES		DO NOT SCALE DRAWING		REVISION
	NAME	SIGNATURE	DATE				TITLE:
DRAWN							
CHK'D							
APPV'D							
MFG							
Q.A				MATERIAL:		DWG NO.	A4
						tekening_manifold	
				WEIGHT:		SCALE:1:2	SHEET 1 OF 1

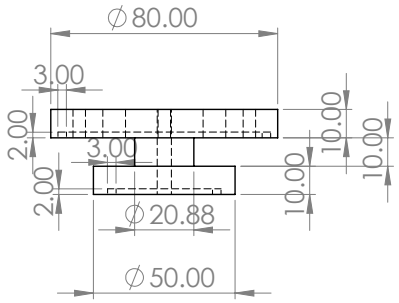

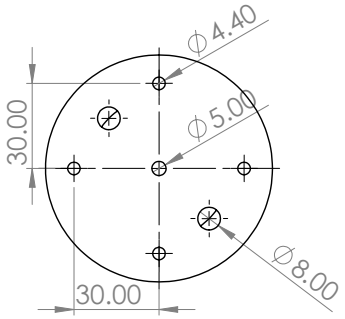

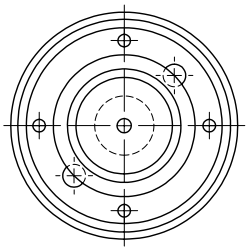

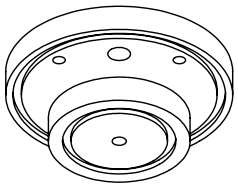

UNLESS OTHERWISE SPECIFIED: DIMENSIONS ARE IN MILLIMETERS SURFACE FINISH: TOLERANCES: LINEAR: ANGULAR:		FINISH:		DEBURR AND BREAK SHARP EDGES		DO NOT SCALE DRAWING	REVISION	
	NAME	SIGNATURE	DATE			TITLE:		
DRAWN								
CHK'D								
APPV'D								
MFG								
Q.A				MATERIAL:		DWG NO.		A4
						Top_mal2		
				WEIGHT:		SCALE:1:2	SHEET 1 OF 1	

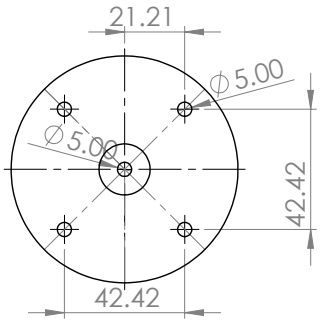

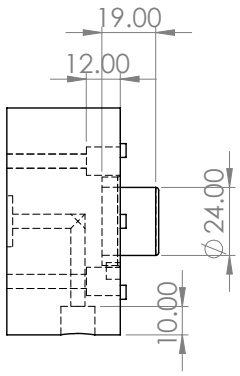

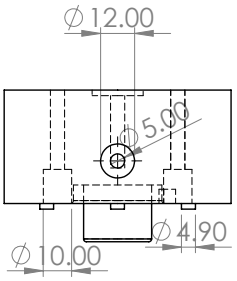

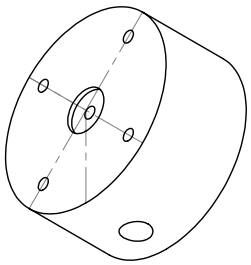

UNLESS OTHERWISE SPECIFIED: DIMENSIONS ARE IN MILLIMETERS SURFACE FINISH: TOLERANCES: LINEAR: ANGULAR:		FINISH:		DEBURR AND BREAK SHARP EDGES	DO NOT SCALE DRAWING	REVISION	
	NAME	SIGNATURE	DATE				TITLE:
DRAWN							
CHK'D							
APPV'D							
MFG							
Q.A				MATERIAL:		DWG NO.	A4
						manifoldV4	
				WEIGHT:		SCALE:1:2	SHEET 1 OF 1

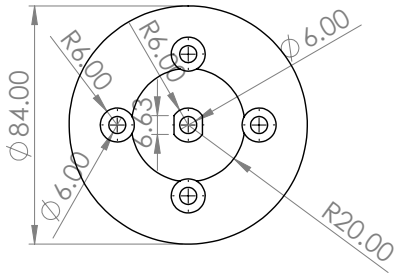

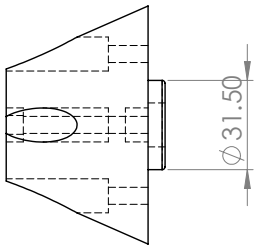

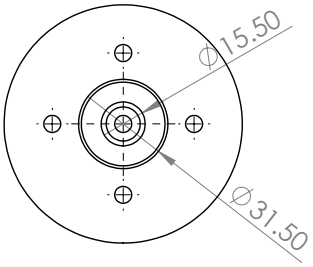

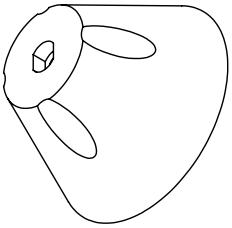

UNLESS OTHERWISE SPECIFIED: DIMENSIONS ARE IN MILLIMETERS SURFACE FINISH: TOLERANCES: LINEAR: ANGULAR:		FINISH:		DEBURR AND BREAK SHARP EDGES		DO NOT SCALE DRAWING	REVISION
	NAME	SIGNATURE	DATE			TITLE:	
DRAWN							
CHK'D							
APPV'D							
MFG							
Q.A				MATERIAL:		DWG NO. FlensV3	A4
				WEIGHT:		SCALE:1:2	SHEET 1 OF 1

Bibliography

[1] Emission absorption spectrum. https://www.aatbio.com/spectrum/Rhodamine_B, . Accessed: 06-01-2020.

[2] Sony imx264 spectral response, . Accessed: 20-4-2020.

[3] *Introduction to Optics*. Pearson Education, 2008. ISBN 9788131720240. URL https://books.google.nl/books?id=-XjoZQVxoNIC.

[4] W. Brian Rowe. *Hydrostatic, Aerostatic and Hybrid Bearing Design*. 2012. ISBN 9780123969941. doi: 10.1016/C2011-0-07331-3.

[5] R. Cameron and R. W. Gregory. Paper 4: Measurement of Oil Film Thickness between Rolling Discs Using a Variable Reluctance Technique. *Proceedings of the Institution of Mechanical Engineers, Conference Proceedings*, 1967. ISSN 0367-8849. doi: 10.1243/pime_conf_1967_182_403_02.

[6] Ziqiang Cui, Chengyi Yang, Benyuan Sun, and Huaxiang Wang. Liquid film thickness estimation using electrical capacitance tomography, 2014. ISSN 13358871.

[7] Alexander P. Demchenko. *Introduction to fluorescence sensing*. 2009. ISBN 9781402090035. doi: 10.1007/978-1-4020-9003-5.

[8] R. S. Dwyer-Joyce, B. W. Drinkwater, and C. J. Donohoe. The measurement of lubricant-film thickness using ultrasound. *Proceedings of the Royal Society A: Mathematical, Physical and Engineering Sciences*, 2003. ISSN 14712946. doi: 10.1098/rspa.2002.1018.

[9] A. Dyson, H. Naylor, and A. R. Wilson. Paper 10: The Measurement of Oil-Film Thickness in Elastohydrodynamic Contacts. *Proceedings of the Institution of Mechanical Engineers, Conference Proceedings*, 1965. ISSN 0367-8849. doi: 10.1243/pime_conf_1965_180_072_02.

[10] Rafael Auras et al. *Poly(lactic Acid): Synthesis, Structures, Properties, Processing, and Applications*. 2010.

[11] P. A. Flournoy, R. W. McClure, and G. Wyntjes. White-Light Interferometric Thickness Gauge. *Applied Optics*, 1972. ISSN 0003-6935. doi: 10.1364/ao.11.001907.

[12] R Haugland, M Spence, I Johnson, and A Basey. *The Handbook: A Guide to Fluorescent Probes and Labelling Technologies*. 2005.

[13] Carlos H. Hidrovo and Douglas P. Hart. Emission reabsorption laser induced fluorescence (ERLIF) film thickness measurement. *Measurement Science and Technology*, 2001. ISSN 13616501. doi: 10.1088/0957-0233/12/4/310.

[14] Kenneth Holmberg, Peter Andersson, and Ali Erdemir. Global energy consumption due to friction in passenger cars. *Tribology International*, 2012. ISSN 0301679X. doi: 10.1016/j.triboint.2011.11.022.

[15] Nicholas M. Husen, Tianshu Liu, and John P. Sullivan. The ratioed image film thickness meter. *Measurement Science and Technology*, 2018. ISSN 13616501. doi: 10.1088/1361-6501/aabd27.

[16] COMSOL INC. Comsol multiphysics, 2020. URL www.Comsol.com.

[17] I. K. Kabardin, V. G. Meledin, I. A. Eliseev, and V. V. Rakhmanov. Optical measurement of instantaneous liquid film thickness based on total internal reflection. *Journal of Engineering Thermophysics*, 2011. ISSN 18102328. doi: 10.1134/S1810232811040072.

[18] Seung-Woo Kim and Gee-Hong Kim. Thickness-profile measurement of transparent thin-film layers by white-light scanning interferometry. *Applied Optics*, 1999. ISSN 0003-6935. doi: 10.1364/ao.38.005968.

[19] Lumileds. Luxeon c color line multiple colors, a single focal length, 2020. URL https://www.lumileds.com/wp-content/uploads/files/DS144-luxeon-c-color-line-datasheet.pdf.

[20] A. A. Mouza, N. A. Vlachos, S. V. Paras, and A. J. Karabelas. Measurement of liquid film thickness using a laser light absorption method. *Experiments in Fluids*, 2000. ISSN 07234864. doi: 10.1007/s003480050394.

[21] T. A. Osman, M. Dorid, Z. S. Safar, and M. O.A. Mokhtar. Experimental assessment of hydrostatic thrust bearing performance. *Tribology International*, 1996. ISSN 0301679X. doi: 10.1016/0301-679X(95)00078-I.

[22] T. Reddyhoff, J. H. Choo, H. A. Spikes, and R. P. Glovnea. Lubricant flow in an elastohydrodynamic contact using fluorescence. *Tribology Letters*, 2010. ISSN 10238883. doi: 10.1007/s11249-010-9592-6.

[23] Tom Reddyhoff, Rob Dwyer-Joyce, and Phil Harper. Ultrasonic measurement of film thickness in mechanical seals. *Sealing Technology*, 2006. ISSN 13504789. doi: 10.1016/S1350-4789(06)71260-0.

[24] D. F. Swinehart. The Beer-Lambert law, 1962. ISSN 00219584.

[25] Yoshio Utaka and Tetsuji Nishikawa. An investigation of liquid film thickness during solutal Marangoni condensation using a laser absorption method: Absorption property and examination of measuring method. *Heat Transfer - Asian Research*, 2003. ISSN 10992871. doi: 10.1002/htj.10124.

[26] Antoon Van Beek and Lubor Lepic. Rubber supported hydrostatic thrust bearings with elastic bearing surfaces of infinite length. *Wear*, 1996. ISSN 00431648. doi: 10.1016/S0043-1648(96)06987-6.

[27] Ron A.J. Van Ostayen, Anton Van Beek, and Mink Ros. A parametric study of the hydro-support. *Tribology International*, 2004. ISSN 0301679X. doi: 10.1016/j.triboint.2004.01.009.

[28] Duqiang Wu, Richard Burton, and Greg Schoenau. An empirical discharge coefficient model for orifice flow. *International Journal of Fluid Power*, 2002. ISSN 14399776. doi: 10.1080/14399776.2002.10781143.